DISSERTATION

INVESTIGATING FLUROXYPYR RESISTANCE IN BASSIA SCOPARIA

Submitted by

Olivia Todd

Department of Agricultural Biology

In partial fulfillment of the requirements

For the Degree of Doctor of Philosophy

Colorado State University

Fort Collins, Colorado

Summer 2021

Doctoral Committee:

Advisor: Todd Gaines

Patricia Bedinger
Cristina Argueso
Courtney Jahn

ABSTRACT

INVESTIGATING FLUROXYPYR RESISTANCE IN BASSIA SCOPARIA

Synthetic auxin herbicides are designed to mimic indole-3-acetic acid (IAA), an integral plant hormone affecting cell growth, development, and tropism. Recent developments in synthetic auxin herbicide research have produced several new reports of synthetic auxin resistant weeds and novel resistance mechanisms, including resistance by cytochrome P450 metabolism to mutations in auxin co-receptors. In this document, we investigate specific genes in the auxin signaling pathway that may be involved in weed resistance to the synthetic auxin herbicide fluroxypyr, an economically important method of broadleaf weed control in wheat. The auxin signaling pathway is well characterized, but for many herbicides in the synthetic auxin group, the specific gene family members for receptors and co-receptors with which they interact in the auxin signaling pathway remain unknown. We characterized this *Bassia scoparia* line using greenhouse studies, dose responses, absorption/translocation and metabolism using ^{14}C-fluroxypyr. To supplement these physiology studies, we conducted an RNA-sequencing experiment using the de novo transcriptome of *Bassia scoparia* to characterize gene expression in response to fluroxypyr using variant calling and differential expression in R. In addition to investigating this resistance case, this document also describes methodologies for creating crop resistance to pendimethalin via EMS mutagenesis. Through this experiment, many individuals have been found to reach full maturity in the northern Colorado region before the growing season ends. Backcrossing to the inbred parent *Sorghum bicolor* to begin genetic characterization

is the next step following completion of the early maturing line characterization and genetic validation.

ACKNOWLEDGEMENTS

I would like to acknowledge the contributing authors here by chapter:

Chapter 1: Todd, Olivia E; Figueiredo, Marcelo RA; Morran, Sarah; Soni, Neeta; Preston, Christopher; Kubeš, Martin F; Napier, Richard; Gaines, Todd A

Chapter 2: Todd, Olivia E; Patterson, Eric; Westra, Eric; Gaines, Todd A

Chapter 3: Todd, Olivia E; Gaines, Todd A; Nissen, Scott J; Dayan, Franck

A sincere thank you to Todd Gaines, Cris Argueso and Courtney Jahn for your investment in me. I thank you so much for your open door, and all you have taught me

Pat Bedinger, thank you for 10 years of your friendship, mentorship and council - it has gotten me far, and I am grateful.

DEDICATION

For my parents and for myself.

TABLE OF CONTENTS

INTRODUCTION

Weeds of agronomic crops cause major yield loss and impact crop quality if uncontrolled (Russo 2012). There are several tactics for controlling weeds in these systems, and chemical application of herbicides is one part of a multi-faceted solution. However, overuse and overreliance on herbicides has lead to herbicide resistance to 17 out of more than 35 different sites of action (Heap 2021). In the great plains of the United States, the nuisance weed species *Bassia scoparia* (kochia) is a tumbling species that reproduces by seed and has a mobile property when it senesces. The base of the plant abscises from the root system and can travel thousands of feet, dropping seeds as it tumbles. Mobility contributes to kochia's high rate of spread, so the plant can obtain and spread dominant, single gene herbicide resistance traits easily (Beckie et al. 2016). Kochia is a preferentially outcrosses and is very fecund, therefore able to drop a large amount of herbicide resistant seeds over a long distance.

Globally, herbicides are used on more than 1.5 billion hectares (Busi et al. 2018). With high use rates, resistance to more than one herbicide of a different site of action, known as multiple resistance, is increasingly common. A summary of information from the International Survey of Herbicide Resistant Weeds by Gaines et al. (2021) slates 107 weed species with multiple resistance to two or more sites of action. Field surveys testing for multiple resistance in kochia have been primarily focused on EPSPS inhibitors, ALS inhibitors and synthetic auxin herbicides (Beckie et al. 2013; Westra et al. 2019; Hall et al. 2014). These herbicides and sites of action comprised the top three globally used herbicides in 2014, where more than 1 billion hectares were treated (Figure 2) (Busi et al. 2018).

Synthetic auxin herbicides (HRAC Group 4) have five subgroups based on similar herbicide chemistry. Fluroxypyr, one chemical within the pyridine carboxylic acid subgroup, is classified as an Indole-3-Acetic Acid (IAA) mimic. Fluroxypyr is efficacious for kochia control, but currently there have been four reported kochia populations in North America that are resistant to fluroxypyr, and two populations in Canada (Heap 2021). Not much is known about the exact site of action, or how an application of fluroxypyr kills broadleaf weeds. However, fluroxypyr is able to directly bind to Auxin F-Box 5 in the auxin signaling pathway (Lee et al. 2014). This interaction is key to stabilizing the TIR1/AFB5 to Indole-3-Acetic Acid Inducible (Aux/IAA) complex (Figure 1). The interaction between fluroxypyr, TIR1/AFB and Aux/IAA proteins facilitates the ubiquitination of transcriptional repressor protein Aux/IAA, allowing for auxin dependent transcription (Lavy and Estelle 2016). The auxin signaling pathway and the role of fluroxypyr as a synthetic auxin provide the groundwork for investigating the resistance mechanism in a resistant population of kochia from eastern Colorado.

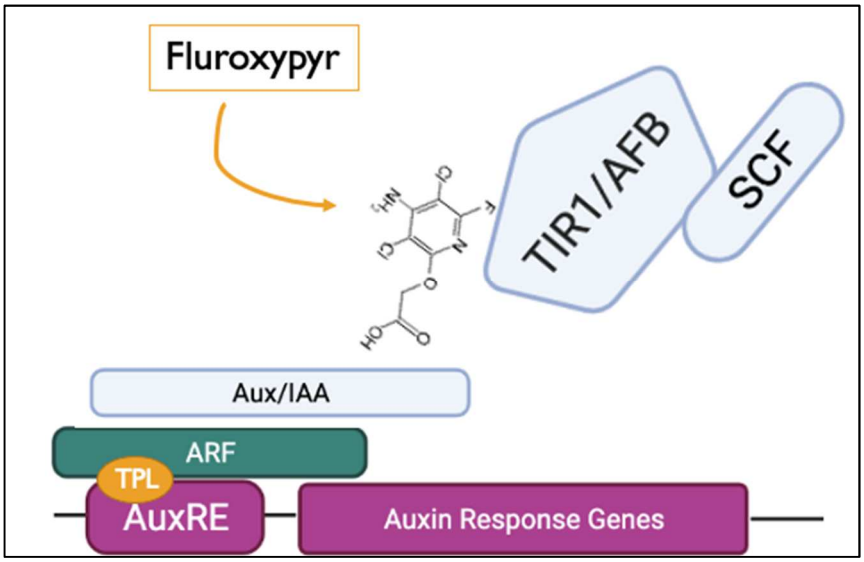

Figure 1. Fluroxypyr acts as the molecular glue, binding the TIR1/AFB – SCF complex to auxin gene transcriptional repressor Aux/IAA, allowing Aux/IAA to be ubiquitinated. In the absence of natural or synthetic auxin, Aux/IAA, Auxin Response Factors (ARF) and Topless (TPL) block the Auxin Response Element (AuxRE). In the presence of a natural or synthetic auxin, after Aux/IAA is ubiquitinated, auxin response gene transcription can begin.

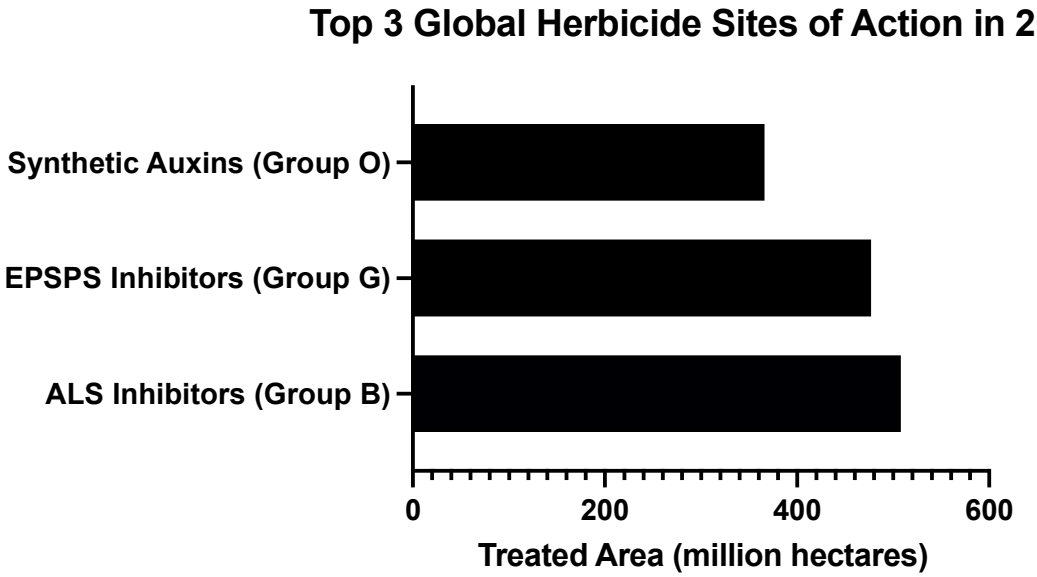

Figure 2. Adapted from Busi et al. (2018): Top three herbicide sites of action over treated hectares globally in 2014. Synthetic auxins were applied over 366 million hectares, EPSPS inhibitors were applied over 477 million hectares, and ALS inhibitors were applied over 508 million hectares globally.

REFERENCES

Beckie HJ, Blackshaw RE, Hall LM, Johnson EN (2016) Pollen-and seed-mediated gene flow in kochia (Kochia scoparia). Weed Sci 64 (4):624-633

Beckie HJ, Blackshaw RE, Low R, Hall LM, Sauder CA, Martin S, Brandt RN, Shirriff SW (2013) Glyphosate-and acetolactate synthase inhibitor–resistant kochia (Kochia scoparia) in western Canada. Weed Sci 61:310-318

Busi R, Goggin DE, Heap IM, Horak MJ, Jugulam M, Masters RA, Napier RM, Riar DS, Satchivi NM, Torra J, Westra P, Wright TR (2018) Weed resistance to synthetic auxin herbicides. Pest Manag Sci 74:2265-2276

Hall LM, Beckie HJ, Low R, Shirriff SW, Blackshaw RE, Kimmel N, Neeser C (2014) Survey of glyphosate-resistant kochia (Kochia scoparia L. Schrad.) in Alberta. Can J Plant Sci 94:127-130

Heap IM (2021) International survey of herbicide resistant weeds. www.weedscience.org.

Lavy M, Estelle M (2016) Mechanisms of auxin signaling. Development 143 (18):3226-3229. doi:10.1242/dev.131870

Lee S, Sundaram S, Armitage L, Evans JP, Hawkes T, Kepinski S, Ferro N, Napier RM (2014) Defining binding efficiency and specificity of auxins for SCF(TIR1/AFB)-Aux/IAA co-receptor complex formation. ACS Chem Biol 9 (3):673-682. doi:10.1021/cb400618m

Russo VM (2012) Peppers: botany, production and uses. CABI International

Westra EP, Nissen SJ, Getts TJ, Westra P, Gaines TA (2019) Survey reveals frequency of multiple resistance to glyphosate and dicamba in kochia (*Bassia scoparia*). Weed Technol 33:664-672

CHAPTER 1: SYNTHETIC AUXIN RESISTANCE: FINDING THE LOCK AND KEY TO WEED RESISTANCE

1. Introduction to synthetic auxin herbicides

Synthetic auxin herbicides (Weed Science Society of America/ Herbicide Resistance Action Committee Group 4/O) are a class of herbicides that mimic the activity of the plant hormone auxin (indole-3- acetic acid, IAA). Synthetic auxins are most commonly used to control broadleaf weeds in small grain cereals, fallow, and rangeland systems, although some are used to control grass and sedge species. On a global scale, synthetic auxin use ranks third behind glyphosate (Group 9/G) and acetolactate synthase inhibitors (Group 2/B) [1]. The two most used synthetic auxins by global treated area are dicamba and 2,4-Dichlorophenoxyacetic acid (2,4-D). Dicamba has been under particular scientific and public scrutiny in the USA in part due to potential offtarget movement and damage to neighboring sensitive vegetation when used later in the growing season during hot summer weather on dicamba-resistant soybean [2,3] and cotton [4]. In the USA, the proceedings of the Weed Science Society of America (WSSA) serve as a timeline for the development of important research topics (Figure 1.1). Research on synthetic auxins was the second most common topic over the 9 meetings included in the meta-analysis from 2011-2019, accounting for 12% of all submitted abstracts. Recently new crop varieties have been commercialized with stacked transgenic herbicide resistance traits such as Enlist cotton and Enlist E3 soybean (2,4-D, glyphosate, and glufosinate resistant) [5] as well as Roundup Ready 2 Xtend soybean (glyphosate and dicamba resistant) and Roundup Ready 3 XtendFlex cotton (glyphosate, glufosinate, and dicamba) [6] by Corteva Agriscience and Bayer CropScience, respectively. Research from WSSA indicates a surge of studies on these traits and herbicide combinations. Over subsequent years as the adoption of these technologies grew and use of

dicamba and 2,4-D increased, WSSA data shows a steady rise in evaluations of crop injury directly related to synthetic auxin use (Figure 1.1).

Reports on synthetic auxin resistance mechanisms in weeds have recently increased [1,7, Figure 1.1]. New publications reporting synthetic auxin resistance, such as in the important weeds kochia (*Bassia scoparia*) [8] and Palmer amaranth (*Amaranthus palmeri)* [9], have also been increasing in frequency in recent years. Research on efficacy and weed management with synthetic auxin herbicides have been at consistent levels at WSSA over the last 10 years, exemplifying the long term interest in studying this growing weed science issue. Since the introduction of 2,4-D as the first synthetic auxin herbicide in 1945, resistance to this class of herbicides has been reported in 41 species, with the first report in 1957 [10]. Despite the importance of this mode of action for weed management, only one molecular resistance mechanism in a weed species has been functionally validated [11]. Due to this lack of information, our scope of understanding of the resistance mechanisms in weedy species for synthetic auxins is relatively poor. The detailed mechanism of action of synthetic auxin herbicides, specifically the exact genes involved in the phytotoxicity, has long been a mystery locked by the complexity of the auxin signaling pathways. Here we discuss the canonical and non-canonical auxin signaling pathways in model plants and consider potential candidate genes which, if mutated, could be the keys to conferring resistance to synthetic auxins in weeds. Herbicide resistance mechanisms involve mutations and/or changes in expression of target-site genes, as well as changes in expression and/or mutations of genes that reduce the concentration of herbicide at the target-site, known as non-target-site mechanisms [12]. For synthetic auxin herbicides, target-site mutations occur in the auxin perception and signaling complex. Non-target-site mechanisms include changes in herbicide movement and enhanced metabolism to

inactive metabolites. We aim to address knowledge gaps in such areas as fitness costs of resistance and effects of ploidy on herbicide resistance. We also identify research needed to understand the differential efficacy of synthetic auxins on different plant families and speculate as to the basis of cross-resistance patterns to chemically dissimilar families of these herbicides.

2. Known and potential resistance mechanisms in the auxin signaling pathway

The canonical path for auxin signaling involves four major classes of proteins: auxin transporters (influx and efflux: PIN, ABCB, AUX/LAX), transcriptional repressors (Aux/IAAs), auxin response factors (ARFs), and the Skp1-Cullin-F-box TIR1/AFB E3 ubiquitin ligase complex ($SCF^{TIR1/AFB}$). Auxin is transported within and between cells via PIN, ABCB and AUX/LAX transporters. Auxin interacts with the $SCF^{TIR1/AFB}$ complex, which upon creation of the SCF-auxin-Aux/IAA complex, causes ubiquitination of Aux/IAA transcriptional repressors allowing induction of auxin response genes (Hagen and Guilfoyle 2002; Lavy and Estelle 2016).

Auxin perception is governed by a molecule of auxin binding to the $SCF^{TIR1/AFB}$ co-receptor complex, which mediates ubiquitination of a family of transcriptional regulators, the Aux/IAA proteins. Functional redundancy exists among the 6 TIR1/AFBs and 29 Aux/IAA proteins in *Arabidopsis*. Some specificity occurs in the interaction of TIR1/AFBs with different auxins and specific Aux/IAA proteins, and the auxin dose dependency of the complexes varies with each specific Aux/IAA protein (Villalobos et al. 2012a).

2.1 Mutations in the $SCF^{TIR1/AFB}$

Assembly of the active $SCF^{TIR1/AFB}$ ubiquitination complex involves several key proteins, some of which affect sensitivity to IAA and synthetic auxins (Table 1.1, Figure 1.2). The effects

of loss of function mutations or even missense mutation in the genes of the ubiquitination complex would ultimately lead to lack of Aux/IAA degradation and would prompt a resistance response. No reports of mutations in the components of the ubiquitin-conjugating enzymes or ubiquitin ligase have been recorded in weeds, but examples in *Arabidopsis* do illustrate the potential for resistance from these target sites. For example, several mutations in *Arabidopsis* SGT1 chaperone confer resistance to IAA and some synthetic auxin herbicides (Walsh et al. 2006). Similarly, mutations in proteins that are involved in the modulation of components of the SCF complex such as AXR1 (Lincoln et al. 1990) show resistance to IAA and 2,4-D. Critically, mutations in the receptors TIR1 and AFB5 in *Arabidopsis* cause insensitivity to dicamba (*tir1-1* and *afb5*) and 2,4-D (*tir1-1*) (Gleason et al. 2011) or to picloram (*afb5*) (Walsh et al. 2006). We speculate that due to the lack of observed field-evolved resistance, loss of function mutations in the $SCF^{TIR1/AFB}$ complex may have severe phenotypic consequences and associated fitness costs. Consequently, their initial frequencies in weed populations are likely to be extremely low in the absence of herbicide selection. Alternative resistance mechanisms that are initially more abundant due to a lower fitness penalty may be more easily selected.

2.2 Mutations in Aux/IAAs

Aux/IAAs are transcriptional repressors and auxin co-receptors. Out of 29 Aux/IAA proteins in Arabidopsis, many different mutants and expression variants with unique physiological responses have been characterized. Of the four domains present in Aux/IAA proteins, domain II stabilizes interactions with TIR1/AFBs by providing the surface that acts as the auxin co-receptor [19]. Mutations in and around the core motif (GWPPV/I), which is known as the degron, are especially dramatic. Several characterized mutants in Arabidopsis showed

drastic phenotypic changes such as reduced plant size, leaf morphology, growth, and formation of lateral roots (Table 1.2). A double base pair mutation within the coding region for domain II of BsIAA16 in kochia causes an amino acid substitution at a core degron position (Gly127Asn, GWPPV to NWPPV) and confers field-level resistance to dicamba [11]. This is the first Aux/IAA mutation identified to date from natural populations of synthetic auxin resistant weed species (Figure 1.2). The authors also suggested that the Gly127Asn mutation in BsIAA16 conferred cross-resistance to fluroxypyr and 2,4-D; however, greenhouse dose response experiments demonstrated that this kochia line is sensitive to fluroxypyr and 2,4-D [20]. This observation highlights that much more work is needed to fully elucidate patterns of cross-resistance across synthetic auxin chemical families conferred by auxin receptor and coreceptor mutations as well as possible effects on weed fitness due to these target-site resistance mechanisms, explored below. In addition to characterized mutations in the degron, variations occurring in the vicinity of the degron [21] could affect auxin-dependent binding to the SCFTIR1/AFB complex, stability of that complex, and/ or ubiquitination rate. Increases in expression or half-life of Aux/IAAs could lead to herbicide resistance as such changes would impact the feedback inhibitor response of auxin-induced gene expression (Figure 1.2).

2.3 Mutations in auxin response factors

Auxin response factors (ARFs) are transcription factors that bind to auxin response elements on the promoter regions of auxin-regulated genes. A critical auxin-responsive gene regulated by ARFs is 9-cisepoxycarotenoid dioxygenase (NCED), which is the rate-limiting step for abscisic acid (ABA) synthesis. A recent report suggested that ABA synthesis is a key marker of the phytotoxicity response to synthetic auxin herbicide application with a role in suppressing

transcription of genes associated with photosynthesis [22]. ARFs comprise four domains, two responsible for DNA binding and regulation, and two for dimerization with Aux/IAAs. The middle region after domain II determines whether the ARF will be a transcriptional activator or repressor [23,24]. In Arabidopsis, there are 23 ARFs; 18 are negative regulators of transcription and five are positive regulators. Due to high functional redundancy, many ARF mutants show only modest changes in plant phenotype, although the arf5 mutant results in extreme loss of body plan and double mutants such as arf7/arf19 show dramatic changes in lateral rooting responses [25]. The double mutant nph4-1 (ARF7) arf19-1 was also highly resistant to 2,4-D and IAA [26]. ARFs 5, 7 and 19 are in the transcriptional activator grouping, and we speculate that it is likely that the reduced redundancy involved with transcriptional activation is more likely to expose auxin insensitivity responses leading to herbicide resistance. However, they will also be more likely to impose fitness costs because there are so few of these activators. No naturally occurring ARF mutants are known to have led to resistant weed populations to date.

2.4 Mutations in transport proteins

Polar transport of auxin is conducted by PIN-formed (PIN) efflux carriers and ATP-Binding Cassette class B (ABCB) pump proteins [27–29]. Influx carrier proteins AUX1/LAX contribute to auxin transport [30–33]. All synthetic auxin herbicides are bioavailable as weak acids, thus they will accumulate inside the plant cells due to the anion trap [34]. Some herbicides are not substrates of the AUX1 uptake carrier [35] and must bypass AUX1/LAX influx carriers via passive or low specificity uptake. On the other hand, the phenoxyacetic acids like 2,4- D have high affinities for AUX1. Therefore, the contribution of AUX1/ LAX proteins to herbicide transport will vary with each herbicide compound. The aux1 mutant of Arabidopsis is resistant to

2,4-D [36]. Mutations reducing AUX1/LAX activity are enough to reduce herbicide transport and confer only modest physiological penalty [33,37], and so loss of AUX1/LAX function could be a candidate for synthetic auxin resistance for phenoxyacetic acids (Figure 1.2). Reduced translocation from application point to meristems has been reported for 2,4-D in wild radish (*Raphanus raphanistrum*) [38], prickly lettuce (*Lactuca serriola*) [39], and corn poppy (*Papaver rhoeas*) [40], and for dicamba in kochia [41]. In wild radish, reduced movement of 2,4-D throughout the plant in a 2,4-D resistant line was attributed to loss of cellular transport mediated by ABC transporters [38]. This conclusion was based on the mimicking of resistance in a sensitive line when treated with 1-naphthylphthalamic acid (NPA), which inhibits ABCB and PIN transporter activity. Resistant wild radish populations varied for reduced 2,4-D translocation as well as the increased expression of plasma-membrane associated receptor-like kinases and ABCB19, with no consistent trend across multiple populations for the role of any single mechanism [42,43]. ABCB4 may be a direct herbicidal target of 2,4-D [44,45]. Binding of 2,4-D to ABCB4 results in increased 2,4-D accumulation in Arabidopsis root epidermal cells and amplifies herbicidal effects such as swelling and loss of root hairs. It seems that ABCB4 has a role to control auxin concentrations within the cell. Functional redundancy within the ABCB protein family helps to combat loss of function mutations and is a trend seen through the analysis of the auxin signaling pathway; however, the ABCB family may have a degree of specificity for synthetic auxins that is not redundant within auxin transporter gene families. A more common association for ABCBs in resistance mechanisms is with upregulation to rapidly pump compounds out of cells as seen in antibiotic and insecticide resistance for broad-spectrum multi-drug resistance, as opposed to loss of function [46]. Upregulation of one or more ABCBs could

readily translate to nontarget site resistance to several synthetic auxins. This type of cross-resistance mechanism has not yet been identified in weeds.

3. Metabolic resistance to synthetic auxins

Herbicide metabolism includes (1) activation of a biologically inactive molecule (pro-herbicide) upon entering the plant, and (2) detoxification of the biologically active chemical. In general, metabolic processes work to maintain homeostasis of IAA in cells [47], although IAA homeostasis is destroyed by the arrival of synthetic auxin herbicides. Such disruptions to endogenous auxin pathways contribute to the phytotoxicity of synthetic auxin herbicides, on top of overload to the downstream genetic signaling responses noted above. Enzymatic activity can contribute to herbicide efficacy through activation of pro-herbicides. An example is the conversion of fluroxypyr meptyl-ester to fluroxypyr acid by esterase enzymes. Several other synthetic auxins are applied as esters including the new aryl-picolinates florpyrauxifen-benzyl and halauxifen-methyl [48]. If the esterase activity is inhibited or reduced, the molecule may not be activated, resulting in no bio-available herbicide to kill the plant. Substantial reduction in metabolic activation of the pro-herbicide triallate to the more toxic triallate sulfoxide confers triallate resistance in wild oats (*Avena fatua*) [49]. Currently no examples of loss of synthetic auxin proherbicide activation have been reported in weeds. We predict that loss of function of an esterase gene is a candidate pathway for evolution of resistance to pro-herbicides such as fluroxypyr meptyl-ester (Figure 1.2), although such resistance would be recessive, may have fitness costs, and could be impacted by functional redundancy among esterase genes. Another pro-herbicide is 2,4-DB. Legumes such as alfalfa (Medicago sativa) do not metabolically activate 2,4-DB to 2,4-D [50], rendering them tolerant to 2,4-DB applications and enabling selective

dicot weed control with 2,4-DB in these crops. Herbicide detoxification can involve one or multiple detoxifying plant enzymes such as glutathione S-transferases, cytochrome P450 monooxygenases, esterases, and glucosyl-transferases [51]. Synthetic auxins are subject to various metabolic pathways including reversible amino acid conjugation in dicots and irreversible hydroxylation followed by sugar conjugation in grasses, with variation among species in the specific metabolic processes [52]. Several examples of enhanced metabolic detoxification of synthetic auxins have been reported as resistance mechanisms in dicot weeds [53] (Figure 1.2), including hemp nettle (*Galeopsis tetrahit*) resistant to MCPA [54], chickweed (*Stellaria media*) resistant to mecoprop [55], and waterhemp (*Amaranthus tuberculatus*) resistant to 2,4-D [56]. Enhanced metabolism by cytochrome P450- mediated 2,4-D hydroxylation was reversed by the cytochrome P450 inhibitor malathion in *A. tuberculatus* [56]. In some cases, a metabolic resistance gene may confer resistance across chemical families within one mode of action, or even to herbicides from unrelated modes of action [51]. Resistance to non-auxin herbicides mediated via enhanced P450 activity can lead to reduced fitness in the absence of the herbicide [57] and the persistence of such resistance alleles will depend on relative fitness. A similar reduction in fitness may occur for plants resistant to synthetic auxins through enhanced detoxification.

4. Limitations in understanding

4.1 Fitness cost of synthetic auxin resistance in weeds

In order for a resistance trait to increase in frequency in a population, the resistance benefit should exceed any fitness cost associated with the resistance trait [58]. Understanding fitness costs linked to synthetic auxin resistance could guide management approaches to exploit

fitness costs to decrease the resistance allele frequency. Several studies investigating fitness cost of synthetic auxin resistance mechanisms in weed species have been conducted in kochia [11,59], wild mustard (*Sinapis arvensis*) [60–62], as well as other weedy species [63–65]. Commonly, a fitness cost has been identified. The field evolved BsIAA16 mutation endowing resistance to dicamba in kochia has a 75% and 50% fitness cost for reduced seed mass in homozygous and heterozygous resistant plants, respectively [11], possibly related to changes in endogenous IAA signaling as a consequence of the degron mutation in the Aux/IAA16 gene. On the other hand, a recent report [66] showed no measurable fitness cost in several wild radish field populations resistant to 2,4-D after a thorough evaluation of physiological responses and crop competition analysis. We conclude that more understanding of the evolutionary trajectory of synthetic auxin herbicide resistance is needed, and the relative lack of such research, in particular on a greater understanding of fitness costs for various resistance mechanisms [67], is illustrated by the lack of reports on the topic presented at WSSA (Figure 1.1).

4.2 Variation in response of broadleaf plant families to different synthetic auxin chemical groups and cross-resistance patterns in weeds

Different chemical families within the synthetic auxins have variable efficacy on certain entire plant families as well as species within the same family. Fluroxypyr, used widely in the USA on rangeland and cereals for broadleaf weed control, is in the pyridine-carboxylic acid group and controls kochia well [68], but has poor control of common lambsquarters (*Chenopodium album*) [69] even though both are members of the Caryophyllales family. Conversely, 2,4-D, a member of the phenoxy-carboxylic acid subfamily, has poor control of kochia [68], but controls common lambsquarters well [70]. The picolinic acid herbicide

clopyralid is used to control Asteraceae and Fabaceae weeds in canola, a crop in the naturally clopyralid-tolerant Brassicaceae family [71]. Similarly, halauxifen-methyl is used selectively in Brassicaceae forage crops to control weeds from several other broadleaf weed families, demonstrating lack of activity on Brassicaceae species but a high activity on other families [72]. We propose that an ambitious research effort into synthetic auxin herbicide/target site interactions is needed to 1) explain why some synthetic auxin chemical families have activity on certain dicot plant families but not others and 2) fully elucidate target-site cross-resistance patterns among synthetic auxin chemical families to guide best practices for herbicide rotation and mixture in resistance management. Potential explanations include physiological differences such as wax cuticle thickness and leaf hairiness leading to changes in herbicide translocation to growing points, differential rates of metabolism, and differences in target-site sensitivity among plant species [52]. We propose that the factorial combinations of target-site auxin receptor/coreceptor complexes in key weeds need further characterization with regards to binding of synthetic auxin herbicide from different chemical groups, particularly across the large gene family of Aux/IAA co-receptors. We currently lack a complete understanding of synthetic auxin herbicide-plant interactions across key weed species, though binding efficiency of some of these herbicides to receptors and co-receptors has been characterized. AFB5 was characterized as the preferred SCFTIR1/ AFB receptor protein for the picolinate auxin herbicides compared to TIR1 in Arabidopsis, whereas other auxin herbicides preferentially bound to TIR1 [73]. We speculate that different synthetic auxin herbicide families may differ from IAA in their main receptor target/coreceptor complex. Currently, only one receptor (TIR1) has been crystallized [74]. A homology model for AFB5 has been published with picloram bound [15]. A limitation of the TIR1 structure is that it was crystallized with a peptide containing only the degron region that

interacts with TIR1 and not the full Aux/IAA co-receptor protein; therefore, questions remain as to how the entire Aux/IAA protein interacts with TIR1. Structures for other auxin signaling proteins have been described, namely ARF5 domain III/IV [75], ARF1 [76], and Aux/IAA17 domain III/IV [77]. Given that at least one auxin herbicide resistance mechanism is based on a mutation in the Aux/IAA co-receptor degron sequence, more structures could help to guide hypotheses regarding mechanisms of resistance, their evolution, and perhaps guide decisions on resistance management using rotations and mixtures among different synthetic auxin chemical families.

4.3 Herbicide interactions with fast acting auxin signaling responses

The auxin signaling pathway via SCFTIR1/AFB (Figure 1.2) has been well characterized and is considered the canonical auxin signaling pathway. Changes in abundance of Aux/IAAs have been recorded within minutes of an auxin stimulus. However, other more rapid pathways involving auxin signaling proteins may also exist. Research within the last three years suggests that there may be another role for the long-described SCFTIR1/AFB auxin receptors that acts in seconds, and at the plasma membrane as opposed to the nucleus [reviewed by 78]. This rapid response mechanism affects primary root and root hair growth, potentially valuable traits for herbicides to target, but it is not yet known how many synthetic auxins activate this pathway. Interestingly, these fast root responses required an AUX1 uptake carrier for activity and so the families of synthetic auxins not carried by AUX1 [35] may not engage with this system. A fascinating recent report describes rapid cell death (visible leaf necrosis within 2 hr after 2,4-D application) induced by 2,4-D in 2,4-D resistant *Conyza sumatrensis* [79]. We speculate that this 2,4-D resistance could involve rapid auxin response signaling pathways such as a plasma

membrane receptor leading to H2O2 production and rapid cell death within 15 min of 2,4-D application, thereby reducing 2,4-D translocation to the apical meristem and causing resistance. Transmembrane kinases have also been associated with rapid auxin signaling. In the presence of auxin the C-terminus on a transmembrane kinase is cleaved and translocated to the nucleus where it stabilizes specific Aux/IAA proteins [80]. This stabilization regulates auxin response factors, inducing transcription of auxin-induced genes [81]. The transmembrane kinase gene family is composed of four functional overlapping members, TMK1-4 [82]. Single mutants in these genes have no observable phenotype. Double null mutants (tmk1; tmk4) are less sensitive to auxin, and triple mutants (tmk1; tmk3; tmk4) completely auxin insensitive and have lower seed production phenotypes and reduced size. Further work is needed to characterize how activity of these transmembrane kinases responses may potentially regulate synthetic auxin herbicide activity and selectivity, as well characterizing a potential role for transmembrane kinases in evolved 2,4-D resistance in weeds [42].

4.4 Resistance to quinclorac in grasses

Quinclorac is a unique synthetic auxin that is primarily used in rice and is selective against annual grasses and broadleaf weeds [83]. Resistance to quinclorac in grass weeds has been a management issue, including quinclorac resistance in smooth crabgrass (*Digitaria ischaemum*) [84] and Echinochloa species. One resistance mechanism reported in Echinochloa has been increased activity in the enzyme betacyanoalanine synthase (β-CAS), the key enzyme in cyanide degradation. The increase in β-CAS activity is proposed to detoxify hydrogen cyanide, which is produced as a consequence of ethylene biosynthesis following quinclorac application [83,85–88]. Several mutations associated with enhanced activity have been identified in β-CAS.

Met-295-Lys was identified in two resistant Echinochloa crus-galli var. zelayensis lines, which is the sequence present in the same position in naturally quinclorac-tolerant rice [86]. Three mutations in Echinochloa crus-galli var. mitis (Asn-105-Lys, Gln-195-Glu, and Gly-298-Val) were determined to expand the binding pocket, conferring higher β-CAS activity [88]. However, in other resistant Echinochloa lines the same overall effect has been achieved by reducing ethylene synthesis, hence alleviating the source of cyanide production [89, 90]. Other mechanisms that reduce the impact of elevated cyanide such as downregulation of genes involved in photosynthesis and electron transport have been reported from Echinochloa crus-galli var. zelayensis, suggesting a broad array of mechanisms have been selected which allow it to survive quinclorac application [87]. Whether these confer resistance to other synthetic auxins as well as quinclorac is unclear, and further investigation into quinclorac resistance mechanisms is needed. Both target-site and non-target-site mechanisms may be involved in quinclorac resistance in grass weeds.

4.5 Impacts of polyploidy on synthetic auxin resistances

Polyploidy is common throughout the angiosperms, with 30-70% of plant species within families estimated to be polyploid [91]. Of the 41 species that have been reported with resistance to synthetic auxins, 35% are polyploid and/or mixed ploidy [10]. Understanding resistance mechanisms in polyploid weed species can be especially complex as the presence of multiple genomes results in a suite of regulatory mechanisms that are not found in diploid species. Many of the cases of quinclorac resistance in grasses occur in the Echinochloa spp., which are frequently polyploid and similar considerations arise. Allele dosage, gene sub-functionalization, silencing and redundancy, inheritance modes, and mutational load all have implications. This

may be particularly true for synthetic auxin resistance mechanisms resulting from target-site mutations, such as a mutation in an Aux/IAA gene. In this instance, resistance in a diploid species may be dominant but the same mutation in a polyploid may have less effect, due to the reduced representation of the resistance allele in the total gene expression of a polyploid. By the same measure, high relative fitness may be maintained in a polyploid that is resistant because this plant may express both mutant and non-mutated versions of the affected gene from homoeologous chromosomes, allowing resistant alleles to remain cryptic with minimal apparent fitness penalty until their selective advantage is uncovered by herbicide application. Genome assembly for polyploids is especially challenging. Therefore, polyploidy in weeds presents a considerable challenge when investigating herbicide resistance mechanisms for synthetic auxins given the complex gene families for auxin co-receptors, transporters, and auxin response factors. The inheritance of synthetic auxin resistance traits has been determined mostly in diploids [e.g., 92,93] as well as identification of specific resistance mechanisms [11], but despite these challenges, further investigation is needed to better understand the evolutionary trajectory of synthetic auxin resistance in polyploid weed populations.

5. Concluding thoughts and available resources

Research to unlock the mysteries of resistance to synthetic auxin herbicides and cross-resistance patterns across weed species will require comprehensive sequence data for the genomes involved. The availability of weed genomics resources is expanding, through efforts of individual groups [e.g., 94,95] and the International Weed Genomics Consortium [96]. With better genomic tools, the identification and validation of synthetic auxin resistance genes will improve and help inform the future development and sustainability of synthetic auxin herbicides.

The research that has been done to date enables predictions of possible genetic mechanisms for evolved synthetic auxin herbicide resistance (Figure 1.2). As we continue to unravel the interactions between synthetic auxin herbicide molecules and auxin signaling pathways, new insights may lead to novel inhibitors that bypass existing resistance mechanisms or enable inhibition of other components of the auxin signaling pathway.

TABLES

Table 1.1 Assembly of the active SCFTIR1/AFB ubiquitination complex involves several key proteins that affect sensitivity to IAA and synthetic auxins

Protein	*Described insensitivity*	*Role in auxin pathway*	*Possible effect on auxin pathway*	*Source*
AXR1 ECR1 RCF1	2,4-D	E1 and E2 ubiquitin-protein ligase complex component	Loss of function could lead to mis/malformation of $SCF^{TIR1/AFB}$ ubiquitination complex	(Lincoln et al. 1990; Del Pozo et al. 2002)
HSP90/SGT1	IAA, 2,4-D, picloram, florpyrauxifen-benzyl	Molecular Chaperone	Loss of function could lead to lack of ubiquitination of Aux/IAAs	(Gray et al. 2003; Wang et al. 2016; Walsh et al. 2006; Watanabe et al. 2016)
RUB NEDD8 CAND1	IAA, 2,4-D	Ubiquitin complex modulators	Loss of function could lead to mis/malformation of $SCF^{TIR1/AFB}$ ubiquitination complex	(Bostick et al. 2004; Zhang et al. 2008)
COP9				(Huang et al. 2012; Schwechheimer et al. 2001)
CUL1		E3 ubiquitin-protein ligase complex component	Missense/loss of function may lead to lowered substrate binding of the $SCF^{TIR1/AFB}$ ubiquitination complex. May lead to incomplete or lowered ubiquitination of the targeted Aux/IAA proteins	(Hellmann et al. 2003; Yu et al. 2015)
TIR1	Dicamba, 2,4-D	Auxin receptor	Lack of auxin perception, lowered posttranslational regulation, leading to lowered/lack of ubiquitination	(Gleason et al. 2011)
AFB5	Dicamba, picloram	Auxin Receptor		

Table 1.2. Several characterized mutants in *Arabidopsis* Aux/IAA genes showed severe phenotypic changes in plant size, leaf morphology, growth, and formation of lateral roots. Auxin insensitivity caused by downregulation of Aux/IAA genes in tomato. Mutation in the degron of *Aux/IAA16* in *Bassia scoparia* caused dicamba resistance.

Described Mutant	*Organism*	*Source*
axr5-1/IAA1	*Arabidopsis thaliana*	(Yang et al. 2004)
shy2/IAA3	*Arabidopsis thaliana*	(Tian and Reed 1999)
axr2/IAA7	*Arabidopsis thaliana*	(Calderon-Villalobos et al. 2010; Nagpal et al. 2000; Walsh et al. 2006)
iaa16	*Arabidopsis thaliana*	(Rinaldi et al. 2012)
iaa28	*Arabidopsis thaliana*	(Rogg et al. 2001)
SlIAA3	*Solanum lycopersicum*	(Chaabouni et al. 2009)
SlIAA15	*Solanum lycopersicum*	(Xu et al. 2015)
SlIAA27	*Solanum lycopersicum*	(Bassa et al. 2012)
Aux/IAA16	*Bassia scoparia*	(LeClere et al. 2018a)

FIGURES

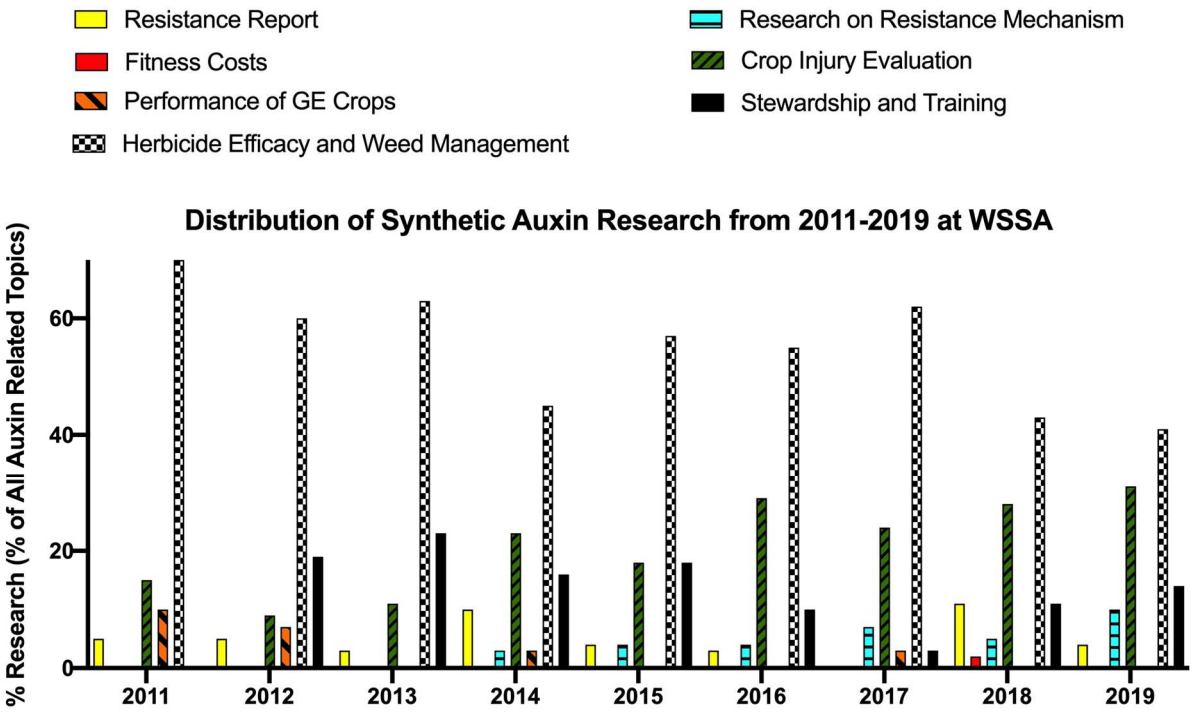

Figure 1.1. Research prevalence on topics related to the use of synthetic auxin herbicides. The numbers of abstracts related to synthetic auxin research at the annual Weed Science Society of America (WSSA) conference proceedings from 2011-2019 have been classified into seven topic categories. Data for each topic was normalized as a percent of the total published abstracts on synthetic auxins.

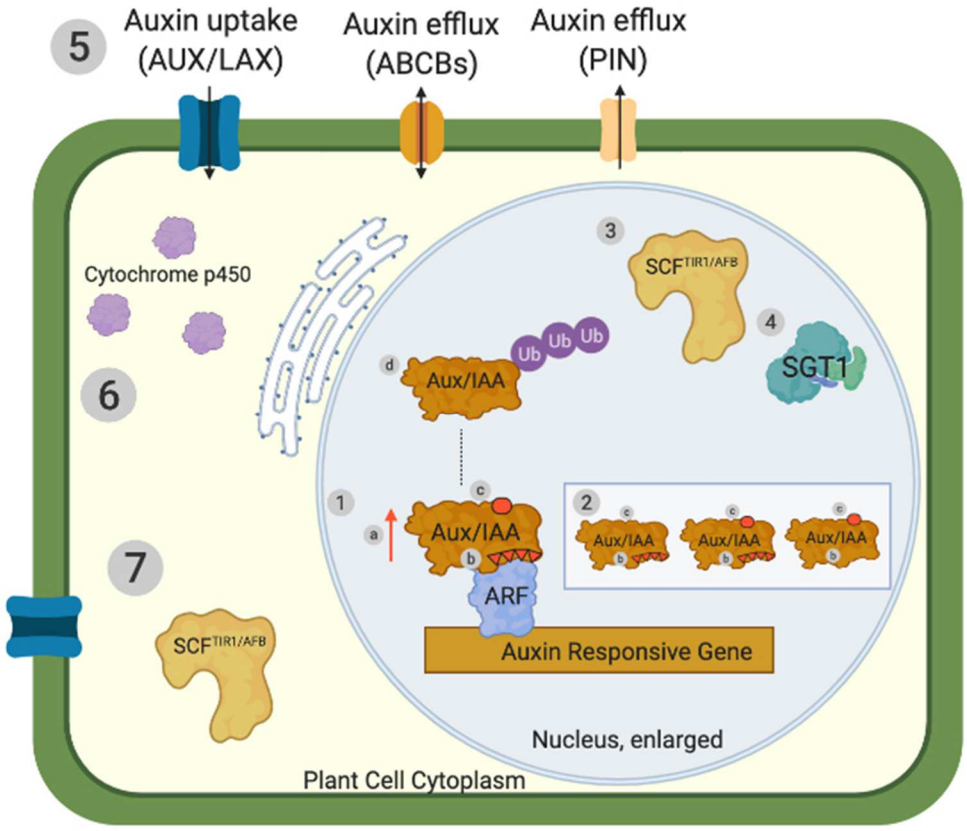

Figure 1.2. Confirmed and proposed resistance mechanisms to synthetic auxin herbicides in weeds. Red X indicates loss of function, red up arrow indicates increased expression. 1) Accumulation of Aux/IAA protein dampens the ubiquitination and degradation responses required to release ARF transcription factor for expression of auxin responsive genes due to a, increased expression of Aux/IAA protein (proposed); b, changes to flexibility of regions near the degron of Aux/IAA protein (shown as set of four red triangles, proposed); c, mutation in degron of Aux/IAA protein co-receptor (shown as red dot) to restrict binding to SCFTIR1/AFB/ auxin complex (confirmed in model systems, Table 2, and in weeds [11]); d, mutations in the regulators of the SCFTIR1/AFB complex restrict ubiquitination of Aux/IAA and subsequent Aux/IAA degradation (proposed). 2) Polyploid containing a mixture of wild-type and resistant mutant Aux/IAA proteins (proposed, mutations in degron and regions near the degron illustrated). 3) Loss of function of SCFTIR1/AFB receptor (confirmed in model systems, proposed in weeds). 4) Loss of function of molecular chaperones such as SGT1 and HSP90 (confirmed in model systems, proposed in weeds). 5) Loss of function of auxin inter-cellular transporters such as AUX/LAX, ABCB transporters, and PIN transporters (proposed). 6) a, loss of activation of pro-herbicide by esterases (proposed); b, enhanced cytochrome P450 metabolism of synthetic auxin herbicides (confirmed in weeds). 7) Changes to fast-acting, non-canonical auxin signaling pathway such as SCFTIR1/AFB/auxin interactions at the plasma membrane (proposed) or transmembrane kinases that can stabilize Aux/IAA proteins (proposed in weeds, [42]). Figure created in BioRender (www.biorender.com).

REFERENCES

[1] R. Busi, et al., Weed resistance to synthetic auxin herbicides, Pest Manage. Sci. 74 (2018) 2265–2276.
[2] G.T. Jones, J.K. Norsworthy, T. Barber, E. Gbur, G.R. Kruger, Off-target movement of DGA and BAPMA dicamba to sensitive soybean, Weed Technol. 33 (2019) 51–65.
[3] N. Soltani, et al., Off-target movement assessment of dicamba in North America, Weed Technol. (2020) in press.
[4] J.T. Buol, et al., Effect of growth stage on cotton response to a sublethal concentration of dicamba, Weed Technol. 33 (2019) 1–8.
[5] T.R. Wright, et al., Robust crop resistance to broadleaf and grass herbicides provided by aryloxyalkanoate dioxygenase transgenes, Proc. Natl. Acad. Sci. USA 107 (2010) 20240–20245.
[6] M.R. Behrens, et al., Dicamba resistance: Enlarging and preserving biotechnologybased weed management strategies, Science 316 (2007) 1185–1188.
[7] V.E. Perotti, A.S. Larran, V.E. Palmieri, A.K. Martinatto, H.R. Permingeat, Herbicide resistant weeds: A call to integrate conventional agricultural practices, molecular biology knowledge and new technologies, Plant Sci. 290 (2020) 110255.
[8] V. Kumar, R.S. Currie, P. Jha, P.W. Stahlman, First report of kochia (Bassia scoparia) with cross-resistance to dicamba and fluroxypyr in western Kansas, Weed Technol. 33 (2019) 335–341.
[9] V. Kumar, R. Liu, G. Boyer, P.W. Stahlman, Confirmation of 2, 4□D resistance and identification of multiple resistance in a Kansas Palmer amaranth (Amaranthus palmeri) population, Pest Manage. Sci. 75 (2019) 2925–2933.
[10] I. Heap, The international survey of herbicide resistant weeds, Available on-line: www.weedscience.com . Accessed April 22, 2020 (2020).
[11] S. LeClere, C. Wu, P. Westra, R.D. Sammons, Cross-resistance to dicamba, 2,4-D, and fluroxypyr in Kochia scoparia is endowed by a mutation in an AUX/IAA gene, Proc. Natl. Acad. Sci. USA 115 (2018) E2911–E2920.
[12] T.A. Gaines, et al., Mechanisms of evolved herbicide resistance, J. Biol. Chem. (2020) in press.
[13] G. Hagen, T. Guilfoyle, Auxin-responsive gene expression: genes, promoters and regulatory factors, Plant Mol. Biol. 49 (2002) 373–385.
[14] M. Lavy, M. Estelle, Mechanisms of auxin signaling, Development 143 (2016) 3226–3229.
[15] L.I.A.C. Villalobos, et al., A combinatorial TIR1/AFB–Aux/IAA co-receptor system for differential sensing of auxin, Nat. Chem. Biol. 8 (2012) 477.
[16] T.A. Walsh, et al., Mutations in an auxin receptor homolog AFB5 and in SGT1b confer resistance to synthetic picolinate auxins and not to 2,4-dichlorophenoxyacetic acid or indole-3-acetic acid in Arabidopsis, Plant Physiol. 142 (2006) 542–552.
[17] C. Lincoln, J.H. Britton, M. Estelle, Growth and development of the axr1 mutants of Arabidopsis, Plant Cell 2 (1990) 1071–1080.
[18] C. Gleason, R.C. Foley, K.B. Singh, Mutant analysis in Arabidopsis provides insight into the molecular mode of action of the auxinic herbicide dicamba, PLoS One 6 (2011) e17245.
[19] T.J. Guilfoyle, The PB1 domain in auxin response factor and Aux/IAA proteins: a versatile protein interaction module in the auxin response, Plant Cell 27 (2015) 33–43.

[20] O.E. Todd, T. Gaines, E.P. Westra, P. Westra, Investigating cross-resistance to the synthetic auxins fluroxypyr and dicamba in Bassia scoparia, Proc. Western Soc. Weed Sci. 72 (2019) 120.
[21] M. Niemeyer, et al., Flexibility of intrinsically disordered degrons in AUX/IAA proteins reinforces auxin co-receptor assemblies, Nature Comm 11 (2020) 2277.
[22] C.L. McCauley, et al., Transcriptomics in Erigeron canadensis reveals rapid photosynthetic and hormonal responses to auxin-herbicide application, J. Exp. Bot. 71 (2020) 3701–3709.
[23] V.V. Mironova, N.A. Omelyanchuk, D.S. Wiebe, V.G. Levitsky, Computational analysis of auxin responsive elements in the Arabidopsis thaliana L. genome, BMC Gen. 15 (2014) S4.
[24] T. Ulmasov, Z.-B. Liu, G. Hagen, T.J. Guilfoyle, Composite structure of auxin response elements, Plant Cell 7 (1995) 1611–1623.
[25] Y. Okushima, et al., Functional genomic analysis of the AUXIN RESPONSE FACTOR gene family members in Arabidopsis thaliana: unique and overlapping functions of ARF7 and ARF19, Plant Cell 17 (2005) 444–463.
[26] M.K. Watahiki, K.T. Yamamoto, The massugu1 mutation of Arabidopsis identified with failure of auxin-induced growth curvature of hypocotyl confers auxin insensitivity to hypocotyl and leaf, Plant Physiol. 115 (1997) 419–426.
[27] J. Petrasek, et al., PIN proteins perform a rate-limiting function in cellular auxin efflux, Science 312 (2006) 914–918.
[28] M. Geisler, B. Aryal, M. Di Donato, P. Hao, A critical view on ABC transporters and their interacting partners in auxin transport, Plant Cell Physiol. 58 (2017) 1601–1614.
[29] P.J. Verrier, et al., Plant ABC proteins–a unified nomenclature and updated inventory, Trends Plant Sci. 13 (2008) 151–159.
[30] B. Peret, et al., AUX/LAX genes encode a family of auxin influx transporters that perform distinct functions during Arabidopsis development, Plant Cell 24 (2012) 2874–2885.
[31] D.J. Carrier, et al., The binding of auxin to the Arabidopsis auxin influx transporter AUX1, Plant Physiol 148 (2008) 529–535.
[32] X. Yang, et al., The IAA1 protein is encoded by AXR5 and is a substrate of SCFTIR1, Plant J. 40 (2004) 772–782.
[33] K. Swarup, et al., The auxin influx carrier LAX3 promotes lateral root emergence, Nat. Cell Biol. 10 (2008) 946–954.
[34] H.K. Takano, E.L. Patterson, S.J. Nissen, F.E. Dayan, T.A. Gaines, Predicting herbicide movement across semi-permeable membranes using three phase partitioning, Pest. Biochem. Physiol. 159 (2019) 22–26.
[35] K. Hoyerova, et al., Auxin molecular field maps define AUX1 selectivity: many auxin herbicides are not substrates, New Phytol. 217 (2018) 1625–1639.
[36] F.B. Pickett, A.K. Wilson, M. Estelle, The aux1 mutation of Arabidopsis confers both auxin and ethylene resistance, Plant Physiol. 94 (1990) 1462–1466.
[37] A. Marchant, et al., AUX1 promotes lateral root formation by facilitating indole-3- acetic acid distribution between sink and source tissues in the Arabidopsis seedling, Plant Cell 14 (2002) 589–597.
[38] D.E. Goggin, G.R. Cawthray, S.B. Powles, 2,4-D resistance in wild radish: reduced herbicide translocation via inhibition of cellular transport, J. Exp. Bot. 67 (2016) 3223–3235.
[39] D.S. Riar, I.C. Burke, J.P. Yenish, J. Bell, K. Gill, Inheritance and physiological basis for 2,4-D resistance in prickly lettuce (Lactuca serriola L.), J. Agric. Food Chem. 59 (2011) 9417–9423.

[40] J. Rey-Caballero, et al., Unravelling the resistance mechanisms to 2, 4-D (2, 4-dichlorophenoxyacetic acid) in corn poppy (Papaver rhoeas), Pest. Biochem. Physiol. 133 (2016) 67–72.
[41] D.J. Pettinga, et al., Increased Chalcone Synthase (CHS) expression is associated with dicamba resistance in Kochia scoparia, Pest Manage. Sci. 74 (2018) 2306–2315.
[42] D.E. Goggin, S. Bringans, J. Ito, S.B. Powles, Plasma membrane receptor-like kinases and transporters are associated with 2,4-D resistance in wild radish, Ann. Bot. 125 (2020) 821–832.
[43] D.E. Goggin, P. Kaur, M.J. Owen, S.B. Powles, 2, 4-D and dicamba resistance mechanisms in wild radish: subtle, complex and population specific? Ann. Bot. 122 (2018) 627–640.
[44] H. Yang, A.S. Murphy, Functional expression and characterization of Arabidopsis ABCB, AUX 1 and PIN auxin transporters in Schizosaccharomyces pombe, Plant J. 59 (2009) 179–191.
[45] M. Kubeš, et al., The Arabidopsis concentration-dependent influx/efflux transporter ABCB4 regulates cellular auxin levels in the root epidermis, Plant J. 69 (2012) 640–654.
[46] W. Dermauw, T. Van Leeuwen, The ABC gene family in arthropods: comparative genomics and role in insecticide transport and resistance, Insect Biochem. Mol. Biol. 45 (2014) 89–110.
[47] V. Skalický, M. Kubeš, R. Napier, O. Novák, Auxins and cytokinins—The role of subcellular organization on homeostasis, Int. J. Mol. Sci. 19 (2018) 3115.
[48] J.B. Epp, et al., The discovery of Arylex™ active and Rinskor™ active: Two novel auxin herbicides, Bioorganic & Medicinal Chemistry 24 (2016) 362–371.
[49] A.J. Kern, D.M. Peterson, E.K. Miller, C.C. Colliver, W.E. Dyer, Triallate resistance in Avena fatua L. is due to reduced herbicide activation, Pest. Biochem. Physiol. 56 (1996) 163–173.
[50] D. Linscott, R. Hagin, J. Dawson, Conversion of 4-(2, 4-dichlorophenoxy) butyric acid to homologs by alfalfa. Mechanism of resistance to this herbicide, J. Agric. Food Chem. 16 (1968) 844–848.
[51] V.K. Nandula, et al., Herbicide metabolism: crop selectivity, bioactivation, weed resistance, and regulation, Weed Sci. 67 (2019) 149–175.
[52] T.M. Sterling, J. Hall, Mechanism of action of natural auxins and the auxinic herbicides Herbicide Activity: Toxicology, Biochemistry and Molecular Biology, IOS Press, Amsterdam, 1997, pp. 111–141.
[53] M. Jugulam, C. Shyam, Non-target-site resistance to herbicides: recent developments, Plants 8 (2019) 417.
[54] T. Weinberg, G.R. Stephenson, M.D. McLean, J.C. Hall, MCPA (4-chloro-2-ethylphenoxyacetate) resistance in hemp-nettle (Galeopsis tetrahit L.), J. Agric. Food Chem. 54 (2006) 9126–9134.
[55] D. Coupland, P.J. Lutman, C. Heath, Uptake, translocation, and metabolism of mecoprop in a sensitive and a resistant biotype of Stellaria media, Pest. Biochem. Physiol. 36 (1990) 61–67.
[56] M.R. Figueiredo, et al., Metabolism of 2,4□dichlorophenoxyacetic acid contributes to resistance in a common waterhemp (Amaranthus tuberculatus) population, Pest Manage. Sci. 74 (2018) 2356–2362.
[57] M.M. Vila-Aiub, P. Neve, S. Powles, Resistance cost of a cytochrome P450 herbicide metabolism mechanism but not an ACCase target site mutation in a multiple resistant Lolium rigidum population, New Phytol. 167 (2005) 787–796.
[58] M.M. Vila□Aiub, P. Neve, S.B. Powles, Fitness costs associated with evolved herbicide resistance alleles in plants, New Phytol. 184 (2009) 751–767.

[59] V. Kumar, P. Jha, Differences in germination, growth, and fecundity characteristics of dicamba-fluroxypyr-resistant and susceptible Kochia scoparia, PLoS One 11 (2016) e0161533.
[60] D.J. Debreuil, L.F. Friesen, I.N. Morrison, Growth and seed return of auxin-type herbicide resistant wild mustard (Brassica kaber) in wheat, Weed Sci. 44 (1996) 871–878.
[61] J.C. Hall, M. Romano, Morphological and physiological differences between the auxinic herbicide-susceptible (S) and-resistant (R) wild mustard (Sinapis arvensis L.) biotypes, Pest. Biochem. Physiol. 52 (1995) 149–155.
[62] M. Jugulam, M.D. McLean, S. Chen, J. Christopher Hall, Development of near□- isogenic lines and identification of markers linked to auxinic herbicide resistance in wild mustard (Sinapis arvensis L.), Pest Manage. Sci. 68 (2012) 548–556.
[63] K. Bonner, A. Rahman, T. James, K. Nicholson, D. Wardle, Relative intra□species competitive ability of nodding thistle biotypes with varying resistance to the herbicide 2, 4□D, New Zealand J. Agric. Res. 41 (1998) 291–297.
[64] H. Watanabe, M.Z. Ismail, N.K. Ho, Response of 2, 4-D resistant biotype of Fimbristylis miliacea (L.) Vahl. to 2, 4-D dimethylamine and its distribution in the Muda Plain, Peninsular Malaysia, J. Weed Sci. Technol. 42 (1997) 240–249.
[65] G. Bourdôt, D. Saville, G. Hurrell, Ecological fitness and the decline of resistance to the herbicide MCPA in a population of Ranunculus acris, J. Appl. Ecol. 33 (1996) 151–160.
[66] D.E. Goggin, H.J. Beckie, C. Sayer, S.B. Powles, No auxinic herbicide–resistance cost in wild radish (Raphanus raphanistrum), Weed Sci. 67 (2019) 539–545.
[67] P. Neve, R. Busi, M. Renton, M.M. Vila□Aiub, Expanding the eco□evolutionary context of herbicide resistance research, Pest Manage. Sci. 70 (2014) 1385–1393.
[68] V. Kumar, P. Jha, Effective preemergence and postemergence herbicide programs for kochia control, Weed Technol. 29 (2015) 24–34.
[69] R.L. Macdonald, C.J. Swanton, J.C. Hall, Basis for the selective action of fluroxypyr, Weed Res. 34 (1994) 333–344.
[70] A.P. Robinson, D.M. Simpson, W.G. Johnson, Summer annual weed control with 2, 4-D and glyphosate, Weed Technol. 26 (2012) 657–660.
[71] J.C. Hall, P.K. Bassi, M.S. Spencer, W.H.V. Born, An evaluation of the role of ethylene in herbicidal injury induced by picloram or clopyralid in rapeseed and sunflower plants, Plant Physiol. 79 (1985) 18–23.
[72] G. Wells, ForageMaxTM herbicide for broadleaf weeds in forage brassicas, in: M. Baker (Ed.), 19th Australasian Weeds Conference Tasmanian Weed Society Hobart, Australia, 2014, pp. 448–449.
[73] S. Lee, et al., Defining binding efficiency and specificity of auxins for SCFTIR1/AFBAux/IAA co-receptor complex formation, ACS Chem. Biol. 9 (2014) 673–682.
[74] X. Tan, et al., Mechanism of auxin perception by the TIR1 ubiquitin ligase, Nature 446 (2007) 640–645.
[75] M.H. Nanao, et al., Structural basis for oligomerization of auxin transcriptional regulators, Nature Comm 5 (2014) 3617.
[76] D.R. Boer, et al., Structural basis for DNA binding specificity by the auxin-dependent ARF transcription factors, Cell 156 (2014) 577–589.
[77] M. Han, et al., Structural basis for the auxin-induced transcriptional regulation by Aux/IAA17, Proc. Natl. Acad. Sci. USA 111 (2014) 18613–18618.
[78] M. Kubeš, R. Napier, Non-canonical auxin signalling: fast and curious, J. Exp. Bot. 70 (2019) 2609.

[79] A. R. S. d. Queiroz, et al., Rapid necrosis: a novel plant resistance mechanism to 2,4-D, Weed Sci. 68 (2020) 1–13.
[80] T. Xu, et al., Cell surface ABP1-TMK auxin-sensing complex activates ROP GTPase signaling, Science 343 (2014) 1025–1028.
[81] M. Cao, et al., TMK1-mediated auxin signalling regulates differential growth of the apical hook, Nature 568 (2019) 240–243.
[82] N. Dai, W. Wang, S.E. Patterson, A.B. Bleecker, The TMK subfamily of receptor-like kinases in Arabidopsis display an essential role in growth and a reduced sensitivity to auxin, PLoS One 8 (2013) e60990.
[83] H. Yasuor, M. Milan, J.W. Eckert, A.J. Fischer, Quinclorac resistance: a concerted hormonal and enzymatic effort in Echinochloa phyllopogon, Pest Manage. Sci. 68 (2012) 108–115.
[84] I. Abdallah, A.J. Fischer, C.L. Elmore, M.E. Saltveit, M. Zaki, Mechanism of resistance to quinclorac in smooth crabgrass (Digitaria ischaemum), Pest. Biochem. Physiol. 84 (2006) 38–48.
[85] J. Xu, B. Lv, Q. Wang, J. Li, L. Dong, A resistance mechanism dependent upon the inhibition of ethylene biosynthesis, Pest Manage. Sci. 69 (2013) 1407–1414.
[86] Y. Gao, et al., Resistance to quinclorac caused by the enhanced ability to detoxify cyanide and its molecular mechanism in Echinochloa crus-galli var. zelayensis, Pest. Biochem. Physiol. 143 (2017) 231–238.
[87] Y. Gao, X. Pan, X. Sun, J. Li, L. Dong, Is the protection of photosynthesis related to the mechanism of quinclorac resistance in Echinochloa crus-galli var. zelayensis? Gene 683 (2019) 133–148.
[88] M. Zia Ul Haq, Z. Zhang, J. Wei, S. Qiang, Ethylene biosynthesis inhibition combined with cyanide degradation confer resistance to quinclorac in Echinochloa crusgalli var. mitis, Int. J. Mol. Sci. 21 (2020) 1573.
[89] P. Chayapakdee, et al., Quinclorac resistance in Echinochloa phyllopogon is associated with reduced ethylene synthesis rather than enhanced cyanide detoxification by β□cyanoalanine synthase, Pest Manage. Sci. 76 (2020) 1195–1204.
[90] Y. Gao, et al., Quinclorac resistance induced by the suppression of the expression of 1-aminocyclopropane-1-carboxylic acid (ACC) synthase and ACC oxidase genes in Echinochloa crus-galli var. zelayensis, Pest. Biochem. Physiol. 146 (2018) 25–32.
[91] P.S. Soltis, D.B. Marchant, Y. Van de Peer, D.E. Soltis, Polyploidy and genome evolution in plants, Curr. Opin. Gen. Devel. 35 (2015) 119–125.
[92] C. Preston, D.S. Belles, P.H. Westra, S.J. Nissen, S.M. Ward, Inheritance of resistance to the auxinic herbicide dicamba in kochia (Kochia scoparia), Weed Sci. 57 (2009) 43–47.
[93] C. Preston, J.M. Malone, Inheritance of resistance to 2, 4-D and chlorsulfuron in a multiple resistant population of Sisymbrium orientale, Pest Manage. Sci. 71 (2015) 1523–1528.
[94] J.M. Kreiner, et al., Multiple modes of convergent adaptation in the spread of glyphosate-resistant Amaranthus tuberculatus, Proc. Natl. Acad. Sci. USA 116 (2019) 21076–21084.
[95] M. Laforest, et al., A chromosome-scale draft sequence of the Canada fleabane genome, Pest Manage. Sci. 76 (2020) 2158–2169.
[96] K. Ravet, et al., The power and potential of genomics in weed biology and management, Pest Manage. Sci. 74 (2018) 2216–2225.
[97] J.C. Del Pozo, et al., AXR1-ECR1–dependent conjugation of RUB1 to the Arabidopsis cullin AtCUL1 is required for auxin response, Plant Cell 14 (2002) 421–433.

[98] W.M. Gray, P.R. Muskett, H.-w. Chuang, J.E. Parker, Arabidopsis SGT1b is required for SCFTIR1-mediated auxin response, Plant Cell 15 (2003) 1310–1319.
[99] R. Wang, et al., HSP90 regulates temperature-dependent seedling growth in Arabidopsis by stabilizing the auxin co-receptor F-box protein TIR1, Nature Comm 7 (2016) 1–11.
[100] E. Watanabe, et al., HSP90 stabilizes auxin-responsive phenotypes by masking a mutation in the auxin receptor TIR1, Plant Cell Physiol. 57 (2016) 2245–2254.
[101] M. Bostick, S.R. Lochhead, A. Honda, S. Palmer, J. Callis, Related to ubiquitin 1 and 2 are redundant and essential and regulate vegetative growth, auxin signaling, and ethylene production in Arabidopsis, Plant Cell 16 (2004) 2418–2432.
[102] W. Zhang, et al., Genetic analysis of CAND1–CUL1 interactions in Arabidopsis supports a role for CAND1-mediated cycling of the SCFTIR1 complex, Proc. Natl. Acad. Sci. USA 105 (2008) 8470–8475.
[103] Y.L. Huang, et al., Transcriptome analysis of an invasive weed Mikania micrantha, Biologia Plantarum 56 (2012) 111–116.
[104] C. Schwechheimer, et al., Interactions of the COP9 signalosome with the E3 ubiquitin ligase SCFTIR1 in mediating auxin response, Science 292 (2001) 1379–1382.
[105] H. Hellmann, et al., Arabidopsis AXR6 encodes CUL1 implicating SCF E3 ligases in auxin regulation of embryogenesis, EMBO J. 22 (2003) 3314–3325.
[106] H. Yu, et al., Untethering the TIR1 auxin receptor from the SCF complex increases its stability and inhibits auxin response, Nature Plants 1 (2015) 1–8.
[107] Q. Tian, J.W. Reed, Control of auxin-regulated root development by the Arabidopsis thaliana SHY2/IAA3 gene, Development 126 (1999) 711–721.
[108] L.I. Calderon-Villalobos, X. Tan, N. Zheng, M. Estelle, Auxin perception—- structural insights, CSH Perspect Biol 2 (2010) a005546.
[109] P. Nagpal, et al., AXR2 encodes a member of the Aux/IAA protein family, Plant Physiol. 123 (2000) 563–574.
[110] M.A. Rinaldi, J. Liu, T.A. Enders, B. Bartel, L.C. Strader, A gain-of-function mutation in IAA16 confers reduced responses to auxin and abscisic acid and impedes plant growth and fertility, Plant Mol. Biol. 79 (2012) 359–373.
[111] L.E. Rogg, J. Lasswell, B. Bartel, A gain-of-function mutation in IAA28 suppresses lateral root development, Plant Cell 13 (2001) 465–480.
[112] S. Chaabouni, et al., Sl-IAA3, a tomato Aux/IAA at the crossroads of auxin and ethylene signalling involved in differential growth, J. Exp. Bot. 60 (2009) 1349–1362.
[113] T. Xu, et al., Solanum lycopersicum IAA15 functions in the 2, 4-dichlorophenoxyacetic acid herbicide mechanism of action by mediating abscisic acid signalling, J. Exp. Bot. 66 (2015) 3977–3990.
[114] C. Bassa, I. Mila, M. Bouzayen, C. Audran-Delalande, Phenotypes associated with down-regulation of Sl-IAA27 support functional diversity among Aux/IAA family members in tomato, Plant Cell Physiol. 53 (2012) 1583–1595.

CHAPTER 2: A FLUROXYPYR AND ALS RESISTANT KOCHIA (*BASSIA SCOPARIA*) POPULATION FROM COLORADO IS NOT CROSS-RESISTANT TO DICAMBA

1. Introduction

Kochia is a broadleaf, annual tumbleweed that is agronomically problematic. Kochia is highly stress tolerant and is able to germinate under a wide range of temperatures, salinity levels, and moisture levels (Friesen et al. 2009). Herbicide resistance in kochia has been reported for several acetolactate synthase (ALS) inhibitors (group 2) (Primiani et al. 1990), atrazine (group 5) (Foes et al. 1999), glyphosate (group 9) (Waite et al. 2013), and dicamba (group 4) (Cranston et al. 2001). Furthermore, multiple resistance to all four of these modes of action has been reported in one population (Varanasi et al. 2015). Herbicide resistance in kochia has widespread distribution for resistance to ALS inhibitors, glyphosate, synthetic auxins, and atrazine (Kumar et al. 2019b).

ALS-inhibitor resistance in kochia was first reported in the United States in 1987, and kochia was one of the first species to evolve resistance to sulfonylureas and other ALS-inhibiting herbicides (Primiani et al. 1990). Photosystem II (PSII)-inhibitor resistance to simazine and atrazine was first documented in common groundsel (*Senecio vulgaris*) in 1970 (Ryan 1970), and atrazine resistance in kochia was first reported in Kansas in 1976 (Heap 2021). Both ALS-inhibitor and PSII inhibitor resistance can result from nucleotide polymorphisms in the gene encoding the site of action (Gaines et al. 2020). Glyphosate resistance in kochia has become increasingly common (e.g., Westra et al. (2019); Kumar et al. (2014); Beckie et al. (2015); Gaines et al. (2016)). The prevalence of glyphosate, atrazine, and ALS inhibitor resistant kochia has resulted in increased use of auxinic herbicides for kochia management, mainly dicamba and

fluroxypyr, for control of kochia in no-till fallow, wheat, and corn in the Great Plains region (Kumar et al. 2019b).

While synthetic auxins have been used for more than 70 years, resistance evolution has lagged behind other herbicide modes-of-action (Busi et al. 2018). Nine reports of synthetic auxin resistance across six states in the U.S. and two provinces in Canada have described resistance in kochia populations as either resistant to dicamba alone, or resistant to both dicamba and fluroxypyr (Heap 2021). One mechanism of resistance to dicamba in kochia has been characterized at the molecular level as a double nucleotide substitution changing the degron motif GWPPV to NWPPV in a key Aux/IAA protein (*IAA*16) in the auxin signaling pathway (LeClere et al. 2018b); however, a reduction in dicamba translocation has also been reported in this population (Pettinga et al. 2018). Cross-resistance to dicamba and fluroxypyr has been reported in kochia populations from the US states of Kansas and Montana (Kumar et al. 2019a; Kumar and Jha 2016) and in Saskatchewan, Canada (Heap 2021). Our objective was to characterize resistance to fluroxypyr, dicamba, chlorsulfuron, and atrazine in a putatively fluroxypyr-resistant kochia population from eastern Colorado. We confirmed fluroxypyr and ALS resistance and found that this population was not cross-resistant to dicamba.

2. Materials and methods

2.1 Plant material

In 2014, a field survey was conducted in eastern Colorado where 171 kochia populations were collected (Westra et al. 2019). These populations were screened with single doses of dicamba, fluroxypyr, and glyphosate to test for resistance. One population, Flur-R, was found to have a few individuals (<2%) surviving fluroxypyr after the fourth week of evaluation. Plants

were subjected to single dose selection at 157 g ae ha^{-1} fluroxypyr (Starane Ultra, Dow Agrosciences, Indianapolis, IN). Survivors at 157g ae ha^{-1} were selected and allowed to bulk pollinate. After two more generations of selection at both 157g ae ha^{-1} and 314g ae ha^{-1}, cross-pollination, and seed production, the progeny were uniformly resistant up to 314g ae ha^{-1} fluroxypyr. Field use history of the collection site is unknown. During the bulking stages, groups of three to four plants per pot were covered with a pollination bag and allowed to cross-pollinate. Seed was harvested per pot, hand threshed and cleaned using an air-column blower. Seeds were stored at 4 C and planted in the spring in a greenhouse maintained at 25 C with a 16 h photoperiod, growth conditions which were uniform over the course of the experiments. An inbred dicamba resistant population homozygous for a mutation in the *IAA16* gene from Colorado State University (9425) (LeClere et al. 2018b; Preston et al. 2009) and a fluroxypyr susceptible field population from the 2014 eastern Colorado field study (J01) (Westra et al. 2019) were included in the dose response and single dose screening as susceptible controls.

2.2 Fluroxypyr and dicamba dose responses

Flur-R, J01, and 9425 were planted in 1.5 cm^2 280-count plug flats. Plants were sub-irrigated and thinned down to one plant per cell. When plants were approximately 4-5 cm tall, uniform seedlings were transplanted to 4 cm^2 plastic pots containing SunGro potting mix (American Clay Works Supply, Denver, CO). During growth, plants were sub-irrigated once a week for three weeks until the plants reached 10 cm height. Plants were kept in the greenhouse with conditions described above for the duration of the experiment. The dose response experiment was repeated. A randomized complete block design was used for each dose, with four plants per dose and three replications. The dose response for fluroxypyr included the

following eight rates: 0, 20, 40, 80, 157, 314, 628, and 1,256 g ae ha^{-1} fluroxypyr (Starane Ultra, Corteva Agrisciences, Indianapolis, IN). The dicamba doses included 0, 35, 70, 140, 280, 560, 1120, and 2240 g ae ha^{-1} of dicamba (Engenia, BASF, Research Triangle Park, NC) mixed with Induce (NIS, 0.25% v/v, Helena Agri-Enterprises, LLC, 24330 US-34 Greely, CO 80631). Applications were made with a DeVries Generation 4 Research Track Sprayer (DeVries Manufacturing, Hollandale, MN, 86956) equipped with a TeeJet (TeeJet Technologies, 1801 Business Park drive, Springfield, IL) 8002EV8 nozzle calibrated to output 187 L ha^{-1}. Plant height was measured by recording the distance in centimeters from the soil to the newest leaf in the meristem before treating and was measured again 30 days after treatment. Survival (dead or alive) was also recorded 30 days after treatment. An individual was considered "dead" if it displayed severe epinasty, stem thickening, yellowing, and had no new growth at the axillary or primary meristems after 30 days. An individual was considered "alive" if it displayed minimal to no epinasty and stem thickening, no yellowing, and had new growth at the axillary or primary meristems after 30 days. Percent survival was chosen for fluroxypyr resistance assessment because while percent change in height does accurately differentiate between resistant and susceptible plants, for this population it did not accurately represent the individuals where axillary meristem growth was the primary source of regrowth.

For data analysis, the response variable "Percent Survival" (Figure 1) was created by transforming binary data according to the equation:

$$Y = \left(\frac{N_1}{N_{total}}\right) * 100 \text{ [1]}$$

Where *Y* is the percent survival at each calculated dose, N_1 is the number of individuals marked as "alive" according to the parameters above. N_{total} is the number of individuals per rate. The change in height over 30 days was normalized using the following equation:

$$Y = (X_{\Delta Height}/A_{Avg}) * 100 \text{ [2]}$$

Where *Y* is the percent change in height as a percent of the 0 g ae ha^{-1} rate for each population. $X_{\Delta Height}$ is the change in height for an individual over 30 days, and A_{Avg} is the average change in height for individuals at the 0 g ae ha^{-1} rate for the corresponding population. The model used by the drm package in R did not converge for the J01 or 9425 lines using "percent change in height (% control)" as a response, so percent survival data were analyzed using a three-parameter log-logistic model (Knezevic et al. 2007) which was determined to be the best model by a lack-of-fit test from the drc package in R (R-Team 2018) with the equation:

$$Y = \frac{d}{1+exp\,[b(log\,[(x- log)\,(e)])]} \text{ [3]}$$

where *Y* is the percent survival 30 days after treatment, *d* is the upper limit parameter, *b* is the regression slope, *x* is the dose of either fluroxypyr or dicamba in g ae ha^{-1} and *e* is the dose at which 50% mortality is achieved (Table 2.1). The data were averaged per treatment and the standard error of the mean is presented per dose. "Rate" and "Population" were used as predictor variables.

2.3 Glyphosate, atrazine, and chlorsulfuron single rate screening

Flur-R and J01 seeds were planted in 4 cm^2 plastic pots containing SunGro potting mix. Plants were sub-irrigated and thinned down to one plant per cell. When plants were

approximately 7 cm in height, n=72 plants for each herbicide were treated with atrazine (AAtrex 4L, Syngenta, Greensboro, NC, 2240 g ai ha^{-1}, 1% crop oil concentrate), chlorsulfuron (Telar XP, Bayer CropScience, St. Louis, MO, 137 g ai ha^{-1}), or glyphosate (RoundUp Powermax, Monsanto Company, St. Louis, MO, 870 g ae ha^{-1}, 2% w/v ammonium sulfate). All treatments were applied with the same equipment and nozzle type described above. Survival (dead or alive) was assessed 30 days after treatment. In a *post hoc* analysis, a random number generator was used to assign each of the 72 individuals to one of three blocks with n=24 to serve as replicates. Standard error of the mean was calculated using the standard deviation from this analysis.

Kompetitive allele specific PCR (KASP)

Approximately 200 mg of meristem tissue was harvested from 9 individuals from Flur-R, 9425, and four additional dicamba resistant populations (J25, J06, J27 and M32) from the field survey described by Westra et al. (2019). Dicamba resistance was verified by spraying individuals from J25, J06, J27, and M32 with 280 g ae ha^{-1} dicamba. Flur-R individuals were verified as resistant by spraying with 157 g ae ha^{-1} fluroxypyr. Tissue was put into a 1.5 mL Eppendorf tube and flash frozen in liquid nitrogen. DNA extraction protocol was adapted from Aboul-Maaty and Oraby (2019) using the established CTAB method. DNA purification was checked using a NanoDrop2000 and diluted to 5 ng uL^{-1}. The FAM fluorophore (in bold) was added to the forward primer specific to the *iaa16* double mutation (allele specific sequence in italics) endowing a protein change from wildtype GWPPV to NWPPV in kochia described by LeClere et al. (2018b)
(5'**GAAGGTGACCAAGTTCATGCT**TGTTCTTCAGGACACAAGTTGTA*AA*) and the HEX fluorophore (in bold) was added to the forward primer specific to the wild type sequence (in italics) (5'**GAAGGTCGGAGTCAACGGATT**TGTTCTTCAGGACACAAGTTGTA*GG*). One

universal reverse primer (5'AGTTTGATCATCGGACGTCTTCTT) and the forward primers were designed with IDT PrimerQuest, The KASP protocol for genotyping for herbicide resistance follows the methodology described by Patterson et al. (2017). The KASP primer master mix was made with 18 µL of 10 uM HEX and FAM primers, 45 µL of 10 uM universal reverse primer, and 69 µL of sterile water. An aliquot of 12 µL of this primer mix was added to the KASP master mix (432 µL mix of polymerase, dNTPs, buffer, cofactors). Using a 96-well plate, 4 µL of KASP master mix was mixed with 4 µL of 5 ng μL^{-1} template DNA or 4 µL of water for two no-template controls (NTCs) were included. The KASP assay was conducted using Bio-Rad CFX Manager 3.1 following the KASP user manual (Technologies 2020) using a 96-well plate. Thermal cycling conditions were as follows: activation at 94 C for 15 minutes, then 10 touchdown cycles of 94 C for 20 seconds (denaturing), 61 C for 1 minute (annealing and elongation), then 35 cycles of 94 C for 20 seconds, 55 C for 1 minute and 30 C for 10 seconds. Fluorescence was recorded at the end of every cycle. Fluorescence at the 35^{th} cycle was used for the allelic discrimination data. Data were plotted using GraphPad Prism version 8.4.2.

3. Results and discussion

3.1 Fluroxypyr and dicamba dose response

The population Flur-R was confirmed to be resistant to fluroxypyr based on change in height (Figure 2.1A) and percent survival (Figure 2.1B) at 30 d after treatment (DAT), with 75% survival up to 628 g ae ha^{-1} of fluroxypyr (Figure 2.1B). Flur-R was approximately 40 times more resistant than the susceptible population J01 and 36 times more resistant than 9425 (Table 2.1). The population 9425, which was previously reported to be fluroxypyr resistant (LeClere et al. 2018b) was subsequently shown to have weak fluroxypyr resistance (Wu et al. 2020). Our

results show 9425 had less than 25% survival at the label rate of 157 g ae ha^{-1} fluroxypyr (Figure 2.1B) and had similar reduction in height as the known susceptible population (Figure 2.1A). The known fluroxypyr susceptible population (J01) and 9425 had an LD_{50} ratio for fluroxypyr not different from 1 (Table 2.1), indicating that 9425 is not resistant to field rates of fluroxypyr.

Flur-R was susceptible to dicamba (Figure 2.1C), with 8% survival at 70 g ae ha^{-1} and an LD_{50} of 56 g ae ha^{-1}. Flur-R is approximately seven times more susceptible than 9425 to dicamba (Table 2.1), the only fluroxypyr-resistant kochia population to be reported without cross-resistance to another synthetic auxin (Heap 2021).

3.2 Glyphosate, atrazine, and chlorsulfuron single rate screening

None of the 72 individuals from Flur-R or J01 survived following treatment with the label rates of glyphosate (870 g ae ha^{-1}) and atrazine (2240 g ai ha^{-1}) 30 days after treatment. However, 94% ($\pm$ 0.5%) of individuals from the Flur-R population survived chlorsulfuron (137 g ai ha^{-1}) treatment while only 7% ($\pm$ 0.5%) of J01 individuals survived. This indicates that there is multiple resistance to ALS inhibitors in this fluroxypyr resistant population.

3.3 KASP

Kompetitive allele specific PCR was used to genotype individuals based on the methods of Patterson et al. (2017) using allelic discrimination in the KASP assay to determine whether or not Flur-R individuals contained the *IAA16* mutation reported by LeClere et al. (2018b). Specific fluorophore sequences were assigned to each forward primer, which generated a fluorescent signal to determine which allele was present in the kochia DNA sample. Relative Fluorescence Units (RFU) were measured to determine which of the fluorophore sequences amplified for each

sample (Figure 2.2). Of the nine individuals tested from the Flur-R population, six displayed high RFU for the HEX labeled primer corresponding to the wildtype allele and three displayed approximately equal RFU for both alleles, indicating heterozygous individuals for the *iaa16* mutation (Figure 2.2B). One known susceptible wild type control was included, as well as one mutant resistant control (9425). These results indicate that the *iaa16* mutation does not cause fluroxypyr resistance, and that the dicamba resistance allele is segregating in the Flur-R population. This mutation is known to be incompletely dominant (Preston et al. 2009), confirmed by our data in which heterozygous individuals with one mutant allele were not dicamba resistant at the label rate. Other target site mutations may exist in proteins of the auxin signaling pathway and these are candidates for future research into the fluroxypyr resistance mechanism (Todd et al. 2020).

The KASP survey of five dicamba resistant populations showed that the *iaa16* mutation was present in some but not all field populations, indicating that additional mechanisms of dicamba resistance remain to be discovered (Figure 2.2A). The KASP genotyping assay will enable diagnostic testing, whereby growers and applicators can determine the presence of the *iaa16* mutation in their kochia populations. As synthetic auxin resistance continues to increase in major weed species (e.g., (Kumar et al. 2019c)), the relationship between cross-resistance patterns and auxin signaling protein-herbicide interaction is still in question. Synthetic auxin resistance mechanisms in weeds may include target site resistance in other IAA proteins and/or enhanced herbicide metabolic degradation. While reports of cross-resistance to synthetic auxins exist, a significant portion of dicamba-resistant kochia may still be able to be controlled by fluroxypyr in an area where dicamba resistance is present. Genetic and physiological details related to cross-resistance incidences in kochia are key contributors to understand cross-

resistance patterns, inform management decisions, and preserve the longevity and utility of synthetic auxin herbicides.

TABLES

Table 2.1. Parameters for Fluroxypyr and Dicamba dose response data in kochia populations Flur-R, 9425 and J01. Confirmation of resistance to fluroxypyr and lack of cross-resistance to dicamba in resistant kochia (*Bassia scoparia)* line Flur-R. Parameters of the fluroxypyr and dicamba dose responses rating percent survival for Flur-R, fluroxypyr/dicamba sensitive line J01-S and fluroxypyr sensitive/dicamba resistant line 9425 are described in Equation 3. Flur-R shows a significant resistance factor ratio (R/S) of 36 and 40 to 9425 and J01 respectively. Flur-R is 7 times more susceptible to dicamba than 9425. (*b,d*) lower and upper limits of regression parameters, respectively. (*LD_{50}*) The dose (g ae ha^{-1}) of either fluroxypyr or dicamba where 50% mortality occurs for each population. (*R/S)* The ratio of resistant LD_{50} to either susceptible LD_{50} and resultant p-values. The resistant population for the fluroxypyr dose response is Flur-R. The resistant population for the dicamba dose response is 9425.

	Herbicide									
	Fluroxypyr					Dicamba				
Line	*b* (± SE)	*d* (± SE)	LD_{50} (± SE)	R/S	P-value	*b* (± SE)	*d* (± SE)	LD_{50} (± SE)	R/S	P-value
	-----g ae ha^{-1}-----					-----g ae ha^{-1}-----				
Flur-R	7.3 (8.4)	94.5 (3.6)	720 (110.3)	36-40	<0.001	7.4 (5.2)	100.0 (4.9)	56 (8.5)	--	--
9425	8.5 (37.7)	100.0 (8.8)	20 (1.5)	--	--	85.1 (10.0)	91.7 (2.72)	415 (10.0)	6-7	<0.001
J01	3.1 (1.8)	100.0 (8.8)	18 (2.7)	--	--	9.3 (8.5)	100.0 (4.93)	64 (5.4)	--	--

FIGURES

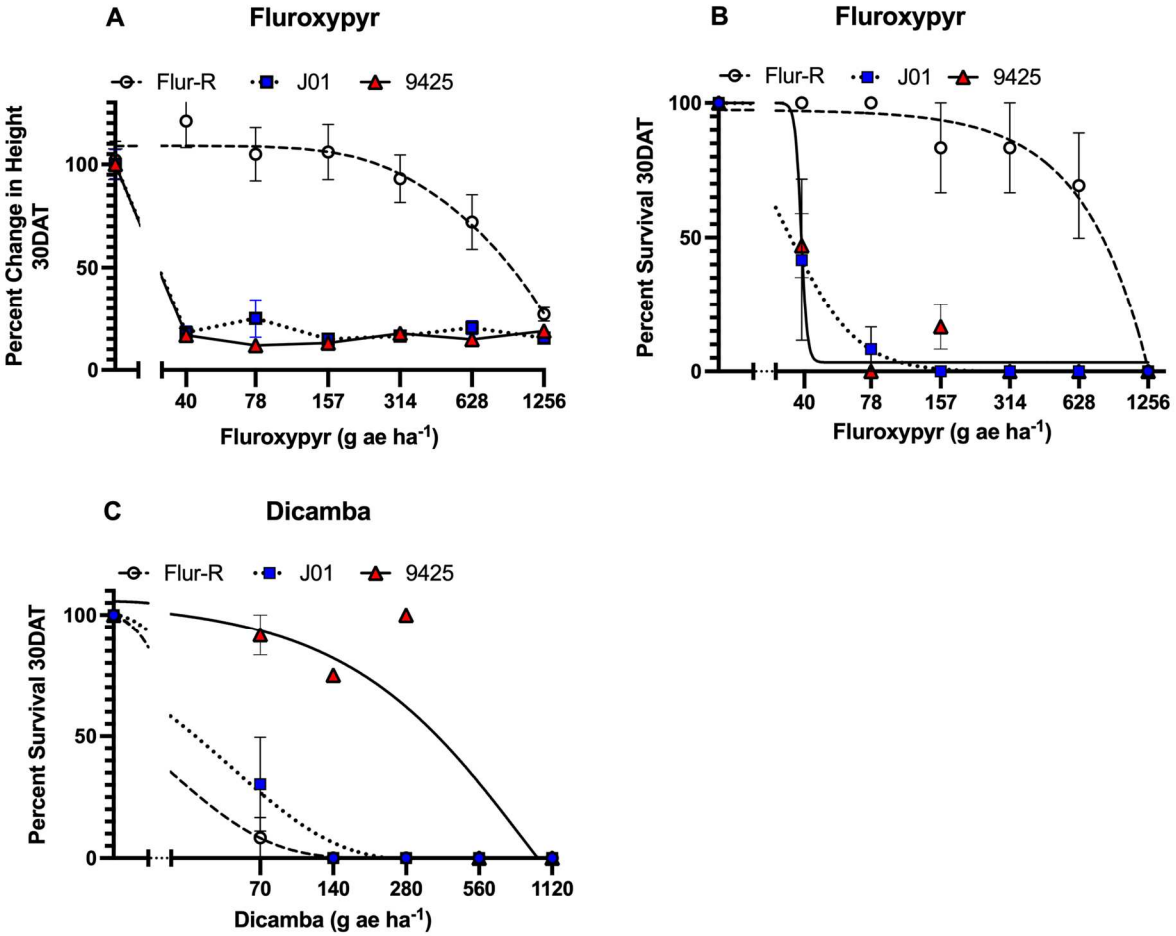

Figure 2.1. Dose response data for (A, B) fluroxypyr (no adjuvant) and (C) dicamba (+ 0.25% NIS) demonstrates fluroxypyr resistance and dicamba sensitivity in fluroxypyr resistant line Flur-R. X-axis is represented in a log10 scale. A. Percent change in height as a percent of the untreated control 30 days after treatment with fluroxypyr shows a 25% reduction in height in Flur-R at 628 g ae ha^{-1} (four times the label rate of 157 g ae ha^{-1}). B. Percent survival for Flur-R with greater than 70% survival to fluroxypyr at 628 g ae ha^{-1} (LD_{50} = 720, p= <0.001). The population 9425 is susceptible to fluroxypyr (LD_{50} = 20 g ae ha^{-1}, p <0.001). C. Flur-R is susceptible to dicamba (LD_{50} = 56 g ae ha^{-1}, p <0.001) and the known dicamba-resistant line, 9425, is resistant to dicamba up to 280 g ae ha^{-1}.

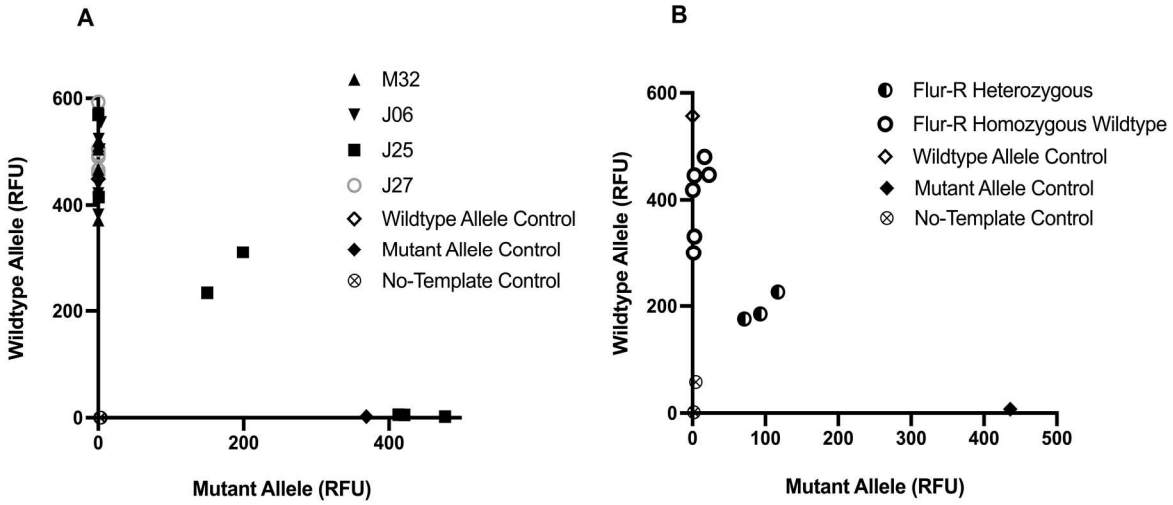

Figure 2.2. KASP assay shows occurrence of the *iaa16* dicamba resistance mutation in (A) four dicamba resistant populations from a field screen in eastern Colorado and (B) nine individuals from the Flur-R population. Each fluorophore sequence and primer correspond to either the *x* or *y* axis. Relative Fluorescence Units (RFU) are used to determine which alleles are present in a DNA sample and if they are present in a homozygous or heterozygous proportion. As a standard for the assay, two non-treated controls, one homozygous wildtype, and one homozygous mutant (kochia line 9425) were used. A. Populations M32, J06, and J27 show dicamba resistance at 280 g ae ha^{-1} and are homozygous for the *IAA16* wild type allele. One population, J25, shows two individuals with heterozygosity and three with homozygous-mutant alleles for *IAA16*. B. Three Flur-R individuals were heterozygous, with one mutant and one wildtype allele, and six individuals are homozygous for the wildtype allele.

REFERENCES

Aboul-Maaty NA-F, Oraby HA-S (2019) Extraction of high-quality genomic DNA from different plant orders applying a modified CTAB-based method. Bulletin of the National Research Centre 43:25

Beckie HJ, Gulden RH, Shaikh N, Johnson EN, Willenborg CJ, Brenzil CA, Shirriff SW, Lozinski C, Ford G (2015) Glyphosate-resistant kochia (*Kochia scoparia* L. Schrad.) in Saskatchewan and Manitoba. Can J Plant Sci 95:345-349

Busi R, Goggin DE, Heap IM, Horak MJ, Jugulam M, Masters RA, Napier RM, Riar DS, Satchivi NM, Torra J, Westra P, Wright TR (2018) Weed resistance to synthetic auxin herbicides. Pest Manag Sci 74:2265-2276

Cranston HJ, Kern AJ, Hackett JL, Miller EK, Maxwell BD, Dyer WE (2001) Dicamba resistance in kochia. Weed Sci 49:164-170

Foes MJ, Liu L, Vigue G, Stoller EW, Wax LM, Tranel PJ (1999) A kochia (*Kochia scoparia*) biotype resistant to triazine and ALS-inhibiting herbicides. Weed Sci 47:20-27

Friesen LF, Beckie HJ, Warwick SI, Van Acker RC (2009) The biology of Canadian weeds. 138. *Kochia scoparia* (L.) Schrad. Can J Plant Sci 89:141-167

Gaines TA, Barker AL, Patterson EL, Westra P, Westra EP, Wilson RG, Jha P, Kumar V, Kniss AR (2016) EPSPS gene copy number and whole-plant glyphosate resistance level in *Kochia scoparia*. PLoS One 11:e0168295

Gaines TA, Duke SO, Morran S, Rigon CAG, Tranel PJ, Kupper A, Dayan FE (2020) Mechanisms of evolved herbicide resistance. J Biol Chem 295:10307-10330

Heap IM (2021) International survey of herbicide resistant weeds. www.weedscience.org.

Knezevic SZ, Streibig JC, Ritz C (2007) Utilizing R software package for dose-response studies: the concept and data analysis. Weed Technol 21:840-848

Kumar V, Currie RS, Jha P, Stahlman PW (2019a) First report of kochia (*Bassia scoparia*) with cross-resistance to dicamba and fluroxypyr in western Kansas. Weed Technol 33:335-341

Kumar V, Jha P (2016) Differences in germination, growth, and fecundity characteristics of dicamba-fluroxypyr-resistant and susceptible *Kochia scoparia*. PLoS One 11:e0161533

Kumar V, Jha P, Jugulam M, Yadav R, Stahlman PW (2019b) Herbicide-resistant kochia (*Bassia scoparia*) in North America: a review. Weed Sci 67:4-15

Kumar V, Jha P, Reichard N (2014) Occurrence and characterization of kochia (*Kochia scoparia*) accessions with resistance to glyphosate in Montana. Weed Technol 28:122-130

Kumar V, Liu R, Boyer G, Stahlman PW (2019c) Confirmation of 2,4-D resistance and identification of multiple resistance in a Kansas Palmer amaranth (*Amaranthus palmeri*) population. Pest Manag Sci 75:2925-2933

LeClere S, Wu C, Westra P, Sammons RD (2018) Cross-resistance to dicamba, 2,4-D, and fluroxypyr in *Kochia scoparia* is endowed by a mutation in an AUX/IAA gene. Proc Natl Acad Sci U S A 115:E2911-E2920

Patterson EL, Fleming MB, Kessler KC, Nissen SJ, Gaines TA (2017) A KASP genotyping method to identify northern watermilfoil, Eurasian watermilfoil, and their interspecific hybrids. Frontiers in plant science 8:752

Pettinga DJ, Ou J, Patterson EL, Jugulam M, Westra P, Gaines TA (2018) Increased chalcone synthase (CHS) expression is associated with dicamba resistance in *Kochia scoparia*. Pest Manag Sci 74:2306-2315

Preston C, Belles DS, Westra PH, Nissen SJ, Ward SM (2009) Inheritance of resistance to the auxinic herbicide dicamba in kochia (*Kochia scoparia*). Weed Sci 57:43-47

Primiani MM, Cotterman JC, Saari LL (1990) Resistance of kochia (*Kochia scoparia*) to sulfonylurea and imidazolinone herbicides. Weed Technol 4:169-172

R-Team (2018) R: A language and environment for statistical computing. Vienna, Austria

Ryan G (1970) Resistance of common groundsel to simazine and atrazine. Weed Sci 18:614-616

Technologies LB (2020) KASP genotyping chemistry user guide and manual. Technologies LB.

Todd OE, Figueiredo MR, Morran S, Soni N, Preston C, Kubeš MF, Napier R, Gaines TA (2020) Synthetic auxin herbicides: finding the lock and key to weed resistance. Plant Sci 300:110631

Varanasi VK, Godar AS, Currie RS, Dille AJ, Thompson CR, Stahlman PW, Jugulam M (2015) Field-evolved resistance to four modes of action of herbicides in a single kochia (*Kochia scoparia* L. Schrad.) population. Pest Manag Sci 71:1207-12

Waite J, Thompson CR, Peterson DE, Currie RS, Olson BL, Stahlman PW, Al-Khatib K (2013) Differential kochia (*Kochia scoparia*) populations response to glyphosate. Weed Sci 61:193-200

Westra EP, Nissen SJ, Getts TJ, Westra P, Gaines TA (2019) Survey reveals frequency of multiple resistance to glyphosate and dicamba in kochia (*Bassia scoparia*). Weed Technol 33:664-672

Wu C, LeClere S, Liu K, Paciorek M, Perez□Jones A, Westra P, Sammons RD (2020) A dicamba resistance□endowing IAA16 mutation leads to significant vegetative growth defects and impaired competitiveness in kochia (*Bassia scoparia*). Pest Manag Sci 77:795-804

CHAPTER 3: RNA-SEQ TRANSCRIPTOME ANALYSIS OF FLUROXYPYR RESISTANT *BASSIA SCOPARIA* IMPLICATES ENHANCED METABOLIC DETOXIFICATION

1. Introduction:

Most synthetic auxin herbicides have been used in grass crops to control broadleaf weeds for more than 75 years (Busi et al. 2018). Though the exact mechanism of action of synthetic auxin herbicides is unknown, it is currently thought that these herbicides mimic the phytohormone indole-3-acetic-acid (IAA). IAA is a plant growth regulating molecule in the auxin hormone group most notably responsible for gravitropism and response to light stimuli (Zhao 2010). While auxins are involved in many cellular processes and signaling with other phytohormones, their function can be understood at the cellular level to primarily coordinate cell elongation (Perrot-Rechenmann 2010). In all plants, auxin homeostasis is tightly regulated through a complex suite of biosynthesis pathways, cellular transport, feedback inhibition, oxidation and conjugation (Rosquete et al. 2012). When the synthetic auxin herbicide fluroxypyr is applied to a plant the result is stem twisting, thickening and lack of new growth at the meristem.

When IAA reaches high levels in the plant, polar auxin carriers such as pin-formed (PIN), efflux transporters ATP Binding Cassettes (ABC class B) and auxin resistant- 1/like AUX1s influx carriers (AUX/LAX) help maintain IAA homeostasis (Cho and Cho 2013). Because fluroxypyr behaves like IAA, these auxin carriers are able to direct the flow of fluroxypyr throughout the plant. Fluroxypyr also mimics the function of IAA, in that it binds to Auxin Signaling F-Box 5, a member of the transport inhibitor response1/auxin signaling F-Box (TIR1/AFB) receptor family (Lee et al. 2014). Fluroxypyr acts to stabilize the complex composed of AFB5 and the auxin dependent transcriptional regulator Indole-3-Acetic Acid

Inducible (Aux/IAA) proteins. Upon creation of this coreceptor-ligand complex Aux/IAA is ubiquitinated and degraded, and no longer negatively regulate Auxin Response Factors (ARF) seated on the Auxin Response Element (AuxRE) in auxin mediated gene promotors (Teale et al. 2006).

In Arabidopsis, treating plants with IAA or synthetic auxin 2,4-D showed expression of early response genes such as Aux/IAAs and small auxin-up RNAs (SAURs). Other auxin induced genes include 1-amincyclopropane-1 synthase (ACS), the first committed step in ethylene production, and GH3, an auxin homeostasis gene. These genes are all transcribed within minutes of high auxin perception (Paponov et al. 2008; Guilfoyle 1999). Many other phytohormone responses are also regulated by auxin perception, such as cytokinin oxidase (CXK6), brassinosteroid biosynthesis gene BAS1, and several gibberellin related genes suggesting that the relationship between these hormones and auxin response is complex (Paponov et al. 2008).

Herbicide resistance is categorized as either target site or non-target site. Target site resistance is characterized by a change (either in conformation or in expression) in a protein that most often decreases binding affinity for the herbicide or affects its interaction with the herbicide (Murphy and Tranel 2019). In synthetic auxin research, LeClere et al. (2018) reports resistance to synthetic auxin herbicide dicamba through the target-site mutation Gly127Asn in Aux/IAA16 which affects the formation of the Aux/IAA-synthetic auxin complex. More recently, Figueiredo et al. (2021) characterized a 27-nucleotide deletion in the gene encoding Aux/IAA2 which confers dicamba resistance in *Sisymbrium orientale;* the deletion also affects formation of the co-receptor/ligand complex. Non-target site resistance is broadly recognized as all other methods unrelated to target site resistance (Delye 2013) and is usually exemplified by metabolic

detoxification of an herbicide, sequestration or a variant in a metabolism catalyzing enzyme which may have a downstream effect by reducing the efficacy of the herbicide. Reports in *Echinochloa* species attribute resistance to quinclorac, a selective synthetic auxin that is effective on grasses, to reduced ethylene production related to ACS and 1-aminocyclopropane-1-carboxylic acid oxidase (ACO) which are processes downstream of auxin induced gene expression (Chayapakdee et al. 2020; Gao et al. 2018). Other reports in *Echinochloa* have attributed resistance responses to cyanide detoxification following ethylene production as a result of beta-cyanoalanine synthase activity (β −CAS) (Gao et al. 2017; Zia Ul Haq et al. 2020). Reduced translocation of 2,4-D via auxin transport proteins was reported by Goggin et al. (2019) in *Raphanus raphanistrum,* and Figueiredo et al. (2018) identified cytochrome P450 involvement in metabolic resistance to 2,4-D in *Amaranthus tuberculatus*. Our objectives in this study were to identify potential candidate genes that may contribute to fluroxypyr resistance in the weed *Bassia scoparia*. Using a de novo genome assembly of *Bassia scoparia* (Patterson et al. 2019), we aligned transcripts using HISAT2 and analyzed the data using differential expression analysis from DESeq2 in R and variant analysis with Platypus and SNPeff. The findings from the differential expression analysis together with differential metabolism data show that fluroxypyr-ester can be converted to fluroxypyr-acid and subsequently converted to metabolites faster in the resistant line, Flur-R, than in the susceptible line J01-S. In addition, it is possible that the transporters, cytochrome P450s and UDP-glucosyl transferases found to be constitutively expressed as well as upregulated after fluroxypyr treatment are contributing to metabolic detoxification of fluroxypyr in Flur-R.

2. Materials and Methods

2.1 Plant material and treatment

In a 2014 field survey (Westra et al. 2019), Flur-R was subjected to single dose selection to fluroxypyr for one generation. Survivors at both 157 g ae ha^{-1} and 314 g ae ha^{-1} fluroxypyr in subsequent generations were bulk pollinated in a greenhouse with a 16 h photoperiod at 25 C. Seeds were sewn into plug flats filled with SunGro potting mix. When plants were 5-7 cm tall, a fluroxypyr dose response was (Starane Ultra, Dow Agrosciences, Indianapolis, IN) made with a Devries Generation 4 Research Track Sprayer equipped with a TeeJet 8002EV8 nozzle calibrated to 187 L ha^{-1} output. An inbred dicamba resistant line with a mutation in the Aux/IAA16 gene conferring dicamba resistance from Colorado State University (9425-S) and a fluroxypyr susceptible field population from the 2014 eastern Colorado field study (J01-S) were included in these experiments as susceptible checks. Flur-R is 36-40 times more resistant to fluroxypyr than J01-S and 9425-S respectively (pvalue = <0.001) based on the rate required to reduce growth of each population by 50% (GR_{50}) calculated in R. A detailed response to fluroxypyr is previously described in previous work (Todd, O. 2021). Kochia seeds from a fluroxypyr resistant line (Flur-R) surviving up to 314 g ae ha^{-1} fluroxypyr from the previous dose response were allowed to cross pollinate, and seed was harvested. Seeds from Flur-R and two susceptible checks (9425-S and J01-S) were sewn into plug flats filled with SunGro potting mix and grown on a light shelf under 700 ME of light at 25 C. When the plants reached 7-10 cm tall, six of the most uniform seedlings from each line were treated as follows: First, all plants were sprayed with water and 0.01 g meristem tissue was harvested for the untreated RNA-sequencing timepoint. Tissue was flash frozen in liquid nitrogen. The same individuals were treated again with 157 g ae ha^{-1} fluroxypyr, the labeled rate to control kochia. Approximately 0.01 g of meristem tissue was harvested at 3 and 10 hours after treatment (h) for the remaining two RNA-sequencing timepoints. Herbicide and water applications were made with a Devries Generation 4

Research Track Sprayer equipped with a TeeJet 8002EV8 nozzle. All plants were in the vegetative stage, except for one Flur-R individual and three J01-S individuals, which were in the early flowering stage at the time of tissue harvest.

2.2 C14-absorption, translocation and metabolism

Bassia scoparia seeds from the fluroxypyr resistant line (Flur-R) and the susceptible check (J01-S) were sown into plug flats filled with SunGro potting mix and grown on a light shelf under 700 ME of light at 25 C. When the plants reached 3-4 cm tall, seedlings from each line were root washed and transplanted into a 25 mL Eppendorf tube filled with silica sand and fertilized with three granules of Osmocote. When plants were 4-5 cm tall and had recovered from transplanting the third and fourth youngest leaf were marked and covered with aluminum foil, so as not to destroy the meristem. Plants were treated with 157 g ae ha^{-1} non-radioactive fluroxypyr using a Devries Generation 4 Research Track Sprayer equipped with a TeeJet 8002EV8 nozzle.

2.3 C14-absorption and translocation

Immediately following non-radioactive fluroxypyr application, 24 plants each of Flur-R and J01-S were treated with a mix of 400 µL cold fluroxypyr and 8,000,000 DPM [^{14}C]-Fluroxypyr to mimic the amount of product the rest of the plant received. A total of 5 µL was applied to each of the two designated treated leaves after removing the aluminum foil. Each plant received a total of 200,000 disintegrations per minute (DPM) (3.33 kBq). After the each timepoint, (6, 12, 24, 48, 96 and 192 h) the treated leaves were removed and washed in 5 mL 90% water, 10% methanol, 0.5% non-ionic surfactant. The 5 mL was mixed with 10 mL scintillation cocktail (Ecoscint XR) and radioactivity was measured in a liquid scintillation

counter. Roots were washed with 5 mL water and mixed with the remaining silica sand mixture. After vortexing, 1 mL of root wash was mixed with 10 mL scintillation cocktail and radioactivity was measured. Four repetitions per timepoint were harvested, and the plant sections were separated as follows: Above treated leaves, treated leaves, below treated leaves and root biomass. Each separate plant part was dried and oxidized using a biological oxidizer. Radioactivity was quantified with a liquid scintillation counter. One individual per timepoint was left in-tact, dried and pressed to a film and imaged with a phosphor imager (Typhoon Trio, GE Healthcare). Dried plants were separated and oxidized in the same manner as above after imaging. The experiment was repeated. Percent absorption and translocation was calculated as follows from (Figueiredo et al. 2018):

$$\%H_{\text{abs}} = [(^{14}\text{C ot}) / (^{14}\text{C ot} + {}^{14}\text{C wl})] \times 100$$

$$\%H_{\text{tr}} = 100 - [(^{14}\text{C al}) / (^{14}\text{C al} + {}^{14}\text{C ot}) \times 100]$$

Where "$\%H_{\text{abs}}$" is percent absorption of [^{14}C]-Fluroxypyr ester, "^{14}C ot" is the sum DPM from the oxidation of all plant parts and "^{14}C ot + ^{14}C wl" is the sum DPM from the oxidation of all plant parts and counts washed from the treated leaf. For herbicide translocation studies, "$\%H_{\text{tr}}$" is percent translocation of [^{14}C]-Fluroxypyr ester out of the treated leaf through the rest of the plant, "^{14}C al" is the DPM [^{14}C]-Fluroxypyr ester counted in the treated leaf.

2.4 C14-metabolism

Immediately following cold fluroxypyr application, plants were treated as described above with a mix of ~1,500,000 DPM (~25 kBq). Four repetitions per timepoint of the whole plant was harvested and flash frozen in liquid nitrogen. The washed treated leaves were placed back with the remaining whole-plant tissue before freezing. Whole plants were then finely

ground in a glass test tube with liquid nitrogen and a glass rod. Five mL extraction solution (90% water, 9% acetonitrile, 1% acetic acid) was added to the tubes and samples were shaken for 30 minutes. All of the liquid from the test tube was added to a 0.45 µm filter tube which was rinsed with an additional 5 mL extraction buffer and centrifuged at ~2600 x g for 10 minutes to separate liquid from ground plant material. A vacuum manifold was used with C-18 columns preconditioned with 1 mL 100% acetonitrile (Waters Co., Sep-Pak Plus). After running all of the extraction buffer from the filter tubes through individual cartridges, 5 mL 100% acetonitrile was run through the same cartridges and collected in new tubes. Samples were evaporated overnight and brought back up in 500 µL solvent A consisting of 10% acetonitrile and 1% formic acid. Each sample was filtered through 25 mm nylon filters (Nalgene) into an injection vial with a 500 µL insert. Injection volume for High Pressure Liquid Chromatography (HPLC) (Hitachi Instruments, Inc., San Jose, CA) was 200 µL. The column (C18 4.6 mm by 150 mm column Column, Zorbax Eclipse XDB-C18, Agilent Technologies, Santa Clara, CA, USA) was attached to a radio-detector (FlowStar LB 513, Berthold Technologies GmbH & Co.) with a flow cell YG-150-U5D solid cell YG-Scintillator (150 µL). Standards showed retention time for [^{14}C]-fluroxypyr ester was 9.8 minutes. Saponification of the [^{14}C]-fluroxypyr to create a [^{14}C]-fluroxypyr acid standard showed a retention time of 2.8 minutes.

2.5 RNA extraction, sequencing and quantification

The RNA-sequencing experiment was conducted first by extracting total RNA following the protocols of the QIAGEN RNeasy plant mini kit in six batches containing two individuals of each line to minimize batch effects. The RNeasy kit was used to extract RNA from the top three fully expanded apical meristem leaves of all three lines of 5-7 cm tall kochia at 0, 3 and 10 h

after 157 g ai ha^{-1} fluroxypyr treatment. Final elution volume was 30 µL. Total RNA samples were diluted to fit the 500-10,000 pg μL^{-1} range to quality check them using an Agilent ScreenTape. Samples which had a RIN score above 6 were submitted to BGI Technologies for quality check following their sample submission guidelines. Following quality check by BGI, 30 samples were used for sequencing. From the total RNA, mRNA enrichment was performed by rRNA depletion or oligo dT selection. Reverse transcription of the mRNA was performed with random N6 primers, followed by end repair, and A-tail and adapter ligation to the fragments. After PCR amplification, single strand separation and single-strand circularization was the final step to sequence paired end 100 base pair fragments with the BGISEQ sequencing platform. In total, 2.8 billion reads were produced, resulting in 92-97 million 100 bp reads per sample.

2.6 Differential expression and variant analysis

Individual fasta files were uploaded to the remote research computing resource SUMMIT (Jonathon Anderson 2017) and files were quality checked with FastQC (version 0.11.9 (Bioinformatics)). Adapters were ligated by BGI Bioinformatics company after sequencing and quality check. Reads were aligned to the *Bassia scoparia* coding sequence version 2 (Patterson et al. 2019) using HISAT2 (version 2.2.0 (Kim et al. 2019)). Differential expression was conducted with resultant reads for each gene feature using the DESeq2 package (version 1.28.1) in the statistical software R (version 4.0.2). Reads were transformed to logarithmic fold change log2 and compared across biological replicates for each population. For each population, the untreated condition was compared to either the 3 or 10 hours after treatment timepoint to determine expression. Mean normalized counts per gene, an adjusted pvalue of < 0.05 and log2 fold change

> 0.5 were the pre-filtering parameters used by DESeq2 for optimal significant genes below the false discovery rate (FDR) of <0.05.

Sorted and indexed bam files were run through the variant calling software Platypus (version 0.8.1 (Rimmer et al. 2014)) to detect single and mono-nucleotide polymorphisms, short and long indels, as well as chromosome rearrangement. The resultant output file was used with the software SnpEff (version 4.3 (Cingolani et al. 2012)) to annotate the variants called from Platypus and give effect predictions. Specific proteins were targeted for variant analysis by checking all proteins annotated as cytochrome P450s against a merged variant file for all individuals of each population. Presence or absence of variants were validated with Integrative Genomics Viewer (IGV) (Robinson et al. 2017).

3. Results

3.1 Absorption, translocation and metabolism

We investigated differences in fluroxypyr absorption and translocation between fluroxypyr-resistant line Flur-R and fluroxypyr-susceptible J01-S. For each of the two lines, two meristem leaves per individual were treated with [^{14}C]-fluroxypyr ester. Differential absorption and translocation were investigated by partitioning all individuals into four plant sections. Radioactivity was counted in each section using biological oxidation and liquid scintillation counting. Maximum percent absorption was determined using a method described by Kniss et al. (2011) in R. Maximum percent absorption of ~3.33 kBq [^{14}C]-fluroxypyr ester for Flur-R was 91.99% ($\pm$3.14), and for J01-S was 85% ($\pm$3.13). No significant differences in maximum absorption between Flur-R and J01-S were found (pvalue = 0.155) (Figure 3.1A). The time (hours) after treatment in which 90% of the herbicide is absorbed based on the model in R was

not statistically between 12 h (± 2.15) for Flur-R, and 9.7 h (± 2.34) for J01-S (pvalue = 0.47). Results from differential translocation of [^{14}C]-fluroxypyr ester between Flur-R and J01-S showed no differences in translocation from the treated leaf to the other plant parts for each line (Figure 3.1A).

The individuals used for [^{14}C]-fluroxypyr metabolism studies were treated as described above. However, whole plant metabolites were extracted, and plants were not partitioned into sections. Analysis of [^{14}C]-fluroxypyr metabolites was conducted using an HPLC equipped with a C18 column. [^{14}C]-fluroxypyr ester and acid standards were analyzed using an HPLC to determine retention time. Analysis of the proportion of [^{14}C]-fluroxypyr ester in each population showed a significant difference at 12 h where the proportion of [^{14}C]-fluroxypyr ester was lower in Flur-R than J01-S, showing rapid conversion from the [^{14}C]-fluroxypyr ester to [^{14}C]-fluroxypyr acid or other [^{14}C]-fluroxypyr metabolites. In Flur-R, the proportionally higher amount of [^{14}C]-fluroxypyr acid at 12 h was significantly reduced at 48 h, and suggests that Flur-R converted the [^{14}C]-fluroxypyr ester to its acid form faster than J01-S, and subsequently converted [^{14}C]-fluroxypyr acid to other metabolites at the later timepoints (Figure 3.2). At 96 h and 192 h, the proportion of metabolites 4 and 2 were in higher Flur-R, respectively (Table 3.1). This suggests that formation of metabolites 2 and 4 is catalyzed by a process that is more active in Flur-R and may play a role in reducing phytotoxic [^{14}C]-fluroxypyr acid.

3.2 Differential expression analysis

To analyze the transcriptome of Flur-R, we sequenced RNA from 4 plants each of fluroxypyr resistant Flur-R, and two fluroxypyr susceptible lines J01-S and 9425-S. BGI Seq was used to obtain between 91 and 95,000,000 clean reads per sample (BGI Bioinformatics, San Jose,

CA). Q20 scores were between 96 – 98%. Alignment was made to the *Bassia scoparia* genome version 2 (Patterson et al. 2019) using HISAT2 (version 2.1.0), and alignment ranged between 59 - 63% for all individuals. Percent unmapped reads ranged between 46 – 51%, and percent uniquely mapped genes ranged from 43 – 48%. Approximately 4% of reads were multi-mapped (Table 2). Following alignment and differential expression with DESeq2, a Wald test was used to obtain pvalues, which were adjusted using the Benjamini-Hochberg method. Filtering parameters were for the adjusted pvalue = < 0.05 and log2 fold change > 0.5.The false discovery rate (FDR) was < 0.05. We identified 439 genes that had higher expression in Flur-R at the untreated timepoint compared to untreated J01-S individuals and 829 genes that had higher expression in Flur-R at the untreated timepoint compared to untreated 9425-S individuals. There were 231 genes that had higher expression in Flur-R at the untreated timepoint compared to both susceptible populations at the untreated timepoint (Figure 3.3). Because we identified differential metabolic degradation in Flur-R, we explored the hypothesis that genes related to herbicide metabolism may have differential regulation or be highly expressed at the untreated timepoint in Flur-R. Of these 231 highly expressed genes at the untreated timepoint, there were six ABC transporters of both class B and G, including genes homologous to ABCG31-like (Bs.00g217020.m01), ABCB28 (Bs.00g454440.m01), ABCG28 (Bs.00g282300.m01), two isoforms of ABCG34 (Bs.00g184080.m01, Bs.00g184080.m02) and ABCG29 (Bs.00g251290.m01) there were five CYP450s between the CYP71 family (CYP82D47 [Bs.00g486870.m01], CYP96A15 [Bs.00g541440.m01], CYP71D10/11 [Bs.00g051830.m01], Ent-Kaurene Oxidase [Bs.00g184110.m01],) and the CYP85 family (CYP90C1/D1 [Bs.00g245700.m01]), and four glucosyltransferases (UDP-glucosyltransferase 73B2 [Bs.00g142060.m01], two isoforms of UDP-glucuronosyl/UDP-glucosyltransferase 89A2-like

[Bs.00g480980.m01 and Bs.00g480980.m03], UDP-glycosyltransferase 87A1 [Bs.00g061050.m01]) (Table 3.3).

When the 3 and 10 h timepoints were contrasted with the untreated timepoint within each line, Flur-R, J01-S and 9425-S showed 188 and 300 common fluroxypyr upregulated genes for the 3 and 10 h timepoints respectively (Figure 3.4). Of those shared upregulated genes, auxin responsive genes such as GH3.2 (Bs.00g477580.m01), Ethylene Responsive Transcription Factors, Small Auxin-Up RNAs (SAURs), Aux/IAAs, and ACS (Bs.00g478760.m01) all showed increased transcription at 3 and 10 h after fluroxypyr treatment (Figure 3.5). The GH3 protein, Ethylene Responsive Transcription Factors and ACS were in the top 20 genes with the highest fold change through the 3 h and 10 h timepoints in Flur-R, 9425-S and J01-S (Tables 3.4, 3.6, 3.8). Two isoforms of the IAA cellular transporter PIN were upregulated in 9425-S at 10h after treatment (Bs.00g190770.m01 and Bs.00g190770.m02), but the response in Flur-R and J01-S did not meet the filtering criteria and therefor the response was not statistically different following fluroxypyr treatment (Figure 3.6). Aux/LAX transcription did not appear to be statistically responsive for all three lines when treated with fluroxypyr at 3 and 10 h (Figure 3.6). There were 288 uniquely upregulated genes at 3 h in the Flur-R line and 303 at 10 h (Figure 3.4). Some unique auxin-induced transcripts such as SAURs and ARF11 were upregulated in Flur-R, but six additional ABC transporters of class G, two ABC transporters of class C, one ABC transporter of class A, six additional UDP-glucosyltransferases and three sugar transporters were upregulated following fluroxypyr treatment (data not shown). CYP81B2 (Bs.00g431990.m01), CYP82D47 and CYP71A9 (Bs.00g241110.m01) were induced by fluroxypyr treatment, as well as 4 Glutathione S-Transferases at 3 h and 10 h compared to the untreated timepoint.

When the 3 and 10 h timepoints were contrasted with the untreated timepoint within each line, Flur-R, J01-S and 9425-S showed 104 and 718 common fluroxypyr downregulated genes for the 3 and 10 h timepoints respectively (Figure 3.4). Twelve of these shared genes were related to photosystem I and II at 10 h. Key proteins related to photosynthetic electron transport such as Chlorophyll A-B Binding protein (Bs.00g240870.m01 and Bs.00g240870.m02) and ATP Synthase (Bs.00g432500.m01) are downregulated in all three lines and are present in the top 20 downregulated genes for all three lines (Tables 3.5, 3.7, 3.9). Uniquely downregulated in both susceptible lines, and among the genes with the highest downregulation are two Early Light Induced Protein-1 genes which are chlorophyll biosynthesis inhibitors (Bs.00g421070.m01 and Bs.00g420960.m01). Additional downregulated proteins of interest unique to the susceptible lines include four cellulose synthase genes (Bs.00g015170.m01, Bs.00g015170.m02, Bs.00g056700.m01 and Bs.00g260720.m01). Genes uniquely downregulated at 10 h in Flur-R included two additional photosystem II subunit genes (Bs.00g059220.m01 and Bs.00g338570.m01), several synthases such as Terpene Synthase (Bs.00g074880.m01), Polyprenyl Synthatase (Bs.00g449610.m01), Strictosidine Synthase (Bs.00g057800.m01), Phosphomethylpyrimidine synthase (Bs.00g253210.m01), Aminodeoxychorismate (ADC) synthase (Bs.00g135570.m01) and ABA biosynthesis gene NCED2 (Bs.00g024060.m01).

3.3 Variant analysis

Of the 147 genes annotated as cytochrome P450s in the kochia genome, none contained a unique polymorphism where all four Flur-R individuals showed a variant that was unique to Flur-R and not found in the two S lines, using manual inspection in IGV. There were 37 genes annotated as having an Aux/IAA domain or function, and 21 genes with an ARF domain or

function. Of these genes, three contained a sequence variant conferring an amino acid change or a deletion. ARF19/7, one of five transcriptional activators in the ARF family, had two nonsynonymous variants (Gly446Ser; Leu486Ile) and two deletions of one codon that are all predicted to have no significant effect on fluroxypyr binding due to their position in the variable middle region described by Ulmasov et al. (1999) (Figure 3.7). A protein annotated as ARF3 also known as ETTIN (ETT) showed one nonsynonymous homozygous variant (Leu293Ser), where three susceptible individuals were heterozygous for the variant found in Flur-R, one was homozygous, and the remaining were wildtype. IAA4 showed one nonsynonymous variant (Glu52Arg) in an non-conserved region 6-10 bases N terminal of Domain II as described by Ramos et al. (2001) (Figure 3.7). Because the region is which the variant is located is not conserved, it is not likely to contribute to the resistance response. We also determined there were no unique variants in any proteins annotated as AFB or TIR1, specifically no mutations in the 18 LRR rich C terminus where Aux/IAA and auxin bind (Villalobos et al. 2012).

4. Discussion and conclusion

Kochia's response to fluroxypyr follows patterns of auxin regulated gene expression studies in Arabidopsis in fluroxypyr resistant line Flur-R and two susceptible lines 9425-S and J01-S (Goda et al. 2004). Expression of auxin response genes suggests that fluroxypyr is being perceived similarly by all three lines and supports our findings that there were no variants in the key target-site proteins that interact with fluroxypyr or IAA (mainly ARF and Aux/IAA) in the auxin signaling pathway. Although we did find a homozygous variant in ARF3, the region boundaries of ARF3 are unlike most other ARFs in that it does not contain Domain III/IV, two key domains for interaction with Aux/IAA proteins relating to auxin gene expression. ARF3

does function in some auxin related pathways (reviewed by Liu et al. (2014)) but the protein has been described to function as a repressor of several proteins causing inhibition of cytokinin activity, a plant hormone which often partners with IAA (Zhang et al. 2018). While we cannot rule out that this variant in ARF3 does not contribute directly to fluroxypyr resistance or affect cytokinin levels in the plant, due to ARF3's described function there is almost no likelihood of ARF3 being a target site for fluroxypyr and is therefore unlikely to cause target site resistance. Additionally, if variants were found which affected synthetic auxin perception or binding, such as the Aux/IAA16 Gly127Asn mutation described by LeClere et al. (2018), the expected auxin response gene expression would likely not be induced as shown by Pettinga et al. (2018).

The translocation data suggest that fluroxypyr, being primarily in its acid form based on the 6 h metabolism results, is moving throughout the plant as the phloem mobile herbicide it is described to be (Schober et al. 1986). IAA transporter transcripts for two PIN isoforms are upregulated in the susceptible lines 9425-S and J01-S when treated with fluroxypyr, suggesting that PIN can transport fluroxypyr in a similar manner to that of IAA. Based on the insignificant differences between translocation in Flur-R and J01-S, the two identified PIN transporters are not moving phytotoxic fluroxypyr acid throughout the resistant or susceptible plants at a significantly different rate. However, other transporters such as ATP Binding Cassette (ABC) class B can move multiple substrates and have been shown to transport xenobiotics; some members of this large protein family serve as auxin transporters (Cho and Cho 2013). ABC transporters from both class B and G are upregulated in Flur-R following fluroxypyr treatment, none of which have been directly implicated in herbicide resistance, but several class G transporters are involved in auxin homeostasis and other phytohormone transport, cellular detoxification of heavy metals and pathogen resistance (Gräfe and Schmitt 2021; Dhara and

Raichaudhuri 2021). The functional suite of ABCG transporters in kochia is yet to be fully described, though cellular export of fluroxypyr conjugates is not too far outside the current described roles.

In Flur-R, ABA biosynthesis gene NCED2 decreased over the course of the RNA-seq experiment contrasting the results from the two susceptible lines, while NCED6 had an increased response at 3 h (Figure 3.4). The implications of this decreased expression in the resistance response are currently unknown, though a small body of literature suggests an increased level of response from NCED following synthetic auxin application (Kraft et al. 2007; McCauley et al. 2020; Raghavan et al. 2005). Among these ABA related downregulated genes, seven subunits of Photosystem I and four subunits of Photosystem II are downregulated in all three lines following fluroxypyr application suggesting that this herbicide may affect light energy harvesting as part of its mechanism of action.

Of the five CYP450s found to be constitutively more highly expressed in Flur-R compared to either J01-S or 9425-S, CYP71D10/11 has been implicated in metabolic herbicide resistance to fenoxaprop-p-ethyl (Bai et al. 2020). Other CYP450s in the CYP71 family have been described as shikimate and shikimate intermediate modifiers (Jun et al. 2015), including Ent-Kaurene Oxidase (CYP701 subfamily) which functions in gibberellin biosynthesis and whose overexpression has been shown to cause partial resistance to plant growth retardant uniconazole-P (Miyazaki et al. 2011). Treatment induced CYP81B2 (Bs.00g431990.m01) was shown in transgenic tobacco to metabolize phenylurea herbicide chlortoluron after the application of synthetic auxin 2,4-D, and was also characterized to be involved in phenylpropanoid biosynthesis and secondary metabolite biosynthesis (Ohkawa et al. 1999). The other two treatment induced CYP450s in Flur-R, CYP82D47 and CYP71A9-like have no

described role in herbicide resistance, however, there are a significant number of CYP450s involved in herbicide metabolism in the CYP71 family, in which they both belong (Siminszky et al. 1999; Gion et al. 2014; Xiang et al. 2006).

The other constitutively expressed CYP450 in the Flur-R line, CYP90C1/D1, belongs to the CYP85 family which is implicated in modification of cyclic terpenes and sterols in the brassinosteroid, abscisic acid and gibberellin biosynthesis (Jun et al. 2015; Ohnishi et al. 2006; Ohnishi et al. 2012). It is not unusual for CYP450s to be multifunctional (Bernhardt 2006), and their function can often be attributed to the selectivity of some herbicides, extensively reviewed by Dimaano and Iwakami (2021).

Given the high untreated and treatment-induced expression of Glutathione S-Transferases (GST) and UDP-Glucosyl Transferases, formation of tripeptide GST or sugar conjugates catalyzed by these enzymes is possible following CYP450 activity via *O*-glucosylation (Ludwig-Müller 2011). GSTs and UDP-Glucosyl Transferases can glycosylate plant hormones and xenobiotics to influence bioactivity, transport, solubility and can be pumped out of the cell via ABC transporters (Li et al. 2001; Moons 2005).

We investigated fluroxypyr resistance using herbicide physiology experiments as well as RNA-sequencing and identified metabolic detoxification as a plausible explanation of fluroxypyr resistance in kochia line Flur-R. Two of the four metabolites in the HPLC metabolite profile are accounted for, having been reported by the Environmental Protection Agency (EPA 2010). The action of conjugation by GST or UDP-Glucosyl Transferases may explain one of the two remaining undescribed metabolites presented in the HPLC data, which were rapidly converted from fluroxypyr acid throughout the time course in Flur-R. Subsequent sequestration of the non-phytotoxic herbicide via ABC transporter may also play a role in the resistance response, though

more work is needed to fully elucidate the metabolic response following fluroxypyr application in Flur-R.

5. Future work

Future work elucidating the fluroxypyr resistance mechanism involves *in vitro* and *in vivo* testing of the four candidate Glutathione S-Transferases, eight UDP Glucosyl Transferases, and eight Cytochrome P450s. Metabolite identification is crucial next step to determine the metabolic path of the fluroxypyr molecule. Identifying the two unknown fluroxypyr metabolites will allow us to identify the enzyme responsible for the catalyzing the molecular transformation and hone our testing on one or two groups of metabolic enzymes. Metabolic information paired with ongoing inheritance studies will be a strong contribution to the understanding of synthetic auxin resistance and elucidation of fluroxypyr resistance in this population of kochia

TABLES

Table 3.1.Mean count estimates for [^{14}C]-Fluroxypyr ester, [^{14}C]-Fluroxypyr acid, and four [^{14}C]-metabolites in Flur-R and J01-S fluroxypyr resistant kochia population Flur-R and fluroxypyr susceptible population J01-S. Mean counts are area under the peak curve calculated in RadioStar for each of the six peaks and six timepoints identified as a result of the HPLC data. Pvalue represents statistical difference for α= 0.05 of a non-directional hypothesis test between Flur-R and J01-S for each timepoint for each HPLC peak.

Time (hr)	Ester			Acid			Metabolite 1			Metabolite 2			Metabolite 3			Metabolite 4		
	Mean counts (±SE)			Mean counts (±SE)			Mean counts (±SE)			Mean counts (±SE)			Mean counts (±SE)			Mean counts (±SE)		
	Flur-R	J01-S	P value	Flur-R	J01-S	P value	Flur-R	J01-S	P value	Flur-R	J01-S	P value	Flur-R	J01-S	P value	Flur-R	J01-S	P value
6	5.90 (3.60)	13.62 (2.54)	*ns*	43.55 (4.97)	39.60 (3.52)	*ns*	1.60 (4.67)	3.60 (3.31)	*ns*	8.70 (3.85)	8.50 (2.72)	*ns*	7.70 (3.30)	0.00 (2.33)	*ns*	3.20 (1.04)	1.13 (0.74)	*ns*
12	8.90 (2.94)	23.35 (2.54)	0.00 ***	33.90 (4.06)	21.70 (3.52)	0.03 *	2.97 (3.82)	9.07 (3.31)	*ns*	6.53 (3.14)	4.90 (2.72)	*ns*	9.93 (2.69)	3.62 (2.33)	*ns*	3.50 (0.85)	0.68 (0.74)	0.02 *
24	11.05 (2.54)	15.53 (2.94)	*ns*	25.23 (3.52)	34.37 (4.06)	*ns*	3.77 (3.31)	7.03 (3.82)	*ns*	10.12 (2.72)	6.20 (3.14)	*ns*	9.95 (2.33)	9.40 (2.69)	*ns*	3.05 (0.74)	1.27 (0.85)	*ns*
48	3.65 (2.54)	5.60 (3.60)	*ns*	13.18 (3.52)	26.75 (4.9)	0.03 *	11.97 (3.31)	12.20 (4.67)	*ns*	13.03 (2.72)	5.60 (3.85)	*ns*	12.82 (2.33)	20.15 (3.30)	*ns*	3.33 (0.74)	1.95 (1.04)	*ns*
96	3.33 (2.54)	1.87 (2.94)	*ns*	10.18 (3.52)	9.40 (4.06)	*ns*	22.57 (3.31)	25.23 (3.82)	*ns*	15.47 (2.72)	7.20 (3.14)	*ns*	13.03 (2.33)	19.27 (2.69)	*ns*	4.63 (0.74)	0.33 (0.85)	0.00 ***
192	1.60 (2.54)	2.90 (2.94)	*ns*	7.95 (3.52)	11.17 (4.06)	*ns*	21.73 (3.31)	24.83 (3.82)	*ns*	20.98 (2.72)	6.17 (3.14)	0.00 **	14.45 (2.33)	21.67 (2.69)	0.05 *	1.85 (0.74)	1.00 (0.85)	*ns*

Table 3.2
Total read counts, total unmapped reads, uniquely mapped reads and multimapped reads following BGI-seq on fluroxypyr resistant kochia population Flur-R and two fluroxypyr susceptible populations, J01-S and 9425-S. Three treatments in the RNA-seq study included untreated, "UNT"; 3 hours after treatment with fluroxypyr, "3HAT"; and 10 hours after treatment with fluroxypyr, "10HAT". Results are taken from the summary text resulting from an alignment of transcripts by HISAT2. Total reads are calculated from the number of pairs given in the summary text. Uniquely mapped reads are calculated from the number of neither concordant nor discordant aligning pairs given in the summary text. Multimapped reads are calculated from the number of concordant pairs that aligned more than once to a given area, given in the summary text.

Sample ID	Rep Number	Total Reads	Unmapped Reads	% Unmapped Reads	Uniquely Mapped Reads	% Uniquely Mapped Reads	Multimapped Reads	% Multimapped Reads	% Alignment
Flur-R-UNT	1	97689782	45858498	46.94	46882608	47.99	4481566	4.59	63.75
Flur-R-UNT	2	95695742	45861354	47.92	45246428	47.28	4144868	4.33	63.23
Flur-R-UNT	3	97519984	45970566	47.14	46406360	47.59	4633858	4.75	63.61
Flur-R-3HAT	1	95413504	45414436	47.60	46002926	48.21	3546352	3.72	62.77
Flur-R-3HAT	2	91184906	43299420	47.49	43985586	48.24	3486156	3.82	63.09
Flur-R-3HAT	3	95425988	46448452	48.67	44617614	46.76	3940164	4.13	61.85
Flur-R-10HAT	1	93693734	45778908	48.86	43823698	46.77	3675860	3.92	60.84
Flur-R-10HAT	2	93129972	46437846	49.86	42670796	45.82	3554876	3.82	60.04
Flur-R-10HAT	3	95618080	47186278	49.35	44128110	46.15	3826944	4.00	60.99
Flur-R-10HAT	4	93585040	46051500	49.21	43362892	46.34	3764776	4.02	60.93
9425-UNT	1	92544840	47348388	51.16	41298246	44.63	3534366	3.82	60.09
9425-UNT	2	94427486	44399484	47.02	45254046	47.92	4286030	4.54	63.2
9425-UNT	3	93239008	44049906	47.24	44570942	47.80	4187108	4.49	63.46
9425-3HAT	1	94771882	48492414	51.17	42537404	44.88	3331316	3.52	59.72
9425-3HAT	2	94873922	49298324	51.96	41903046	44.17	3278096	3.46	58.78

9425-3HAT	3	95517488	46581770	48.77	44650670	46.75	3815516	3.99	61.89
9425-10HAT	1	94999072	47433958	49.93	43022690	45.29	4108722	4.33	60.68
9425-10HAT	2	94852474	48913844	51.57	41679738	43.94	3791352	4.00	59.01
9425-10HAT	3	94430284	47108688	49.89	42689258	45.21	4167778	4.41	60.12
9425-10HAT	4	93345484	46996468	50.35	41932346	44.92	3991146	4.28	59.94
J01-UNT	1	94110422	45996468	48.87	44077502	46.84	4036452	4.29	62.26
J01-UNT	2	94684556	43865012	46.33	46031172	48.62	4303572	4.55	64.28
J01-3HAT	1	93575648	48396434	51.72	41217110	44.05	3496888	3.74	59.14
J01-3HAT	2	94616826	46806866	49.47	43718792	46.21	3618904	3.82	61.18
J01-10HAT	1	94437294	45321298	47.99	44828044	47.47	3852384	4.08	61.64
J01-10HAT	2	94714112	47245290	49.88	42739518	45.12	4292828	4.53	60.34
J01-10HAT	3	94407492	46128594	48.86	43538298	46.12	4283476	4.54	61.23

Table 3.3. Genes with higher expression at the untreated timepoint in Flur-R compared to J01-S and 9425-S lines at the untreated timepoint. Raw normalized counts and Log2 fold change for highly expressed ABC transporters, UDP glucosyltransferases and cytochrome p450 monooxygenases in the fluroxypyr resistant population Flur-R compared to either susceptible population 9425-S or J01-S. Genes which are higher expressed in Flur-R compared to both susceptible populations and are denoted with † and represented with the normalized count and fold change comparison to 9425-S.

Gene ID	Mean of normalized counts		Fold Change	Log2 Fold Change (±SE)	Pvalue (adjusted)	Gene Description
	Flur-R	9425-S				
Bs.00g282300.m01†	108	6	18	5.18 (1.47)	0.0028	ABC-G 28-like
Bs.00g217020.m01†	63	0	63	8.98 (2.85)	1.31E-06	ABC-G 31-like
Bs.00g454440.m01†	276	52	5	2.28 (0.44)	0.0003	Putative ABC-B 28-like
Bs.00g184080.m01	2147	3	716	9.63 (0.75)	9.86E-32	ABC-G 34 Isoform 1
Bs.00g184080.m02	2258	3	753	9.70 (0.75)	1.85E-32	ABC-G 34 Isoform 2
Bs.00g251290.m01	1462	341	4	1.98 (0.38)	0.0008	ABC-G 29-like
Bs.00g142060.m01	38	0	38	8.02 (2.81)	6.52E-05	UDP-glucosyltransferase 73B2 related
Bs.00g480980.m01†	510	14	36	5.01 (0.63)	2.11E-11	UDP-glucuronosyl/UDP-glucosyltransferase 89A2-like
Bs.00g480980.m03†	538	15	36	4.99 (0.63)	2.72E-11	UDP-glucuronosyl/UDP-glucosyltransferase 89A2-like
Bs.00g061050.m01	6018	1187	5	2.08 (0.59)	0.027	UDP-glycosyltransferase 87A1 related
Bs.00g541440.m01	232	10	23	4.21 (0.72)	2.00E-06	CYP96A15
Bs.00g051830.m01	233	5	47	4.03 (1.48)	0.0231	CYP71D10/11
Bs.00g245700.m01	417	114	4	1.72 (0.40)	0.0113	CYP90C1/D1 (3-Epi-6-Deoxocathasterone 23-Monooxygenase)
Bs.00g184110.m01	133	2	67	6.24 (0.96)	3.59E-08	CYP701 subfamily (Ent- Kaurene Oxidase)
	Flur-R	J01-S				
Bs.00g142720.m01	8246	3606	2	1.17 (0.15)	0.0001	7-deoxyloganetin glucosyltransferase-like 85A23
Bs.00g486870.m01	1847	61	31	4.85 (0.55)	1.29E-13	CYP82D47-like

Table 3.4. Top 20 upregulated genes in fluroxypyr resistant line Flur-R at 3 hours after treatment (HAT) and 10HAT compared to the untreated timepoint. Fold change was calculated using the mean of normalized counts which was produced using the DESeq2 package in R. Log2 Fold Change was calculated in DESeq2, log2 fold change standard error and adjusted pvalue were also calculated in DESeq2. The Wald-test obtained pvalues were adjusted using the Benjamini-Hochberg method. The FDR was < 0.05.

Gene ID	Mean of normalized counts		Fold Change	Log2 Fold Change (±SE)	Pvalue (adjusted)	Gene Description
	Flur-R Untreated	Flur-R 3HAT				
Bs.00g016210.m01[j] †	0.71	607	855	5.30 (0.39)	1.59E-14	Precursor of CEP13/CEP14
Bs.00g306100.m01	8	383	48	4.79 (0.33)	2.84E-28	Transcription Factor, MADS-Box
Bs.00g477580.m01[c] †	67	15681	980	4.63 (0.40)	1.22E-35	GH3 Family Protein
Bs.00g523550.m01	20	1131	57	4.57 (0.380	8.34E-24	Reverse Transcriptase Zinc-Binding Domain
Bs.00g418990.m01	34	1534	45	4.48 (0.37)	3.11E-23	Ethylene-Responsive Transcription Factor
Bs.00g010340.m01	1187	24154	20	4.43 (0.28)	3.94E-42	Membrane Attack Complex Component/Perforin (MACPF) Domain
Bs.00g435130.m01	34	1425	42	4.11 (0.39)	2.77E-19	Proton-Dependent Oligopeptide Transporter Family
Bs.00g315820.m01	242	7163	30	4.03 (0.37)	2.01E-18	Amino Acid Transporter
Bs.00g520970.m01	4	791	198	3.98 (0.47)	3.34E-13	Uncharacterized Protein
Bs.00g419000.m01[a]	4	1779	445	3.99 (0.49)	3.20E-11	Dehydration-Responsive Element-Binding Protein 1A-Related
Bs.00g315840.m01	184	5117	28	3.92 (0.38)	1.28E-16	Amino Acid Transporter
Bs.00g301780.m01	650	24203	37	3.90 (0.40)	2.28E-17	ABC Transporter G Family Member 40
Bs.00g087440.m01	17	547	32	3.88 (0.40)	5.86E-14	Amino Acid Transporter
Bs.00g181270.m02[a]	150	5353	36	3.87 (0.42)	4.17E-14	Protein NLP6-Related
Bs.00g257560.m01	1	330	330	3.85 (0.45)	3.93E-11	C2 Domain (Calcium/Lipid-Binding Domain, Calb)
Bs.00g200680.m01	1	80	80	3.85 (0.42)	2.58E-07	Uncharacterized Protein
Bs.00g244620.m01	75	1873	25	3.85 (0.34)	7.44E-20	Uncharacterized Protein
Bs.00g301770.m01	65	2253	35	3.82 (0.40)	3.74E-16	ABC Transporter G Family Member 40
Bs.00g428240.m01	3	126	42	3.78 (0.42)	3.22E-10	Extended Synaptotagmin-Related
Bs.00g036810.m01	750	16564	22	3.73 (0.36)	1.72E-17	Protein Phosphatase 2C

	Flur-R Untreated	Flur-R 10HAT				
Bs.00g016210.m01[j] †	0.71	2485	4007	7.43 (0.36)	9.28E-23	Precursor of CEP13/CEP14
Bs.00g477580.m01[c] †	67	29708	443	6.01 (0.41)	6.01E-57	GH3
Bs.00g239120.m01[k]	7	1135	162	5.82 (0.39)	1.82E-33	Aquaporin Transporter
Bs.00g168520.m01[k]	35	3260	93	5.25 (0.35)	1.44E-36	Cold Regulated Protein 27
Bs.00g168520.m02[d]	37	3298	89	5.41 (0.38)	1.41E-43	Cold Regulated Protein 27
Bs.00g107600.m01	13	2990	230	5.21 (0.43)	7.35E-34	Barwin-like endoglucanases
Bs.00g370370.m01	3	495	65	5.14 (0.41)	1.50E-22	Ethylene-Responsive Transcription Factor 13 Related
Bs.00g431740.m01	33	4437	134	5.12 (0.44)	2.94E-27	Heme-Dependent Peroxidases
Bs.00g057300.m01	0.34	142	418	5.06 (0.49)	3.98E-08	CYP71D10-like
Bs.00g217150.m01	6	1485	248	4.92 (0.44)	4.39E-28	Bet v I/Major Latex Protein
Bs.00g122020.m01	42	16883	393	4.88 (033)	2.86E-36	Uncharacterized Protein
Bs.00g261130.m01	43	6160	143	4.83 (0.33)	1.71E-23	Bet v I/Major Latex Protein
Bs.00g291860.m01	0	153	153	4.78 (0.47)	7.06E-11	Secoisolariciresinol Dehydrogenase
Bs.00g478760.m01[h]	1	930	930	4.48 (0.46)	5.42E-19	1-Aminocyclopropane-1-Carboxylate Synthase 4 Related
Bs.00g282410.m01	6	730	122	4.43 (0.45)	2.22E-19	Cysteine-Rich Repeat Secretory Protein 38
Bs.00g056520.m01	532	16588	31	4.39 (0.33)	5.82E-31	Alanine Dehydrogenase/Pyridine Nucleotide Transhydrogenase
Bs.00g370420.m01	0.37	76	205	4.35 (0.45)	5.86E-07	Uncharacterized Protein
Bs.00g422990.m01[d]	4681	137203	29	4.28 (0.32)	4.34E-32	4-Hydroxyphenylpyruvate Dioxygenase-like
Bs.00g020740.m01	5	709	142	4.27 (0.48)	1.40E-16	WRKY Transcription Factor
Bs.00g148640.m01[m]	1158	32325	28	4.26 (0.30)	7.67E-36	2-Oxoisovalerate Dehydrogenase Subunit Alpha 2

[a] Shared between J01-S 3HAT and Flur-R 3HAT top 20 upregulated genes
[c] Shared between 9425-S 10HAT up, J01-S 10HAT up and Flur-R 3/10HAT top 20 upregulated genes
[d] Shared between J01-S 10HAT and Flur-R 3HAT upregulated top 20 upregulated genes
[h] Shared between 9425-S 3HAT, Flur-R 10HAT and J01-S 10HAT top 20 upregulated genes
[j] Shared between 9425-S 10HAT, Flur-R 3HAT /10HAT and J02-S 10HAT top 20 upregulated genes
[k] Shared between 9425-S 10HAT, Flur-R 10HAT and J01-S 10HAT top 20 upregulated genes
[m] Shared between 9425-S 10HAT and Flur-R 10HAT top 20 upregulated genes
† Shared between Flur-R 3HAT/10HAT top 20 upregulated genes

Table 3.5. Top 20 downregulated genes in fluroxypyr resistant line Flur-R at 3 hours after treatment (HAT) and 10HAT compared to the untreated timepoint. Fold change was calculated using the mean of normalized counts which was produced using the DESeq2 package in R. Log2 Fold Change was calculated in DESeq2, log2 fold change standard error and adjusted pvalue were also calculated in DESeq2. The Wald-test obtained pvalues were adjusted using the Benjamini-Hochberg method. The FDR was <0.05.

Gene ID	Mean of normalized counts		Fold Change	Log2 Fold Change (±SE)	Pvalue (adjusted)	Gene Description
	Flur-R Untreated	Flur-R 3HAT				
Bs.00g258890.m01†	136	2	-66	-3.96 (0.44)	5.28E-11	LRR
Bs.00g104620.m01[e] †	7356	172	-43	-3.64 (0.43)	4.34E-13	Protein Kinase
Bs.00g354480.m01[r]	4017	217	-19	-3.35 (0.37)	4.39E-13	SAM Dependent Carboxyl Methyltransferase
Bs.00g370120.m01[r]	197	7	-29	-3.19 (0.45)	2.63E-08	Lipid Binding Domain
Bs.00g362240.m01	574	29	-20	-3.16 (0.42)	7.22E-09	Bicarbonate Transporter
Bs.00g195790.m01[b]	234	10	-24	-3.10 (0.44)	2.63E-08	Proton Dependent Oligopeptide Transporter
Bs.00g056860.m01	127	1	-95	-3.01 (0.48)	1.48E-06	Peptidase/Proteinase Inhibitor I9
Bs.00g119650.m01	1565	66	-24	-2.97 (0.44)	4.39E-08	Nicotianamine Synthase
Bs.00g251440.m01[r]	687	51	-13	-2.97 (0.37)	3.33E-10	Multicopper Oxidase
Bs.00g126000.m01 †	66186	1694	-39	-2.94 (0.47)	3.76E-08	NADH Cytochrome B5 Reductase
Bs.00g123470.m01	475	38	-13	-2.92 (0.37)	3.95E-10	Glycoside Hydrolase
Bs.00g264170.m01[r]	5895	687	-9	-2.87 (0.23)	6.32E-23	Glycoside Hydrolase
Bs.00g195800.m01	205	14	-15	-2.82 (0.42)	3.44E-07	Proton Dependent Oligopeptide Transporter
Bs.00g403960.m01 †	36087	2902	-12	-2.75 (0.39)	1.81E-08	Carotenoid Oxygenase
Bs.00g528960.m01[r]	1273	96	-13	-2.73 (0.40)	1.24E-07	Auxin-Inducible
Bs.00g348080.m01	965	77	-13	-2.73 (0.40)	9.58E-08	Uncharacterized Protein
Bs.00g420960.m01[p]	1713	12	-148	-2.65 (049)	1.28E-08	Chlorophyll A-B Binding Protein
Bs.00g421070.m01[p]	2101	12	-177	-2.63 (0.49)	4.44E-09	Chlorophyll A-B Binding Protein
Bs.00g429620.m01	67	4	-16	-2.63 (0.44)	2.53E-05	Multicopper Oxidase
Bs.00g372170.m02	220	11	-20	-2.62 (0.46)	6.13E-06	Uncharacterized Protein
	Flur-R Untreated	Flur-R 10HAT				

Bs.00g253530.m01[u]	3988	31	-131	-6.56 (0.29)	2.06E-91	Tetratricopeptide-Like Helical Domain Superfamily
Bs.00g240870.m01[u]	389614	3606	-108	-6.40 (0.26)	1.25E-104	Chlorophyll A-B Binding Protein
Bs.00g240870.m02[u]	246956	2360	-105	-6.35 (0.27)	5.04E-101	Chlorophyll A-B Binding Protein
Bs.00g060850.m01[u]	59810	959	-62	-5.34 (0.36)	1.12E-37	Thiamine Thiazole Synthase
Bs.00g126000.m01†	66186	447	-148	-5.12 (0.50)	4.64E-19	NADH-Cytochrome B5 Reductase
Bs.00g258890.m01†	136	1	-126	-5.10 (0.48)	1.28E-14	Tyrosine-Protein Kinase, Active Site
Bs.00g205780.m01	1166	26	-44	-4.99 (0.32)	8.66E-41	Cytochrome P450 90A1
Bs.00g133350.m02	459	11	-44	-4.88 (0.34)	8.43E-35	Serine Protease Family S10 Serine Carboxypeptidase
Bs.00g104620.m01[e]†	7356	100	-73	-4.81 (0.45)	7.39E-21	Phosphoenolpyruvate Carboxylase Kinase 1-Related
Bs.00g133350.m01	507	12	-41	-4.69 (0.36)	3.06E-28	Peptidase S10, Serine Carboxypeptidase
Bs.00g192330.m01	293420	9287	-32	-4.60 (0.31)	1.24E-37	Magnesium-Chelatase, Subunit H
Bs.00g279710.m01[f]	7847	165	-48	-4.59 (0.42)	6.82E-20	Aerolysin-Like Toxin
Bs.00g299020.m01	794	16	-50	-4.58 (0.44)	9.29E-19	O-Acyltransferase WSD1
Bs.00g116620.m01	2862	91	-31	-4.54 (0.31)	2.96E-37	Coenzyme Q-Binding Protein Coq10
Bs.00g480400.m01[v]	498	8	-62	-4.52 (0.49)	4.12E-14	Plc-Like Phosphodiesterase
Bs.00g206320.m01	10980	18	-609	-4.48 (0.58)	5.73E-15	Cytochrome P450 Superfamily
Bs.00g058520.m01[u]	1710	65	-26	-4.47 (0.26)	1.29E-47	Acyl-CoA N-Acyltransferases
Bs.00g205800.m01	868	23	-38	-4.45 (0.41)	1.42E-19	Cytochrome P450 90A1
Bs.00g403960.m01†	36087	952	-38	-4.45 (0.38)	4.49E-23	Carotenoid Cleavage Dioxygenase 4, Chloroplastic-Related
Bs.00g471400.m01	279	6	-43	-4.44 (0.43)	3.69E-17	Voltage-gated potassium channels

[b] Shared between J01-S 3HAT and Flur-R 3HAT top 20 downregulated genes
[e] Shared between J01-S 3HAT and Flur-R 3HAT/10HAT top 20 downregulated genes
[f] Shared between J01-S 10HAT and Flur-R 10HAT top 20 downregulated genes
[p] Shared between 9425-S 3HAT, J01-S 3HAT and Flur-R 3HAT op 20 downregulated genes
[r] Shared between 9425-S 3HAT and Flur-R 3HAT op 20 downregulated genes
[v] Shared between 9425-S 10HAT and Flur-R 10HAT op 20 downregulated genes
† Shared between Flur-R 3HAT/10HATop 20 downregulated genes

Table 3.6. Top 20 upregulated genes in fluroxypyr susceptible line J01-S at 3 hours after treatment (HAT) and 10HAT compared to the untreated timepoint. Fold change was calculated using the mean of normalized counts which was produced using the DESeq2 package in R. Log2 Fold Change was calculated in DESeq2, log2 fold change standard error and adjusted pvalue were also calculated in DESeq2. The Wald-test obtained pvalues were adjusted using the Benjamini-Hochberg method. The FDR was <0.05.

Gene ID	Mean of normalized counts		Fold Change	Log2 Fold Change (±SE)	Pvalue (adjusted)	Gene Description
	J01-S Untreated	J01-S 3HAT				
Bs.00g058350.m01	4	3428	763	7.33 (0.40)	2.01E-40	NADH Oxidoreductase-Related
Bs.00g144030.m01	173	40872	237	6.42 (0.44)	1.39E-37	Glycoside Hydrolase, Family 16
Bs.00g487370.m01	3	694	247	5.84 (0.46)	1.66E-17	Alpha/Beta Hydrolase Fold
Bs.00g397110.m01	0	494	494	5.46 (0.51)	1.71E-09	Zinc Finger, RING/FYVE/PHD-Type
Bs.00g435120.m01	31	2720	87	5.44 (0.37)	2.45E-36	Proton-Dependent Oligopeptide Transporter Family
Bs.00g419000.m01[a]	0	762	762	5.43 (0.53)	4.51E-10	AP2/ERF
Bs.00g122020.m01†	20	10546	515	5.43 (0.46)	4.17E-37	Uncharacterized Protein
Bs.00g142660.m01	232	13906	60	5.39 (0.32)	6.56E-47	Exordium-Like
Bs.00g430680.m01	5	8380	1847	5.38 (0.53)	2.75E-25	Protein Phosphatase 2C Family
Bs.00g167370.m01	23	2527	110	5.23 (0.48)	2.31E-18	Elo, Fatty Acid Acyl Transferase-Related
Bs.00g058830.m01	337	54400	162	5.20 (0.50)	5.41E-20	Harbinger Transposase-Derived Nuclease Domain
Bs.00g415260.m01	328	31294	95	5.12 (0.46)	4.78E-21	WRKY Domain
Bs.00g361960.m01	24	1628	67	4.96 (0.43)	1.07E-20	Gibberellin 2-Beta-Dioxygenase 4
Bs.00g428250.m02	34	5275	154	4.87 (0.52)	7.13E-16	C2 Domain (Calcium/Lipid-Binding Domain, Calb)
Bs.00g244130.m01	100	15352	154	4.70 (0.51)	3.15E-17	Protein TIFY 11A-Related
Bs.00g181270.m02[a]	74	6520	88	4.65 (0.49)	2.26E-16	Uncharacterized Protein
Bs.00g428250.m01	34	4864	142	4.64 (0.53)	5.42E-14	Extended Synaptotagmin-Related
Bs.00g512260.m01[i]	552	20157	37	4.63 (0.42)	9.41E-18	Glyoxalase/Fosfomycin Resistance/Dioxygenase Domain
Bs.00g228950.m01	2	333	207	4.56 (0.55)	1.44E-07	Dehydration-Responsive Element-Binding Protein 1a-Related

Bs.00g481180.m01	11	762	70	4.55 (0.46)	1.44E-15	Malectin-Like Carbohydrate-Binding Domain
	J01-S Untreated	J01-S 10HAT				
Bs.00g122020.m01†	20	13981	683	6.76 (0.41)	3.41E-61	Uncharacterized Protein
Bs.00g016210.m01[j]	2	1874	811	6.29 (0.43)	2.46E-24	Precursor of CEP13/CEP14
Bs.00g176460.m01	7	1155	173	5.88 (0.39)	3.91E-32	At-Hook Motif Nuclear-Localized Protein 27
Bs.00g218880.m01	3	529	183	5.30 (0.43)	3.47E-17	D-Arabinono-1,4-Lactone Oxidase
Bs.00g168520.m01[k]	43	3475	80	5.23 (0.40)	6.91E-31	Cold Regulated Protein 27
Bs.00g168520.m02[k]	42	3334	78.7	5.08 (0.42)	1.54E-27	Cold Regulated Protein 27
Bs.00g176480.m01	1	295	511	5.07 (0.46)	6.62E-07	At-Hook Motif Nuclear-Localized Protein 27
Bs.00g239120.m01[k]	6	1088	176	4.96 (0.49)	3.49E-18	Aquaporin Tip3-1-Related
Bs.00g478760.m01[h]	2	793	457	4.70 (0.49)	3.96E-14	1-Aminocyclopropane-1-Carboxylate Synthase 4-Related
Bs.00g112620.m01	7	731	110	4.56 (0.47)	8.44E-17	Lipase/Lipooxygenase Domain
Bs.00g044610.m01[l]	263	9925	37.7	4.54 (0.35)	1.05E-29	Uncharacterized Protein
Bs.00g304090.m01[g]	154	4039	26.3	4.28 (0.31)	7.03E-32	AP2/ERF Domain
Bs.00g477580.m01[c]	279	45370	162	4.28 (0.50)	7.01E-23	Indole-3-Acetic Acid-Amido Synthetase GH3.2-Related
Bs.00g112710.m01	416	34778	83.5	4.24 (0.48)	7.24E-20	Lipoxygenase, C-Terminal
Bs.00g275080.m01	2	376	228	4.23 (0.48)	5.48E-11	Heme-Dependent Peroxidases
Bs.00g364070.m01	380	9639	25.4	4.22 (0.36)	2.28E-22	NAC Domain-Containing Protein 10-Related
Bs.00g422990.m01[d]	3600	120541	33.5	4.15 (0.40)	8.07E-20	4-Hydroxyphenylpyruvate Dioxygenase
Bs.00g359220.m02[n]	12	14262	1145	4.10 (0.58)	4.71E-22	Proteinase Inhibitor I13
Bs.00g520060.m01	448	8022	17.9	3.93 (0.24)	1.18E-46	B-Box Domain Protein 26-Related
Bs.00g058370.m01	1	152	131	3.92 (0.47)	3.23E-07	Metacaspase-4-Related

[a] Shared between J01-S 3HAT and Flur-R 3HAT top 20 upregulated genes
[c] Shared between 9425-S 10HAT, J01-S 10HAT and Flur-R 3/10HAT top 20 upregulated genes
[d] Shared between J01-S 10 HAT and Flur-R 10HAT top 20 upregulated genes
[g] Shared between 9425-S 3HAT and J01-S 10HAT top 20 upregulated genes

[h] Shared between 9425-S 3HAT, Flur-R10HAT and J01-S 10HAT top 20 upregulated genes
[i] Shared between J01-S 3HAT and 9425-S 3HAT upregulated top 20
[j] Shared between 9425-S 10HAT, Flur-R 3/10HAT and J01-S 3HAT/10HAT top 20 upregulated genes
[k] Shared between 9425-S 10HAT, Flur-R 10HAT and J01-S 10HAT top 20 upregulated genes
[l] Shared between 9245-S 3HAT/10HAT and J01-S 10HAT top 20 upregulated genes
[n] Shared between 9425-S 10HAT and J01-S 10HAT top 20 upregulated genes
† Shared between J01-S 3HAT /10HAT top 20 upregulated genes

Table 3.7. Top 20 downregulated genes in fluroxypyr susceptible line J01-S at 3 hours after treatment (HAT) and 10HAT compared to the untreated timepoint. Fold change was calculated using the mean of normalized counts which was produced using the DESeq2 package in R. Log2 Fold Change was calculated in DESeq2, log2 fold change standard error and adjusted pvalue were also calculated in DESeq2. The Wald-test obtained pvalues were adjusted using the Benjamini-Hochberg method. The FDR was <0.05.

Gene ID	Mean of normalized counts		Fold Change	Log2 Fold Change (±SE)	Pvalue (adjusted)	Gene Description
	J01-S Untreated	J01-S 3HAT				
Bs.00g420960.m01[p]	2805	114	-25	-7.08 (0.43)	3.21E-37	Early Light-Induced Protein 1, Chloroplastic-Related
Bs.00g421070.m01[p]	3659	129	-28	-6.40 (0.46)	1.24E-31	Early Light-Induced Protein 1, Chloroplastic-Related
Bs.00g104620.m01[e]†	6485	87	-74	-5.07 (0.37)	1.81E-33	Phosphoenolpyruvate Carboxylase Kinase 1-Related
Bs.00g518390.m01[o]	1330	91	-15	-4.38 (0.45)	8.59E-17	Chalcone/Stilbene Synthase
Bs.00g383340.m01[q]†	62541	614	-102	-4.23 (0.38)	5.29E-22	S-Adenosyl-L-Methionine-Dependent Methyltransferase
Bs.00g383340.m02[q]†	63412	627	-101	-4.22 (0.38)	6.99E-22	S-Adenosyl-L-Methionine-Dependent Methyltransferase
Bs.00g479050.m01	1337	71	-19	-4.00 (0.37)	2.08E-19	Multicopper Oxidase, Type 1, 2, 3
Bs.00g150590.m01	19150	874	-22	-3.52 (0.23)	6.20E-37	Carboxyvinyl-Carboxyphosphonate Phosphorylmutase, Chloroplastic
Bs.00g417520.m01	3342	727	-5	-3.51 (0.46)	1.48E-09	Cytochrome P450 86a7
Bs.00g196880.m01	12374	621	-20	-3.40 (0.29)	7.21E-22	Haloacid Dehalogenase-Like Hydrolase Domain-Containing Protein
Bs.00g228740.m01	3131	464	-7	-3.36 (0.43)	4.71E-10	Glucose-Methanol-Choline Oxidoreductase
Bs.00g488230.m02[s]	493	30	-16	-3.27 (0.39)	4.26E-11	BTB/POZ Domain-Containing Protein Dot3
Bs.00g091650.m01	5414	1641	-3	-3.24 (0.40)	1.94E-10	Cytochrome P450 77A4-Related
Bs.00g179870.m01	560	21	-27	-3.20 (0.48)	1.00E-07	Thioredoxin-LIK
Bs.00g488230.m01[s]	589	39	-15	-3.15 (0.38)	3.15E-11	BTB/POZ Domain-Containing Protein DOT3
Bs.00g124100.m01	25716	1786	-14	-3.14 (0.37)	1.34E-11	Multi Antimicrobial Extrusion Protein
Bs.00g195790.m01[b]	661	34	-20	-3.11 (0.53)	1.62E-06	Proton-Dependent Oligopeptide Transporter Family
Bs.00g247060.m01	1115	125	-9	-3.08 (0.36)	3.19E-11	Major Facilitator Protein

Bs.00g418430.m01	2076	95	-22	-3.05 (0.24)	3.85E-24	Peptidase S10, Serine Carboxypeptidase
Bs.00g310680.m01	4294	815	-5	3.02 (0.39)	3.14E-09	Aquaporin transporter
	J01-S Untreated	J01-S 10HAT				
Bs.00g237950.m01	31050	185	-168	-6.11 (0.47)	2.24E-29	Purine and Uridine Phosphorylases
Bs.00g383340.m01[q]†	62541	614	-102	-5.98 (0.34)	5.59E-55	S-Adenosyl-L-Methionine-Dependent Methyltransferase
Bs.00g383340.m02[q]†	63412	627	-101	-5.97 (0.34)	7.93E-55	S-Adenosyl-L-Methionine-Dependent Methyltransferase
Bs.00g060850.m01[u]	61097	963	-63	-5.71 (0.25)	7.00E-96	Thiamine Thiazole Synthase
Bs.00g253530.m01[u]	3380	51	-66	-5.61 (0.30)	2.91E-59	Tetratricopeptide-Like Helical Domain Superfamily
Bs.00g104620.m01[e]†	6485	87	-74	-5.57 (0.33)	7.03E-51	Phosphoenolpyruvate Carboxylase Kinase 1-Related
Bs.00g002550.m01[t]	6898	56	-123	-5.53 (0.50)	1.28E-19	Glucose-6-Phosphate/Phosphate Translocator 2, Chloroplastic
Bs.00g058520.m01[u]	2423	35	-69	-5.51 (0.36)	1.50E-39	Acyl-CoA N-Acyltransferase
Bs.00g279710.m01[f]	25350	388	-65	-5.38 (0.41)	1.01E-26	Aerolysin-Like Toxin
Bs.00g240870.m01[u]	407872	5349	-76	-5.26 (0.45)	3.48E-22	Chlorophyll A-B Binding Protein
Bs.00g240870.m02[u]	265402	3480	-76	-5.24 (0.46)	1.70E-21	Chlorophyll A-B Binding Protein
Bs.00g236450.m01	13388	387	-35	-4.88 (0.24)	4.84E-72	Protein Proton Gradient Regulation 5
Bs.00g115330.m01	71272	1829	-39	-4.85 (0.34)	7.75E-34	Photosystem I Reaction Center Subunit Iv A, Chloroplastic-Related
Bs.00g020870.m01	209812	6578	-32	-4.69 (0.28)	3.26E-46	Chlorophyll A/B Binding Protein
Bs.00g412900.m01	18823	572	-33	-4.65 (0.31)	1.54E-39	Granule-Bound Starch Synthase 1, Chloroplastic/Amyloplastic
Bs.00g476760.m01	699	11	-62	-4.63 (0.50)	4.10E-14	Z -3-Hexen-1-Ol Acetyltransferase
Bs.00g527540.m01	7607	68	-112	-4.47 (0.58)	7.97E-10	Proteinase Inhibitor I3, Kunitz Legume
Bs.00g472680.m01	1623	58	-28	-4.35 (0.36)	3.49E-23	Uncharacterized Protein
Bs.00g383860.m01	33142	1574	-21	-4.31 (0.15)	7.02E-130	Fructose-1,6-Bisphosphatase-Related
Bs.00g055990.m01	635	21	-30	-4.28 (0.40)	3.67E-19	Uncharacterized Protein

[b] Shared between J01-S 3HAT and Flur-R 3HAT top 20 downregulated genes
[e] Shared between 9425-S 3HAT, J01-S 3HAT/10HAT and Flur-R 3HAT/10HAT top 20 downregulated genes
[f] Shared between J01-S 10HAT and Flur-R 10HAT top 20 downregulated genes

[o] Shared between 9425-S 3HAT/10HAT and J01-S 3HAT top 20 downregulated genes
[p] Shared between 9425-S 3HAT, J01-S 3HAT and Flur-R 3HAT top 20 downregulated genes
[q] Shared between 9425-S 3HAT and J01-S 3HAT/10HAT top 20 downregulated genes
[s] Shared between 9425-S 3HAT and J01-S 3HAT top 20 downregulated genes
[t] Shared between 9425-S 10HAT and J01-S 10HAT top 20 downregulated genes
[u] Shared between 9425-S 10HAT, J01-10HAT, Flur-R 10HAT top 20 downregulated genes
[w] Shared between 9425-S 10HAT and J01-S 3HAT top 20 downregulated genes

Table 3.8. Top 20 upregulated genes in fluroxypyr susceptible line 9425-S at 3 hours after treatment (HAT) and 10HAT compared to the untreated timepoint. Fold change was calculated using the mean of normalized counts which was produced using the DESeq2 package in R. Log2 Fold Change was calculated in DESeq2, log2 fold change standard error and adjusted pvalue were also calculated in DESeq2. The Wald-test obtained pvalues were adjusted using the Benjamini-Hochberg method. The FDR was <0.05.

Gene ID	Mean of normalized counts		Fold Change	Log2 Fold Change (±SE)	Pvalue (adjusted)	Gene Description
	9425-S Untreated	9425-S 3HAT				
Bs.00g044610.m01[l]†	188	9324	50	4.69 (0.32)	3.31E-39	Uncharacterized Protein
Bs.00g301680.m01	973	17616	18	3.73 (0.27)	8.83E-32	Auxin-Responsive Protein IAA15
Bs.00g174320.m01†	39	664	17	3.36 (0.31)	6.95E-19	Histidine Kinase/HSP90-Like ATPase Superfamily
Bs.00g050510.m01	150	1971	13	3.36 (0.26)	1.40E-24	Cytochrome P450 734A1
Bs.00g229060.m01	84	2342	28	3.34 (0.41)	1.90E-11	Multi Antimicrobial Extrusion Protein/Protein Detoxification 50
Bs.00g107340.m01	474	5929	13	3.34 0.24)	5.55E-30	Auxin-Responsive Protein IAA1-Related
Bs.00g293750.m01	16	283	18	3.32 (0.34)	6.03E-14	Uncharacterized Protein
Bs.00g478760.m01[h]	7	583	83	3.31 (0.44)	3.80E-13	1-Aminocyclopropane-1-Carboxylate Synthase 4-Related
Bs.00g506330.m01	49	1128	23	3.27 (0.41)	4.61E-10	Chaperone J-Domain Superfamily
Bs.00g044350.m01	605	9804	16	3.14 (0.36)	7.06E-12	Uncharacterized Protein
Bs.00g512260.m01[i]	100	4635	46	3.13 (0.47)	1.83E-05	Lactoylglutathione Lyase Glyoxalase I
Bs.00g305330.m01	79	2260	29	3.06 (0.45)	5.39E-07	Cytochrome P450 76c1-Related
Bs.00g357520.m01	2	88	41	2.96 (0.42)	2.21E-07	Late Embryogenesis Abundant Protein
Bs.00g364640.m01	641	7072	11	2.94 (0.31)	4.70E-13	Signal Transduction Response Regulator, Receiver Domain
Bs.00g304090.m01[g]	196	2097	11	2.91 (0.30)	1.87E-14	AP2/ERF Transcription Factor ERF/PTI6
Bs.00g204690.m01	249	4008	16	2.90 (0.41)	1.21E-07	Zinc Finger, RING/FYVE/PHD-Type
Bs.00g048560.m01	768	8441	11	2.88 (0.31)	4.70E-13	Auxin-Responsive Protein IAA29
Bs.00g112660.m01	352	9548	27	2.87 (0.42)	7.59E-10	Linoleate 9S-Lipoxygenase 5, Chloroplastic
Bs.00g415260.m01	263	9451	36	2.86 (0.47)	3.22E-06	WRKY Transcription Factor 46-Related
Bs.00g290110.m01	336	3706	11	2.85 (0.35)	7.53E-10	Uncharacterized Protein

	9425-S Untreated	9425-S 10HAT				
Bs.00g427230.m01	28	5143	183	6.20	1.09E-37	Member of 'GDXG' Family of Lipolytic Enzymes
Bs.00g168520.m01[k]	46	4282	94	5.64	6.80E-40	Cold Regulated Protein 27
Bs.00g168520.m02[k]	53	4276	81	5.44	1.36E-35	Cold Regulated Protein 27
Bs.00g174320.m01†	39	2571	66	5.40	1.17E-53	Histidine Kinase/HSP90-Like ATPase Superfamily
Bs.00g044610.m01[l]†	188	10766	57	5.07	3.35E-49	Uncharacterized Protein
Bs.00g261820.m01	0	77	77	4.93	4.95E-07	Pectin Lyase Fold/Virulence Factor
Bs.00g016210.m01[j]	2	1675	988	4.87	9.19E-22	Precursor of CEP13/CEP14
Bs.00g413330.m01	620	71783	116	4.85	4.01E-22	Cystathionine Gamma-Lyase
Bs.00g148640.m01[m]	660	27633	42	4.71	1.26E-34	2-Oxoisovalerate Dehydrogenase Subunit Alpha 2, Mitochondrial
Bs.00g305280.m01	0	52	52	4.65	1.41E-05	Allergen V5/TPX-1-Related, Conserved Site
Bs.00g142300.m01	0	48	48	4.58	2.08E-05	Pectin Lyase Fold/Virulence Factor
Bs.00g477660.m01	9	4426	510	4.56	1.47E-25	Gibberellin-Regulated GASA/GAST/SNAKIN Family Protein-Related
Bs.00g359220.m02[n]	41	15538	383	4.56	1.16E-25	Proteinase Inhibitor I13, Potato Inhibitor I Superfamily
Bs.00g239120.m01[k]	2	1207	619	4.54	5.71E-14	Aquaporin TIP3-1-Related
Bs.00g208750.m01	287	11553	40	4.52	1.72E-25	CASP-Like Protein 1E1-Related
Bs.00g430360.m01	60	2663	44	4.44	7.76E-24	Protein Early Flowering 4
Bs.00g100040.m01	3	789	228	4.43	5.81E-09	Bet V I/Major Latex Protein
Bs.00g477580.m01[c]	92	39708	431	4.41	8.98E-30	Indole-3-Acetic Acid-Amido Synthetase GH3.2-Related
Bs.00g526000.m01	228	9711	43	4.40	4.47E-21	NAC Domain
Bs.00g447890.m01	0	73	73	4.36	6.43E-07	Pectinesterase

[c] Shared between 9425-S 10HAT, J01-S 10HAT and Flur-R 3HAT/10HAT top 20 upregulated genes
[g] Shared between 9425-S 3HAT and J01-S 10HAT top 20 upregulated genes
[h] Shared between 9425-S 3HAT, Flur-R 10HAT and J01-S 10HAT top 20 upregulated genes
[I] Shared between 9425-S 3HAT and J01-S 3HAT top 20 upregulated genes
[j] Shared between 9425-S 10HAT, Flur-R 3HAT /10HAT and J01-S 3HAT/10HAT top 20 upregulated genes
[k] Shared between 9425-S 10HAT, Flur-R 10HAT and J01-S 10HAT top 20 upregulated genes
[l] Shared between 9245-S 3HAT/10HAT and J01-S 10HAT top 20 upregulated genes

[m] Shared between 9425-S 10HAT and Flur-R 10HAT top 20 upregulated genes
[n] Shared between 9425-S 10HAT and J01-S 10HAT top 20 upregulated genes
† Shared between 9425-S 3HAT/10HAT top 20 upregulated genes

Table 3.9. Top 20 downregulated genes in fluroxypyr susceptible line 9425-S at 3 hours after treatment (HAT) and 10HAT compared to the untreated timepoint. Fold change was calculated using the mean of normalized counts which was produced using the DESeq2 package in R. Log2 Fold Change was calculated in DESeq2, log2 fold change standard error and adjusted pvalue were also calculated in DESeq2. The Wald-test obtained pvalues were adjusted using the Benjamini-Hochberg method. The FDR was <0.05.

Gene ID	Mean of normalized counts		Fold Change	Log2 Fold Change (±SE)	Pvalue (adjusted)	Gene Description
	9425-S Untreated	9425-S 3HAT				
Bs.00g518390.m01[o†]	4504	68	67	-5.06	1.80E-41	Chalcone/Stilbene Synthase
Bs.00g421070.m01[p]	1918	8	238	-3.69	1.06E-14	Early Light-Induced Protein 1, Chloroplastic-Related
Bs.00g420960.m01[p]	1557	7	210	-3.61	9.55E-14	Early Light-Induced Protein 1, Chloroplastic-Related
Bs.00g543360.m01	2375	98	24	-3.38	1.15E-11	Oxoglutarate/Iron-Dependent Dioxygenase
Bs.00g383340.m01[q]	13230	691	19	-3.31	1.70E-12	S-Adenosyl-L-Methionine-Dependent Methyltransferase
Bs.00g383340.m02[q]	13404	701	19	-3.31	1.82E-12	S-Adenosyl-L-Methionine-Dependent Methyltransferase
Bs.00g354480.m01[r]	1542	87	18	-3.25	1.69E-11	S-Adenosyl-L-Methionine-Dependent Methyltransferase
Bs.00g370120.m01[r]	364	8	45	-3.20	6.65E-09	CRAL-TRIO Lipid Binding Domain
Bs.00g268300.m01†	724	5	140	-3.16	2.50E-10	Early Light-Induced Protein 1, Chloroplastic-Related
Bs.00g364920.m01	453	37	12	-3.13	1.87E-15	Serine-Threonine/Tyrosine-Protein Kinase, Catalytic Domain
Bs.00g488230.m01[s]	532	38	14	-3.11	2.63E-12	BTB/POZ Domain-Containing Protein DOT3
Bs.00g488230.m02[s]	447	37	12	-3.02	1.55E-12	BTB/POZ Domain-Containing Protein DOT3
Bs.00g475340.m01	478	38	13	-2.95	1.42E-09	Camp-Response Element Binding Protein-Related
Bs.00g528960.m01[r]	880	51	17	-2.89	1.17E-07	Auxin_Inducible
Bs.00g180610.m01	1127	60	19	-2.86	1.87E-07	Glycoside Hydrolase Family 1
Bs.00g251440.m01[r]	1535	140	11	-2.81	4.78E-10	Multicopper Oxidase, Type 2
Bs.00g396960.m01	646	57	11	-2.70	3.62E-08	UDP-Glycosyltransferase/Glycogen Phosphorylase
Bs.00g420270.m01	1575	133	12	-2.67	2.39E-06	Glucose-Methanol-Choline Oxidoreductase
Bs.00g104620.m01[e]	1497	106	14	-2.67	9.72E-07	Serine/Threonine-Protein Kinase
Bs.00g264170.m01[r]	11365	1301	9	-2.66	1.13E-10	Beta-Glucosidase 1-Related
	9425-S Untreated	9425-S 10HAT				

Bs.00g002550.m01[t]	10014	41	242	-6.95	3.36E-47	Glucose-6-Phosphate/Phosphate Translocator 2, Chloroplastic
Bs.00g518390.m01[o]†	4504	21	213	-6.94	7.61E-75	Chalcone/Stilbene Synthase, C-Terminal
Bs.00g240870.m01[u]	419016	3501	120	-6.09	2.32E-35	Chlorophyll A-B Binding Protein
Bs.00g240870.m02[u]	274431	2301	119	-6.09	4.32E-35	Chlorophyll A-B Binding Protein
Bs.00g058520.m01[u]	3828	37	103	-6.08	4.85E-49	Acyl-CoA N-Acyltransferase
Bs.00g060850.m01[u]	105278	1179	89	-5.75	2.70E-36	Thiamine Thiazole Synthase
Bs.00g253530.m01[u]	3725	49	76	-5.63	1.99E-37	Tetratricopeptide-Like Helical Domain Superfamily
Bs.00g535160.m01	480	4	110	-5.57	2.65E-21	WAT1-Related Protein
Bs.00g124870.m01	18471	116	160	-5.33	8.61E-16	Lipoxygenase
Bs.00g480400.m01[v]	684	8	85	-5.33	1.31E-20	PLC-Like Phosphodiesterase
Bs.00g418430.m01	3350	46	73	-5.33	6.52E-27	Peptidase S10, Serine Carboxypeptidase
Bs.00g535430.m01	143	1	108	-5.30	7.70E-15	Cyclin_A_B_D_E
Bs.00g518030.m01	721	2	412	-5.13	1.43E-12	Chalcone/Stilbene Synthase, Polyketide Synthase, Type III, Hydroxymethylglutaryl-CoA Synthase
Bs.00g055200.m01	754	15	51	-5.06	7.48E-28	Glyceraldehyde-3-Phosphate Dehydrogenase-Like
Bs.00g535430.m02	121	1	92	-5.05	2.97E-13	Cyclin_A_B_D_E
Bs.00g249240.m01	212	2	117	-5.02	5.87E-13	Uncharacterized Protein
Bs.00g268300.m01†	724	4	171	-5.01	6.54E-14	Early Light-Induced Protein 1
Bs.00g435140.m01	1573	29	55	-4.95	4.56E-22	Proton-Dependent Oligopeptide Transporter Family
Bs.00g136920.m01	1931	16	123	-4.92	1.48E-13	Cupin_1
Bs.00g478150.m01	781	6	138	-4.90	1.45E-11	Glycoside Hydrolase Family 17

[e] Shared between 9425 3HAT, J01-3HAT/10HAT and Flur-R 3HAT/10HAT top 20 downregulated genes
[o] Shared between 9425-S 3HAT/10HAT and J01-S 3HAT top 20 downregulated genes
[p] Shared between 9425-S 3HAT, J01-S 3HAT and Flur-R 3HAT top 20 downregulated genes
[q] Shared between 9425-S 3HAT and J01-S 3HAT/10HAT top 20 downregulated genes
[r] Shared between 9425-S 3HAT and Flur-R 3HAT top 20 downregulated genes
[s] Shared between 9425-S 3HAT and J01-S 3HAT top 20 downregulated genes
[t] Shared between 9425-S 10HAT and J01-S 10HAT top 20 downregulated genes
[v] Shared between 9425-S 10HAT and Flur-R 10HAT top 20 downregulated genes

[w] Shared between 9425-S 10HAT and J01-S 3HAT top 20 downregulated genes
†Shared between 9425-S 3HAT and 10HAT top 20 downregulated genes

FIGURES

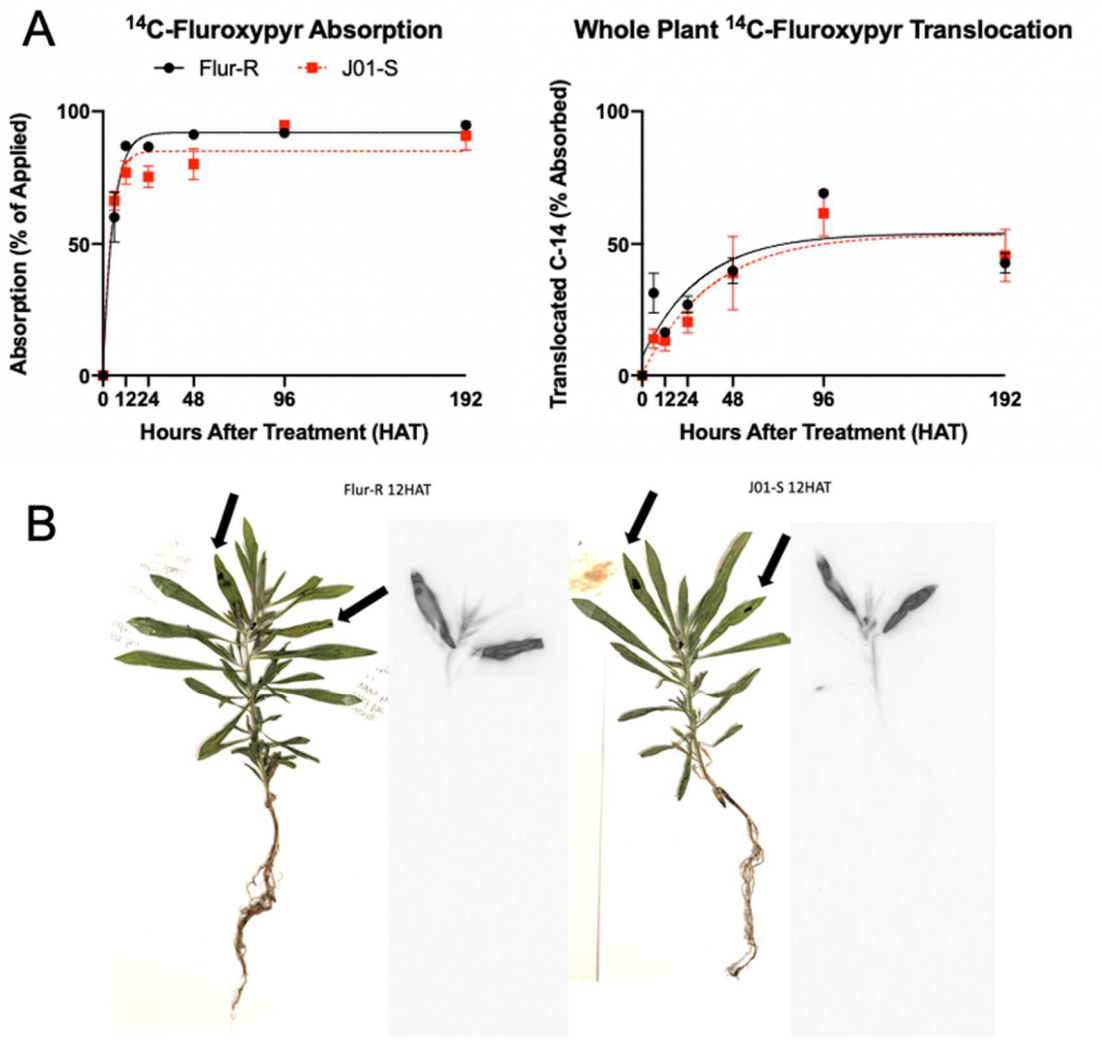

Figure 3.1. A. Whole plant absorption and translocation study conducted on fluroxypyr resistant line, Flur-R and fluroxypyr susceptible line, J01-S assessed over 6,12, 24, 48, 96 and 192 hours after treatment with [^{14}C]-fluroxypyr ester. The absorption/translocation graphs depict percent absorption and translocation normalized to account for slight variation in application rates with SEM. There are no differences between Flur-R and J01-S in absorption or translocation of [^{14}C]-fluroxypyr ester. B. Real plant and phosphor-images showing translocation of [^{14}C]-fluroxypyr ester in Flur-R (left) and J01-S (right) at 12 h, the time at which max absorption is at 90% in both lines. The black arrows mark the two treated leaves on each individual. The phosphor image to the right of each pressed plant photo shows where [^{14}C]-fluroxypyr ester has translocated throughout the plant in 12 hours after treatment.

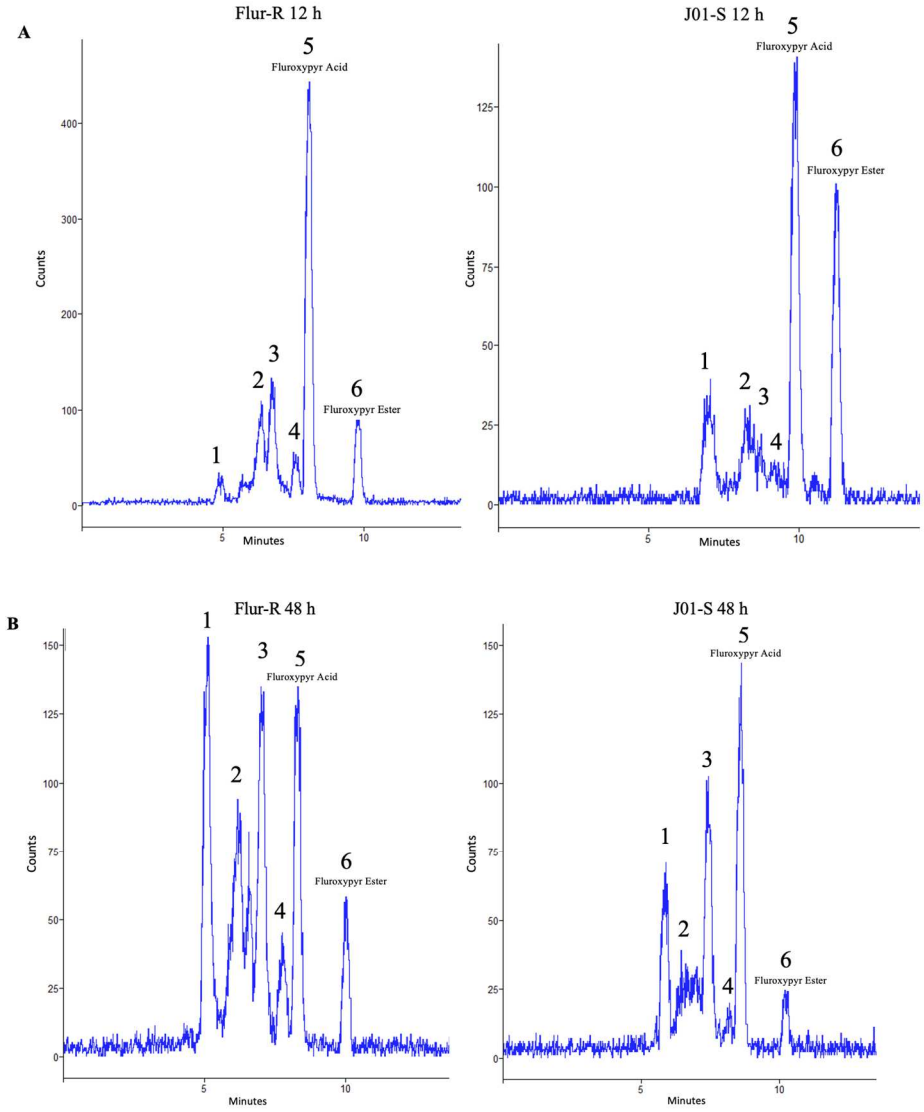

Figure 3.2. A. HPLC metabolite profile for fluroxypyr resistant line Flur-R and fluroxypyr susceptible line J01-S at 24 hours after treatment (h) with [^{14}C]-fluroxypyr ester shows a significant reduction in proportion of [^{14}C]-fluroxypyr ester in Flur-R. B. HPLC metabolite profile for Flur-R and J01-S 48 h shows a higher proportion of metabolites in Flur-R. Retention time for [^{14}C]-fluroxypyr ester (peak 6) was ~ 10.2 minutes. Retention time for [^{14}C]-fluroxypyr acid (peak 5) was ~ 9.8 minutes. Unknown metabolites (peaks 1-4) had retention times varying from ~4.9 to ~9.2 minutes.

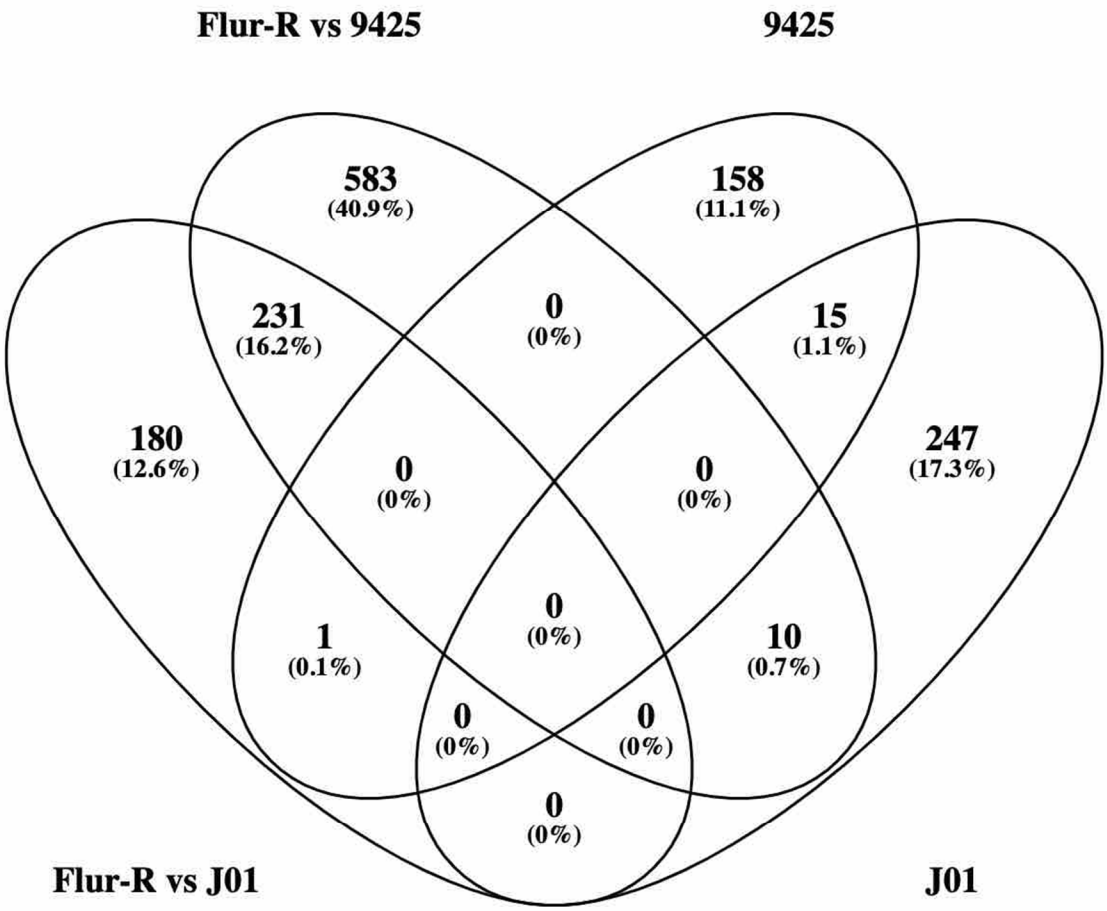

Figure 3.3. Upregulation between the untreated condition in Flur-R compared to both untreated conditions in fluroxypyr susceptible lines 9425-S and J01-S in DESeq2 (Flur-R vs 9425; Flur-R vs J01). Upregulation for both 9425-S and J01-S compared to Flur-R in DESeq2 are represented by their singular line name in the diagram (J01, 9425). Overlapping ovals represent genes that are commonly expressed at the untreated condition between comparisons.

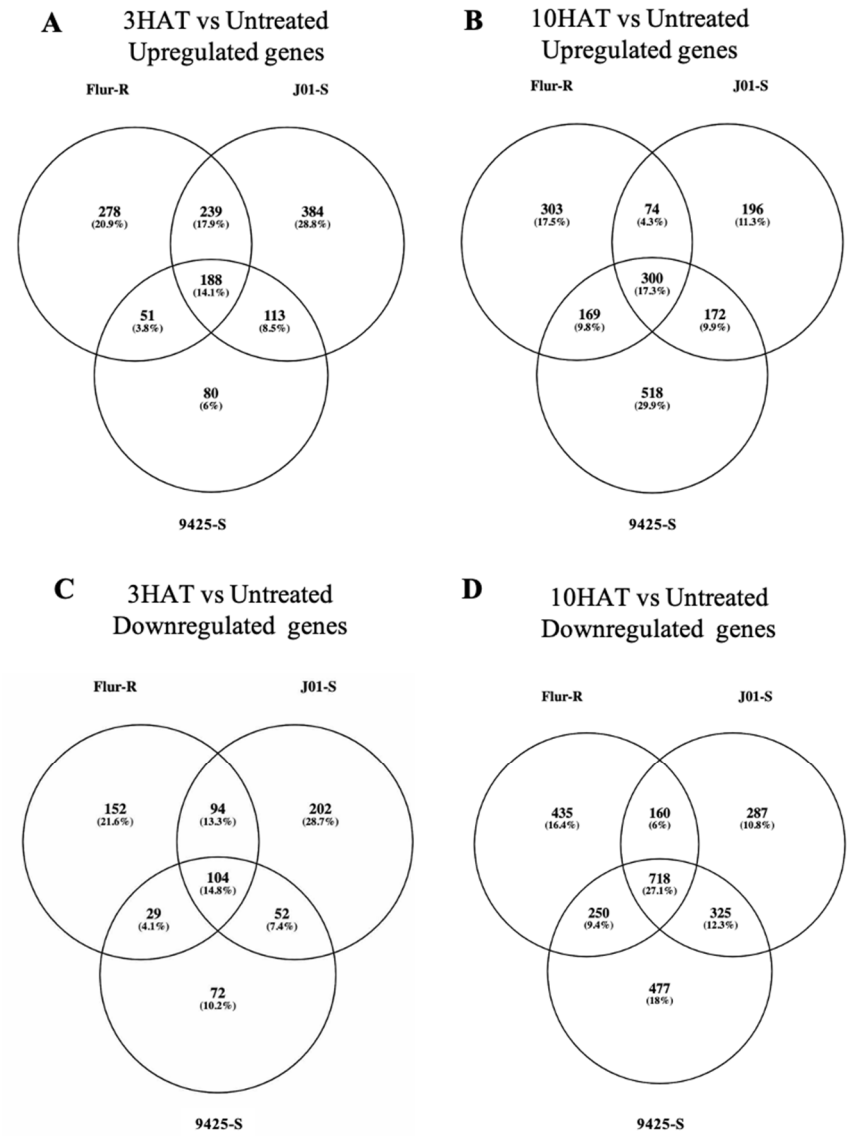

Figure 3.4. Venn diagrams showing transcripts that were either up or down regulated between the untreated condition and either 3 or 10 hours after treatment (HAT) with fluroxypyr in fluroxypyr resistant line Flur-R and susceptible lines 9425-S and J01-S. A. Venn diagram depicting shared and uniquely upregulated transcripts at 3HAT between all three lines. B. Venn diagram depicting shared and uniquely upregulated transcripts at 10HAT between all three lines. C. Venn diagram depicting shared and uniquely downregulated transcripts at 10HAT between all three lines. D. Venn diagram depicting shared and uniquely downregulated transcripts at 10HAT between all three lines.

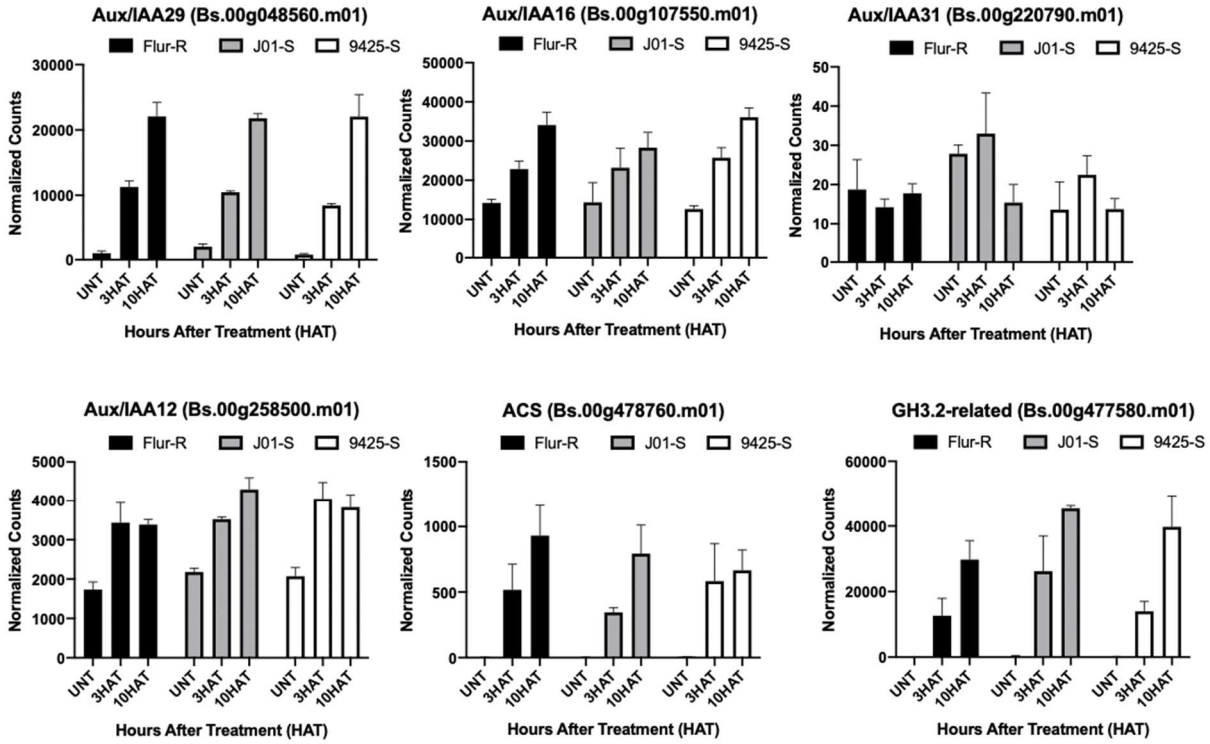

Figure 3.5. Expression profiles for auxin induced genes GH3.2, ACS, and various high confidence Aux/IAAs in fluroxypyr resistant Flur-R, susceptible J01-S, and susceptible 9425-S following differential expression analysis. X-axis shows treatments: untreated, 3 and 10 hours after treatment grouped by line. Normalized counts on the y-axis is a result of the DESeq2 function and model fitting in R package "deseq2". Our non-high confidence Aux/IAA protein identification is included in supplementary table 1, and show similar expression patterns. NCBI Blast results showed mixed results for protein annotation for most Aux/IAA proteins in *Bassia scoparia.*

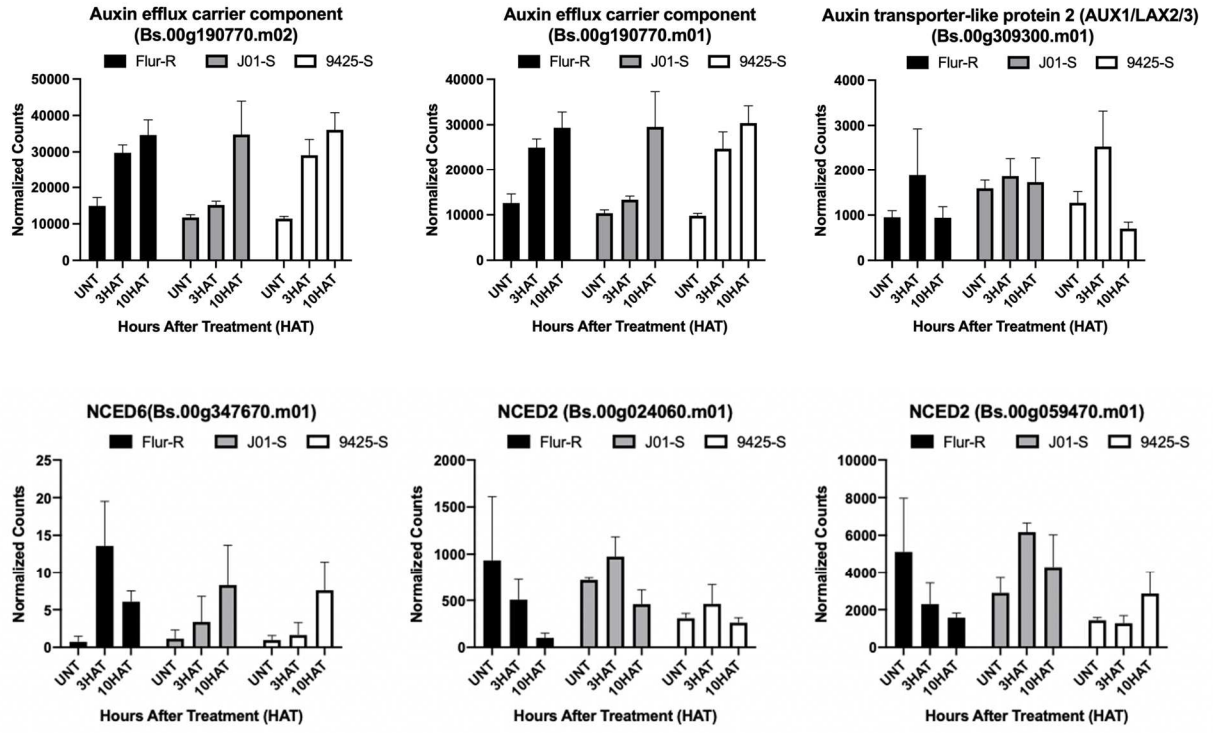

Figure 3.6. Expression profiles for auxin induced influx and efflux transporters and NCED in fluroxypyr resistant Flur-R, susceptible J01-S, and susceptible 9425-S following differential expression analysis. X-axis shows treatments: untreated, 3 and 10 hours after treatment grouped by line. Normalized counts on the y-axis is a result of the DESeq2 function and model fitting in R package "deseq2". Both isoforms of the auxin efflux carrier component were upregulated in response to fluroxypyr in the 9425-S line. There were no differences in expression for the Aux/LAX transporter. NCED6 was responsive at both 3 h and 10 h in Flur-R, but NCED2 was downregulated in Flur-R.

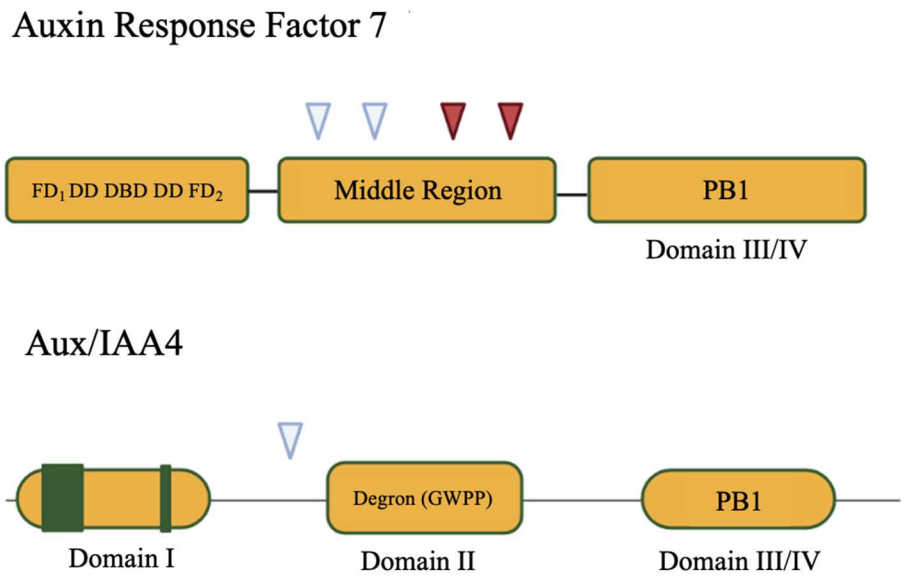

Figure 3.7. Variants in the ARF and Aux/IAA proteins of fluroxypyr resistant line Flur-R. Non-synonymous single nucleotide polymorphisms are represented by the white triangles, and deletions are represented by the red triangles. Because these variants lie in the variable middle region of ARF7, and significantly outside the degron domain of Aux/IAA4, it is unlikely that they influence auxin binding and interaction.

REFERENCES

Bai S, Zhao Y, Zhou Y, Wang M, Li Y, Luo X, Li L (2020) Identification and expression of main genes involved in non-target site resistance mechanisms to fenoxaprop-p-ethyl in Beckmannia syzigachne. Pest Manag Sci 76 (8):2619-2626. doi:10.1002/ps.5800

Bernhardt R (2006) Cytochromes P450 as versatile biocatalysts. J Biotechnol 124 (1):128-145. doi:10.1016/j.jbiotec.2006.01.026

Bioinformatics B FastQC: a quality control tool for high throughput sequence data. https://www.bioinformatics.babraham.ac.uk/projects/fastqc/.

Busi R, Goggin DE, Heap IM, Horak MJ, Jugulam M, Masters RA, Napier RM, Riar DS, Satchivi NM, Torra J, Westra P, Wright TR (2018) Weed resistance to synthetic auxin herbicides. Pest Manag Sci 74 (10):2265-2276. doi:10.1002/ps.4823

Chayapakdee P, Sunohara Y, Endo M, Yamaguchi T, Fan L, Uchino A, Matsumoto H, Iwakami S (2020) Quinclorac resistance in Echinochloa phyllopogon is associated with reduced ethylene synthesis rather than enhanced cyanide detoxification by beta-cyanoalanine synthase. Pest Manag Sci 76 (4):1195-1204. doi:10.1002/ps.5660

Cho M, Cho HT (2013) The function of ABCB transporters in auxin transport. Plant Signal Behav 8 (2):e22990. doi:10.4161/psb.22990

Cingolani P, Platts A, Wang LL, Coon M, Nguyen T, Wang L, Land SJ, Lu X, Ruden DM (2012) A program for annotating and predicting the effects of single nucleotide polymorphisms, SnpEff: SNPs in the genome of Drosophila melanogaster strain w1118; iso-2; iso-3. Fly 6 (2):80-92

Delye C (2013) Unravelling the genetic bases of non-target-site-based resistance (NTSR) to herbicides: a major challenge for weed science in the forthcoming decade. Pest Manag Sci 69 (2):176-187. doi:10.1002/ps.3318

Dhara A, Raichaudhuri A (2021) ABCG transporter proteins with beneficial activity on plants. Phytochemistry 184:112663. doi:10.1016/j.phytochem.2021.112663

Dimaano NG, Iwakami S (2021) Cytochrome P450-mediated herbicide metabolism in plants: current understanding and prospects. Pest Manag Sci 77 (1):22-32. doi:10.1002/ps.6040

EPA (2010) Analytical method for fluroxypyr-MHE and and its metabolites, fluroxypyr acid, fluroxypyr-DCP and fluroxypyr-MP in water

Figueiredo MR, Kuepper A, Malone JM, Petrovic T, Figueiredo ABT, Campagnola G, Peersen OB, Prasad KV, Patterson EL, Reddy AS (2021) An in-frame deletion mutation in the degron tail of auxin co-receptor IAA2 confers resistance to the herbicide 2, 4-D in Sisymbrium orientale. bioRxiv

Figueiredo MRA, Leibhart LJ, Reicher ZJ, Tranel PJ, Nissen SJ, Westra P, Bernards ML, Kruger GR, Gaines TA, Jugulam M (2018) Metabolism of 2,4-dichlorophenoxyacetic acid contributes to resistance in a common waterhemp (Amaranthus tuberculatus) population. Pest Manag Sci 74 (10):2356-2362. doi:10.1002/ps.4811

Gao Y, Li J, Pan X, Liu D, Napier R, Dong L (2018) Quinclorac resistance induced by the suppression of the expression of 1-aminocyclopropane-1-carboxylic acid (ACC) synthase and ACC oxidase genes in Echinochloa crus-galli var. zelayensis. Pestic Biochem Physiol 146:25-32. doi:10.1016/j.pestbp.2018.02.005

Gao Y, Pan L, Sun Y, Zhang T, Dong L, Li J (2017) Resistance to quinclorac caused by the enhanced ability to detoxify cyanide and its molecular mechanism in Echinochloa crus-galli var. zelayensis. Pestic Biochem Physiol 143:231-238. doi:10.1016/j.pestbp.2017.08.009

Gion K, Inui H, Takakuma K, Yamada T, Kambara Y, Nakai S, Fujiwara H, Miyamura T, Imaishi H, Ohkawa H (2014) Molecular mechanisms of herbicide-inducible gene expression of tobacco CYP71AH11 metabolizing the herbicide chlorotoluron. Pesticide biochemistry and physiology 108:49-57

Goda H, Sawa S, Asami T, Fujioka S, Shimada Y, Yoshida S (2004) Comprehensive comparison of auxin-regulated and brassinosteroid-regulated genes in Arabidopsis. Plant Physiol 134 (4):1555-1573. doi:10.1104/pp.103.034736

Goggin DE, Bringans S, Ito J, Powles SB (2019) Plasma membrane receptor-like kinases and transporters are associated with 2,4-D resistance in wild radish. Ann Bot. doi:10.1093/aob/mcz173

Gräfe K, Schmitt L (2021) The ABC transporter G subfamily in Arabidopsis thaliana. J Exp Bot 72 (1):92-106

Guilfoyle TJ (1999) Auxin-regulated genes and promoters. Biochemistry and molecular biology of plant hormones

Jonathon Anderson PJB, Daniel Milroy, Peter Ruprecht, Thomas Hauser, and Howard Jay Siegel (2017) Deploying RMACC Summit: an HPC resource for the rocky mountain region. PEARC17. doi:10.1145/3093338.3093379

Jun X, WANG X-y, GUO W-z (2015) The cytochrome P450 superfamily: Key players in plant development and defense. Journal of Integrative Agriculture 14 (9):1673-1686

Kim D, Paggi JM, Park C, Bennett C, Salzberg SL (2019) Graph-based genome alignment and genotyping with HISAT2 and HISAT-genotype. Nature biotechnology 37 (8):907-915

Kniss AR, Vassios JD, Nissen SJ, Ritz C (2011) Nonlinear Regression Analysis of Herbicide Absorption Studies. Weed Sci 59 (4):601-610. doi:10.1614/Ws-D-11-00034.1

Kraft M, Kuglitsch R, Kwiatkowski J, Frank M, Grossmann K (2007) Indole-3-acetic acid and auxin herbicides up-regulate 9-cis-epoxycarotenoid dioxygenase gene expression and abscisic acid accumulation in cleavers (Galium aparine): interaction with ethylene. J Exp Bot 58 (6):1497-1503. doi:10.1093/jxb/erm011

LeClere S, Wu C, Westra P, Sammons RD (2018) Cross-resistance to dicamba, 2,4-D, and fluroxypyr in *Kochia scoparia* is endowed by a mutation in an AUX/IAA gene. Proc Natl Acad Sci U S A 115 (13):E2911-E2920. doi:10.1073/pnas.1712372115

Lee S, Sundaram S, Armitage L, Evans JP, Hawkes T, Kepinski S, Ferro N, Napier RM (2014) Defining binding efficiency and specificity of auxins for SCF(TIR1/AFB)-Aux/IAA co-receptor complex formation. ACS Chem Biol 9 (3):673-682. doi:10.1021/cb400618m

Li Y, Baldauf S, Lim E-K, Bowles DJ (2001) Phylogenetic analysis of the UDP-glycosyltransferase multigene family of Arabidopsis thaliana. J Biol Chem 276 (6):4338-4343

Liu X, Dinh TT, Li D, Shi B, Li Y, Cao X, Guo L, Pan Y, Jiao Y, Chen X (2014) AUXIN RESPONSE FACTOR 3 integrates the functions of AGAMOUS and APETALA 2 in floral meristem determinacy. The Plant Journal 80 (4):629-641

Ludwig-Müller J (2011) Auxin conjugates: their role for plant development and in the evolution of land plants. J Exp Bot 62 (6):1757-1773

McCauley CL, McAdam SAM, Bhide K, Thimmapuram J, Banks JA, Young BG (2020) Transcriptomics in Erigeron canadensis reveals rapid photosynthetic and hormonal responses to auxin herbicide application. J Exp Bot 71 (12):3701-3709. doi:10.1093/jxb/eraa124

Miyazaki S, Katsumata T, Natsume M, Kawaide H (2011) The CYP701B1 of Physcomitrella patens is an ent-kaurene oxidase that resists inhibition by uniconazole-P. Febs Lett 585 (12):1879-1883. doi:10.1016/j.febslet.2011.04.057

Moons A (2005) Regulatory and functional interactions of plant growth regulators and plant glutathione S-transferases (GSTs). Vitamins & hormones 72:155-202

Murphy BP, Tranel PJ (2019) Target-Site Mutations Conferring Herbicide Resistance. Plants-Basel 8 (10). doi:ARTN 382
10.3390/plants8100382

Ohkawa H, Tsujii H, Ohkawa Y (1999) The use of cytochrome P450 genes to introduce herbicide tolerance in crops: a review. Pestic Sci 55 (9):867-874

Ohnishi T, Godza B, Watanabe B, Fujioka S, Hategan L, Ide K, Shibata K, Yokota T, Szekeres M, Mizutani M (2012) CYP90A1/CPD, a brassinosteroid biosynthetic cytochrome P450 of Arabidopsis, catalyzes C-3 oxidation. J Biol Chem 287 (37):31551-31560

Ohnishi T, Szatmari A-M, Watanabe B, Fujita S, Bancos S, Koncz C, Lafos M, Shibata K, Yokota T, Sakata K (2006) C-23 hydroxylation by Arabidopsis CYP90C1 and CYP90D1 reveals a novel shortcut in brassinosteroid biosynthesis. The Plant Cell 18 (11):3275-3288

Paponov IA, Paponov M, Teale W, Menges M, Chakrabortee S, Murray JA, Palme K (2008) Comprehensive transcriptome analysis of auxin responses in Arabidopsis. Mol Plant 1 (2):321-337. doi:10.1093/mp/ssm021

Patterson EL, Saski CA, Sloan DB, Tranel PJ, Westra P, Gaines TA (2019) The Draft Genome of Kochia scoparia and the Mechanism of Glyphosate Resistance via Transposon-Mediated EPSPS Tandem Gene Duplication. Genome Biol Evol 11 (10):2927-2940. doi:10.1093/gbe/evz198

Perrot-Rechenmann C (2010) Cellular responses to auxin: division versus expansion. Cold Spring Harb Perspect Biol 2 (5):a001446. doi:10.1101/cshperspect.a001446

Pettinga DJ, Ou J, Patterson EL, Jugulam M, Westra P, Gaines TA (2018) Increased chalcone synthase (CHS) expression is associated with dicamba resistance in *Kochia scoparia*. Pest Manag Sci 74 (10):2306-2315. doi:10.1002/ps.4778

Raghavan C, Ong EK, Dalling MJ, Stevenson TW (2005) Effect of herbicidal application of 2,4-dichlorophenoxyacetic acid in Arabidopsis. Funct Integr Genomics 5 (1):4-17. doi:10.1007/s10142-004-0119-9

Ramos JA, Zenser N, Leyser O, Callis J (2001) Rapid degradation of auxin/indoleacetic acid proteins requires conserved amino acids of domain II and is proteasome dependent. The Plant Cell 13 (10):2349-2360

Rimmer A, Phan H, Mathieson I, Iqbal Z, Twigg SR, Wilkie AO, McVean G, Lunter G (2014) Integrating mapping-, assembly-and haplotype-based approaches for calling variants in clinical sequencing applications. Nature genetics 46 (8):912-918

Robinson JT, Thorvaldsdóttir H, Wenger AM, Zehir A, Mesirov JP (2017) Variant review with the integrative genomics viewer. Cancer research 77 (21):e31-e34

Rosquete MR, Barbez E, Kleine-Vehn J (2012) Cellular auxin homeostasis: gatekeeping is housekeeping. Mol Plant 5 (4):772-786. doi:10.1093/mp/ssr109

Schober A, McMaster S, Gantz R Fluroxypyr: a new environmentally compatible herbicide. In: Proceedings-Western Society of Weed Science (USA), 1986.
Siminszky B, Corbin FT, Ward ER, Fleischmann TJ, Dewey RE (1999) Expression of a soybean cytochrome P450 monooxygenase cDNA in yeast and tobacco enhances the metabolism of phenylurea herbicides. P Natl Acad Sci USA 96 (4):1750-1755. doi:DOI 10.1073/pnas.96.4.1750
Teale WD, Paponov IA, Palme K (2006) Auxin in action: signalling, transport and the control of plant growth and development. Nat Rev Mol Cell Biol 7 (11):847-859. doi:10.1038/nrm2020
Ulmasov T, Hagen G, Guilfoyle TJ (1999) Activation and repression of transcription by auxin-response factors. Proceedings of the National Academy of Sciences 96 (10):5844-5849
Villalobos LIAC, Lee S, De Oliveira C, Ivetac A, Brandt W, Armitage L, Sheard LB, Tan X, Parry G, Mao HB, Zheng N, Napier R, Kepinski S, Estelle M (2012) A combinatorial TIR1/AFB-Aux/IAA co-receptor system for differential sensing of auxin. Nature Chemical Biology 8 (5):477-485. doi:10.1038/Nchembio.926
Westra EP, Nissen SJ, Getts TJ, Westra P, Gaines TA (2019) Survey reveals frequency of multiple resistance to glyphosate and dicamba in kochia (*Bassia scoparia*). Weed Technol 33 (5):664-672
Xiang WS, Wang XJ, Ren TR (2006) Expression of a wheat cytochrome P450 monooxygenase cDNA in yeast catalyzes the metabolism of sulfonylurea herbicides. Pesticide Biochemistry and Physiology 85 (1):1-6. doi:10.1016/j.pestbp.2005.09.001
Zhang K, Wang R, Zi H, Li Y, Cao X, Li D, Guo L, Tong J, Pan Y, Jiao Y (2018) AUXIN RESPONSE FACTOR3 regulates floral meristem determinacy by repressing cytokinin biosynthesis and signaling. The Plant Cell 30 (2):324-346
Zhao Y (2010) Auxin biosynthesis and its role in plant development. Annu Rev Plant Biol 61:49-64
Zia Ul Haq M, Zhang Z, Wei J, Qiang S (2020) Ethylene Biosynthesis Inhibition Combined with Cyanide Degradation Confer Resistance to Quinclorac in Echinochloa crus-galli var. mitis. Int J Mol Sci 21 (5). doi:10.3390/ijms21051573

APPENDICIES

Supplementary Table 1. Full *Bassia scoparia* IAA proteins as assigned by UNIPROT annotation and as assigned by top 3 NCBI BLAST-P results.

Bassia scoparia IAA	NCBI Description	% Identity	E-Value	Organism
*IAA29 (Bs.00g048560.m01)	IAA31-like	100	0.0	*Bassia scoparia*
	IAA29-like	66.79	4e-100	*Beta vulgaris*
	IAA29-like	63.77	5e-93	*Chenopodium quinoa*
IAA1 (Bs.00g107340.m01)	Auxin-induced protein 22D-like	79.88	2e-90	*Spinacia oleracea*
	IAA4-like	77.51	2e-87	*Chenopodium quinoa*
	IAA4-like isoform X1	76.33	2e-86	*Chenopodium quinoa*
*IAA16 (Bs.00g107550.m01)	IAA16-like	77.66	2e-136	*Spinacia oleracea*
	Hypothetical Protein	78.21	5e-132	*Spinacia oleracea*
	IAA16-like	74.74	4e-129	*Chenopodium quinoa*
*IAA31 (Bs.00g220790.m01)	IAA31-like	76.83	5e-77	*Chenopodium quinoa*
	IAA4-like	76.43	9e-75	*Beta vulgaris*
	IAA31-like	73.71	2e-74	*Chenopodium quinoa*
*IAA12 (Bs.00g258500.m01)	IAA13-like	88.22	0.0	*Bassia scoparia*
	IAA12-like isoform X2	84.65	6e-127	*Chenopodium quinoa*
	IAA12-like isoform X1	82.73	1e-124	*Chenopodium quinoa*
IAA27 (Bs.00g300610.m01)	IAA8-like	100	0.0	*Bassia scoparia*
	IAA27-like	75.55	2e-157	*Beta vulgaris*
	Hypothetical Protein	75.31	2e-157	*Beta vulgaris*
IAA15 (Bs.00g301680.m01)	IAA7-like	99.48	8e-138	*Bassia scoparia*
	IAA1-like	77.23	1e-105	*Spinacia oleracea*
	IAA1-like	76.35	6e-105	*Chenopodium quinoa*
IAA14 (Bs.00g358730.m01)	Hypothetical Protein	92.49	2e-113	*Beta vulgaris*
	IAA14-like	92.49	6e-113	*Spinacia oleracea*
	Hypothetical Protein	89.08	1e-108	*Spinacia oleracea*
*IAA9 (Bs.00g523560.m01)	IAA9-like	99.04	0.0	*Bassia scoparia*

	IAA9-like	83.54	0.0	*Beta vulgaris*
	IAA9-like	78.59	4e-180	*Spinacia oleracea*

Supplementary Table 2. Partial *Bassia scoparia* IAA proteins as assigned by UNIPROT annotation and as assigned by top 3 NCBI BLAST-P results.

Bassia scoparia IAA	NCBI Description	% Identity	E-Value	Organism
IAA18-like (Bs.00g038420.m01)	IAA18-like	90.70	4e-18	*Bassia scoparia*
	Hypothetical Protein GH714	70.37	9e-17	*Hevea brasiliensis*
	IAA2-like	81.82	2e-16	*Beta vulgaris*
IAA18-like (Bs.00g038420.m02)	IAA18-like	90.70	9e-18	*Bassia scoparia*
	Hypothetical Protein GH714	70.37	2e-16	*Hevea brasiliensis*
	IAA2-like	81.82	3e-16	*Beta vulgaris*
IAA18-like (Bs.00g261040.m01)	IAA18-like	96.32	3e-87	*Bassia scoparia*
	IAA2-like	84.62	1e-70	*Beta vulgaris*
	IAA26-like	85.38	2e-70	*Chenopodium quinoa*
IAA18-like (Bs.00g274940.m01)	IAA18-like	90.70	3e-17	*Bassia scoparia*
	Hypothetical Protein Lal	51.22	4e-17	*Lupinus albus*
	Hypothetical Protein GH714	60.61	1e-16	*Hevea brasiliensis*
IAA18-like (Bs.00g277900.m01)	IAA18-like	90.70	2e-17	*Bassia scoparia*
	Hypothetical Protein GH714	70.37	2e-16	*Hevea brasiliensis*
	IAA2-like	83.72	7e-16	*Beta vulgaris*
IAA18-like (Bs.00g299920.m01)	IAA18-like	99.60	3e-180	*Bassia scoparia*
	IAA2-like	70.35	2e-158	*Beta vulgaris*
	IAA26-like	65.27	2e-139	*Chenopodium quinoa*
IAA18-like (Bs.00g395050.m01)	Hypothetical Protein GOBAR	75.93	2e-19	*Gossypium barbadense*
	IAA2-like	80.00	2e-19	*Beta vulgaris*
	IAA18-like	80.00	4e-19	*Bassia scoparia*
IAA18-like (Bs.00g454800.m01)	IAA18-like	93.83	1e-43	*Bassia scoparia*
	IAA26-like	77.78	2e-31	*Chenopodium quinoa*
	IAA2-like	76.54	1e-30	*Beta vulgaris*
IAA18-like (Bs.00g487380.m01)	IAA18-like	90.70	3e-17	*Bassia scoparia*

	Hypothetical Protein GH714	70.37	4e-16	*Hevea brasiliensis*
	IAA2-like	83.72	1e-15	*Beta vulgaris*

FIGURES

A

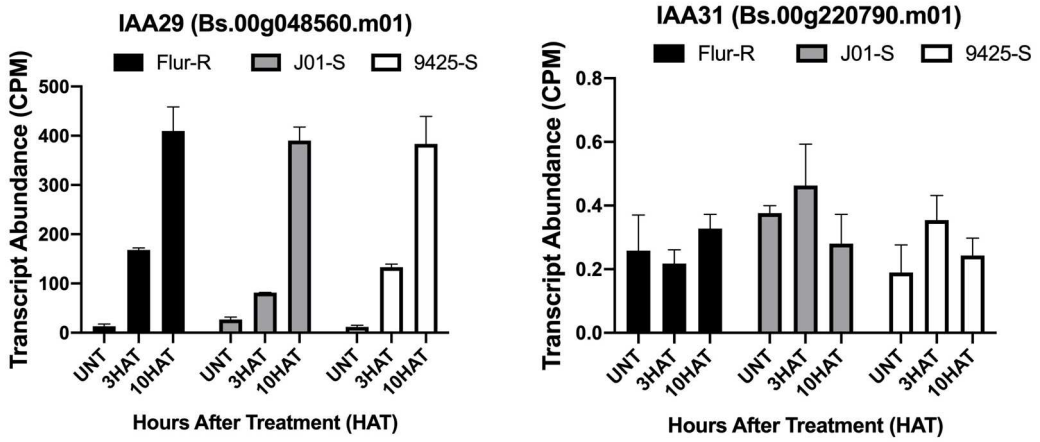

B

>Bs.00g048560.m01
MELELGLAISNGPPKIQTLKELDLISYVNYKGKQANEDENYSNLSSENSVNDVDCANQE
ANCGGVYQLKENDKKKRGFDETNEVESCVTLPLLLWDKHPNEDDKLPPKRLCNSTSFT
LNKNDGDNIV**GWPP**IKSYRKKLNDEQQQQRRRRHVEDFPAIDNGGRGGGGCGGLQTM
FVKVQIEGCFITRKIDLKLYHSYKTLVCSLLSMFGKGHDCMDDYKLTYQDEDGDWLLA
GDVPWRTFIESVQRLKLRKKD

>Bs.00g220790.m01
MGRNKNDDRNRRRNNMPPSSSSSTDSNTNNGCDGEFCSNDLSTDLRLGLSISSQDLSSSP
RGQYSEWAPKQLLRSTLGAGKSNCRRDDTLYVKVYMEGIPIGRKLDLLAHHGYHSLLS
TLVQMFRTTILSPDTNCHGSVDNCHILTYEDKDGDWMMVGDVPWEMFLTTVKRLKIV
AFEKCQ

Supplementary Figure 1. A. Proposed reassignment of IAA31 based on sequencing results. What has been annotated on NCBI as *Bassia scoparia* IAA31 by LeClere et al. (2018b) has been shown to hit to the protein Bs.00g048560.m01 in our genome annotation. This protein's transcript levels in response to fluroxypyr do not align with previous research. Dreher et al. (2006) shows a decrease in IAA31 transcript levels in Arabidopsis as a response to 2,4-D. Additionally, information from TAIR notes that overexpression of IAA31 causes a suite of defects related to development and response to tropisms. In the Arabidopsis protein sequence of IAA31, there is no "GWPP" motif in degron II, although it does share few residues. B. Residues in Bs.00g048560.m01 showing the "GWPP" motif, and our proposed IAA31, Bs.00g220790.m01, which does not have the GWPP" motif.

SUMMARY OF *SORGHUM BICOLOR* EMS MUTAGENESIS FOR HERBICIDE RESISTANCE TRAITS

In spring of 2018, we prepared a dose response with EMS to determine optimal rate for treatment of the M_0 *sorghum bicolor* population TX2737. This dose response included a 12-hour pre-soak to soften seed coats followed by submergence in 10 rates with seven timepoints. Germination, vigor, and number of mutations were measured two weeks after planting. Optimal dose was chosen based on number of seedlings germinated, how well they compared to untreated plant in terms of number of leaves, growth stage, and by how many mutations were present in the treatment as a whole. The dose response was repeated.

In the summer of 2019, 7.5lb (~ 110,000) sorghum seeds of line TX2737 were pre-soaked for 12 hours in water, treated with 0.25% EMS in phosphate buffer for 6 hours and rinsed for 1 hour in clean water. Seeds were dried and planted over 1 acre at the Agricultural Research Development and Education Center in Fort Collins, Colorado. Germination was determined to be ~50% and mutation rate was ~8% based on chlorophyll mutation visual assessment. Notably, Fort Collins on average contains 1,383 growing degree days (Celsius) and does not reach the average ~1600 required by short season varieties (Supplementary Figure 4). Seeds from approximately 20 individuals were collected and cleaned from this 2019 planting. There were 16 individuals with red grain that were also able to reach physiological maturity despite the short growing season in Fort Collins. Only 4 individuals with white grain similar to that of the non-mutagenized population were able to reach physiological maturity in Fort Collins. We hypothesize that there may be developmental advantage for short growing seasons that was induced by EMS treatment where red grain can be used as a trait marker. The presence of red grain was seen during independent mutagenesis events in both 2018 and 2019 where individuals

displaying this trait were harvested individually. From the 2018 data, it is estimated that this red grain trait occurred in 10% of the sorghum harvested at Rocky Ford, Colorado.

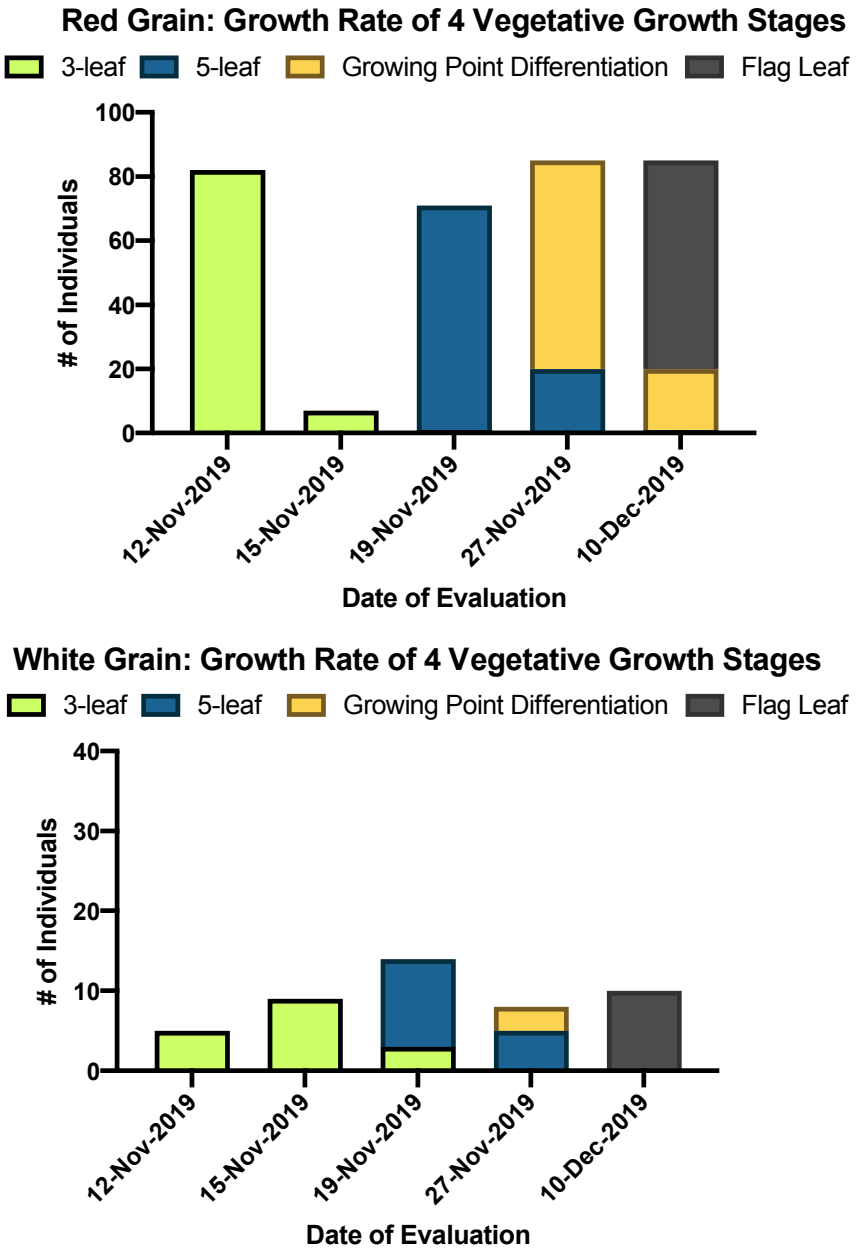

Supplementary Figure 2. Growth rate of the first 4 vegetative growth stages for red grain (top) vs. white grain (bottom) *sorghum bicolor* over a one-month period harvested from an EMS experiment. In the summer of 2019, 7.5lb (~ 110,000) sorghum seeds of line TX2737 were pre-soaked for 12 hours in water, treated with 0.25% EMS in phosphate buffer for 6 hours and rinsed for 1 hour in clean water. More than 80% of the individuals with red grain reached the flag leaf stage within a one-month time period. 10% of individuals with white grain reached the flag leaf stage in this time, with the remaining 80% in growth stages prior to flag leaf emergence.

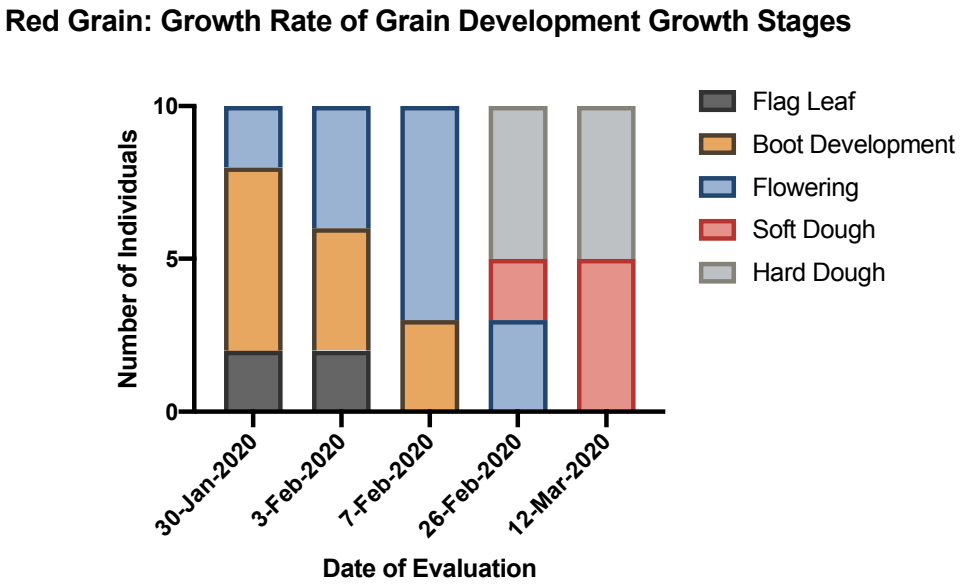

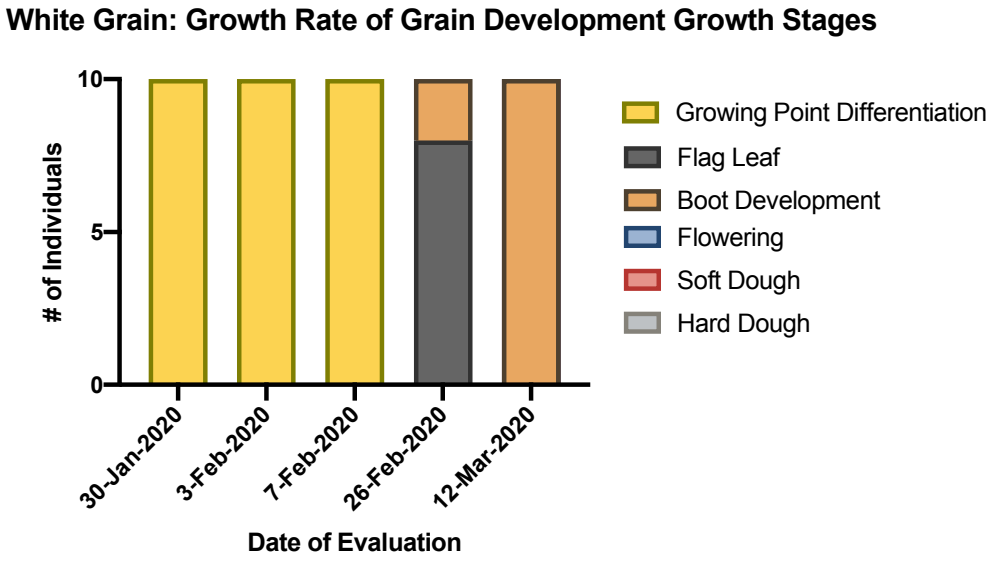

Supplementary Figure 3. Ten *Sorghum bicolor* individuals of line TX2737 in the M2 generation following an EMS mutagenesis application of 0.25%. Ten random individuals were selected per seed color on January 8th, 2020 to continue with the physiology study. Evaluations were made on those 10 individuals until March 12th, 2020. Growth rates significantly differ through the reproductive stages. Red grain reached near physiological maturity (top) by the last evaluation date before the University closures began for COVID-19. As of March 12th, 2020 the white grained plants had not started to flower (bottom).

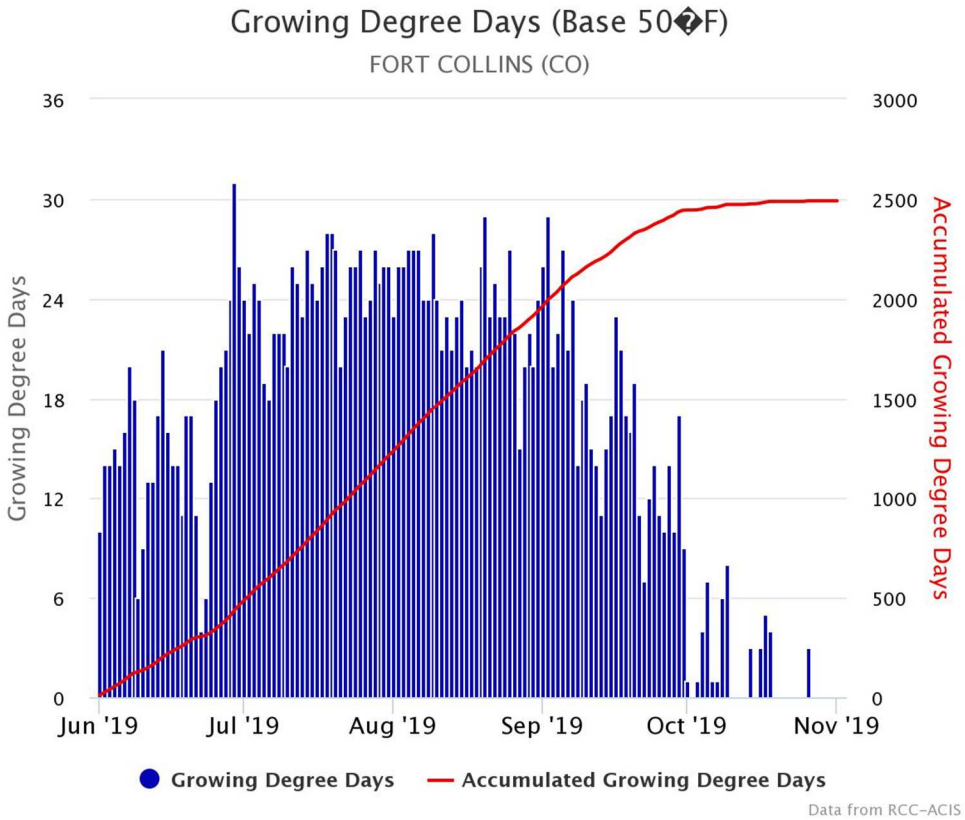

Supplementary Figure 4. Growing Degree Days (GDD) in Fort Collins from June 2019-November 2019, the months during which the 2019 EMS first mutagenized genetaion (M_1) was grown for seed. GDD are displayed here in Farenheit. Using a base temperature of 50F is standard. Converstion from Faranheit GDD to Celsius GDD is as follows:

$$GDD_{Celsius} = (5/9)\ GDD_{Faranheit}$$

REFERENCES

Colorado State University. *Growing Degree Days.* Accessed April 22, 2020. URL: https://climate.colostate.edu/gdd.html, Fort Collins, CO, 80252 USA

Dreher KA, Brown J, Saw RE, Callis J (2006) The Arabidopsis Aux/IAA protein family has diversified in degradation and auxin responsiveness. Plant Cell 18 (3):699-714. doi:10.1105/tpc.105.039172

LeClere S, Wu C, Westra P, Sammons RD (2018) Cross-resistance to dicamba, 2,4-D, and fluroxypyr in *Kochia scoparia* is endowed by a mutation in an AUX/IAA gene. Proc Natl Acad Sci U S A 115 (13):E2911-E2920. doi:10.1073/pnas.1712372115